

BORDERED FLOER HOMOLOGY FOR MANIFOLDS WITH TORUS BOUNDARY VIA IMMERSSED CURVES

JONATHAN HANSELMAN, JACOB RASMUSSEN, AND LIAM WATSON

ABSTRACT. This paper gives a geometric interpretation of bordered Heegaard Floer homology for manifolds with torus boundary. If M is such a manifold, we show that the type D structure $\widehat{CFD}(M)$ may be viewed as a set of immersed curves decorated with local systems in ∂M . These curves-with-decoration are invariants of the underlying three-manifold up to regular homotopy of the curves and isomorphism of the local systems. Given two such manifolds and a homeomorphism h between the boundary tori, the Heegaard Floer homology of the closed manifold obtained by gluing with h is obtained from the Lagrangian intersection Floer homology of the curve-sets. This machinery has several applications: We establish that the dimension of \widehat{HF} decreases under a certain class of degree one maps (pinches) and we establish that the existence of an essential separating torus gives rise to a lower bound on the dimension of \widehat{HF} . In particular, it follows that a prime rational homology sphere Y with $\widehat{HF}(Y) < 5$ must be geometric. Other results include a new proof of Eftekhary's theorem that L-space homology spheres are atoroidal; a complete characterisation of toroidal L-spaces in terms of gluing data; and a proof of a conjecture of Hom, Lidman, and Vafaee on satellite L-space knots.

1. INTRODUCTION

Bordered Floer homology is a suite of invariants, introduced by Lipshitz, Ozsváth and Thurston [25], assigned to three-manifolds with boundary. These invariants are particularly well-adapted to cut-and-paste techniques. In the case of manifold with torus boundary, this theory has been developed in various ways yielding effective combinatorial tools for studying certain classes of toroidal three-manifolds [7, 13, 14, 15, 17, 18, 23]. The goal of this paper is to provide a geometric interpretation of bordered Floer homology for manifolds with torus boundary in terms of one-dimensional objects in the boundary of the manifold.

1.1. Bordered invariants as immersed curves. If M is a closed orientable 3-manifold with torus boundary, we define T_M to be the complement of 0 in $H_1(\partial M; \mathbb{R})/H_1(\partial M; \mathbb{Z})$. The punctured torus T_M can be identified with the complement of a point z in ∂M , and this identification is well-defined up to isotopy.

In order to define the bordered invariant $\widehat{CFD}(M, \alpha, \beta)$, we must choose a parametrization (α, β) of ∂M . That is, α and β are the cores of the 1-handles in a handle decomposition of ∂M . Starting from $\widehat{CFD}(M, \alpha, \beta)$ we will define a collection $\gamma = \{\gamma^1, \dots, \gamma^n\}$ of immersed closed curves $\gamma^i: S^1 \looparrowright T_M$, each decorated with a local system (V_i, Φ_i) consisting of a finite dimensional vector space over $\mathbb{F} = \mathbb{Z}/2\mathbb{Z}$ and an automorphism $\Phi_i: V_i \rightarrow V_i$; we denote this data by $\widehat{HF}(M)$.

Date: October 20, 2017.

JH was partially supported by NSF RTG grant DMS-1148490; JR was partially supported by EPSRC grant EP/M000648/1; LW was partially supported by a Marie Curie career integration grant, by a CIRGET research fellowship, and by a Canada Research Chair; JR and LW were Isaac Newton Institute program participants while part of this work was completed and acknowledge partial support from EPSRC grant EP/K032208/1; additionally, LW was partially supported by a grant from the Simons Foundation while at the Isaac Newton Institute.

Theorem 1. *The collection of decorated curves $\widehat{HF}(M)$ is a well defined invariant of M , up to regular homotopy of curves and isomorphism of local systems. In particular, $\widehat{HF}(M)$ does not depend on the choice of parametrization (α, β) .*

This data is equivalent to bordered Floer homology: $\widehat{HF}(M)$ is determined by $\widehat{CFD}(M, \alpha, \beta)$ and, for any choice of parametrization (α, β) , $\widehat{CFD}(M, \alpha, \beta)$ can be recovered from $\widehat{HF}(M)$.

Now suppose that M_0 and M_1 are manifolds as above, and that $Y = M_0 \cup_h M_1$ is the closed manifold obtained by gluing them together by the orientation reversing homeomorphism $h: \partial M_1 \rightarrow \partial M_0$. The Heegaard Floer homology $\widehat{HF}(Y)$ can be recovered from $\gamma_0 = \widehat{HF}(M_0)$ and $\gamma_1 = \bar{h}(\widehat{HF}(M_1))$, where the homeomorphism \bar{h} is the composition of h with the elliptic involution on ∂M_0 .

Theorem 2. *For $Y = M_0 \cup_h M_1$ as above,*

$$\widehat{HF}(Y) \cong HF(\gamma_0, \gamma_1)$$

where $HF(\cdot, \cdot)$ is an appropriately defined version of the Lagrangian intersection Floer homology in T_{M_0} .

1.2. Trivial local systems. In order to illustrate the content of Theorem 1 and Theorem 2, it is instructive to consider the case where the local systems are trivial. In this case the associated vector spaces are 1-dimensional and can be dropped from the notation; the resulting invariants are simply (systems of) immersed curves. As a very simple example, the invariant $\widehat{HF}(D^2 \times S^1)$ consists of a single closed circle parallel to the longitude $\lambda = \partial D^2 \times \{\text{pt}\}$.

A more interesting example is illustrated in Figure 1: The invariant associated with the complement of the figure eight knot has two components. When the curves are more complicated, it is generally easier to represent them by drawing some of their lifts to the cover $\tilde{T} = H_1(M; \mathbb{R}) \setminus H_1(M; \mathbb{Z}) \cong \mathbb{R}^2 \setminus \mathbb{Z}^2$. From this point of view, the effect of orientation reversal on bordered invariants corresponds to reflection in the line determined by the longitude. Figure 2 shows the invariant associated with the right-hand trefoil. We note that, in this context, calculation is extremely efficient:

Corollary 3. *In the case of trivial local systems, following the notation of Theorem 2, if no two components of γ_0 and γ_1 are parallel then $\dim \widehat{HF}(Y)$ is the minimal geometric intersection number between γ_0 and γ_1 .*

For example, let Y_1 be the manifold obtained by splicing the complements of the left-hand trefoil K_L and the right-hand trefoil K_R ; that is by taking $M_0 = S^3 \setminus \nu(K_L)$, $M_1 = S^3 \setminus \nu(K_R)$, and $h: \partial M_0 \rightarrow \partial M_1$ such that $h(\mu) = \lambda$ and $h(\lambda) = \mu$, where μ and λ are the preferred meridian and longitude of each trefoil in S^3 . Similarly, let Y_2 be the manifold obtained by splicing two copies of the complement of the right-hand trefoil. Consulting Figure 3, we see that $\widehat{HF}(Y_1)$ has dimension 9, while $\widehat{HF}(Y_2)$ has dimension 7, as calculated by Hedden and Levine [18].

Manifolds for which the local systems are trivial are precisely the loop-type manifolds introduced by the first and third author [17]; the graphical formalism can thus be viewed as a geometric

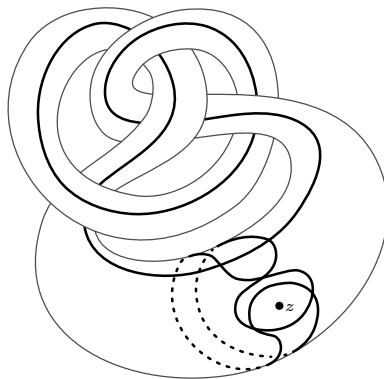


Figure 1. The marked exterior of the figure eight knot, together with its bordered invariant as a pair of immersed curves.

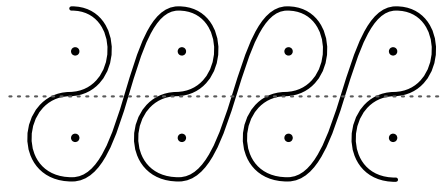


Figure 2. A curve for the right-hand trefoil: the horizontal direction corresponds to the preferred longitude λ , and the vertical direction to the standard meridian of the knot.

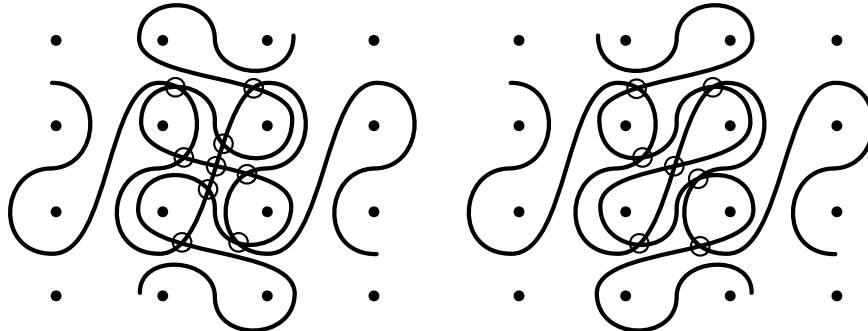


Figure 3. Splicing trefoils: The diagram on the left illustrates the intersection (carried out in \tilde{T}_M) calculating $\dim \widehat{HF}(Y_1) = 9$ where Y_1 is the splice of a right-hand and left-hand trefoil, while the diagram on the right illustrates the intersection calculating $\dim \widehat{HF}(Y_2) = 7$ where Y_2 is the splice of two right-hand trefoils.

representation of the loop calculus. We remark that no explicit examples of three-manifolds are known for which the associated bordered invariant gives rise to a non-trivial local system. In practice – for instance for the gluing theorem needed in [15] – it is often enough to restrict attention to loop-type manifolds. As such, this class of manifolds seems interesting in its own right, and is discussed in further detail in a companion article [16].

1.3. Train tracks and a structure theorem. We now discuss the ideas behind the proof of Theorem 1. If M is as in the statement of the theorem, the bordered Floer homology $\widehat{CFD}(M, \alpha, \beta)$ is a type D structure (in the sense of Lipshitz, Ozsváth, and Thurston [25]) over an algebra \mathcal{A} , known as the *torus algebra*. In this case, a type D structure over \mathcal{A} is simply a chain complex over \mathcal{A} satisfying certain conditions. These are equivalent to differential modules.

In this paper, we will restrict our attention to a certain class of type D structures over \mathcal{A} , which we call *extendable*. (An *extended type D structure* is a curved differential module over an algebra $\tilde{\mathcal{A}}$ which has \mathcal{A} as a quotient; these have certain properties in common with matrix factorizations.) The following theorem, which is essentially due to Lipshitz, Ozsváth and Thurston [25, Chapter 11], shows that this is not much of a restriction.

Theorem 4. *If M is a compact oriented manifold with torus boundary, $\widehat{CFD}(M, \alpha, \beta)$ is extendable.*

We introduce a new graphical calculus, based on immersed train tracks in the punctured torus, which describes extended type D structures. The graphical calculus provides an effective practical method for reducing a given extended type D structure to a collection of curves decorated with local systems. Using it, we prove the following structure theorem:

Theorem 5. *Every extendable type D structure over \mathcal{A} can be represented by a collection of immersed curves in the punctured torus, decorated with local systems.*

The class of extendable type D structures which are known to arise as $\widehat{CFD}(M, \alpha, \beta)$ for some three-manifold M is considerably smaller than the set of all extendable type D structures. Indeed, as mentioned above, we do not have any explicit examples of a manifold M for which $\widehat{HF}(M)$ has a non-trivial local system (though we expect that such M should exist). Even in the case of trivial local systems there are curve sets that do not correspond to three-manifold invariants. For instance, Proposition 50 shows that certain configurations of *loose* curves (introduced in Section 7.2) do not arise as invariants of three-manifolds. This improves on a result due to Gillespie [9], and should be compared with work of Alishahi and Lipshitz [1].

1.4. Relation with the Fukaya category. Theorem 1 can be interpreted as saying that if M is a manifold with torus boundary then $\widehat{HF}(M)$ is a compactly supported element of the Fukaya

category $\mathcal{F}(T_M)$, while Theorem 2 says that the Floer homology of a closed manifold $Y = M_0 \cup_h M_1$ is given by the Hom pairing in the Fukaya category:

$$\widehat{HF}(Y) = \text{Hom}(\widehat{HF}(M_0), \bar{h}(\widehat{HF}(M_1)))$$

The connection between the Heegaard Floer theory and the Fukaya category dates back to the introduction of Heegaard Floer homology, whose definition was motivated by a Seiberg-Witten analog of the Atiyah-Floer conjecture [28]. Following the introduction of bordered Floer homology [24, 25], Auroux [2, 3] and Lekili and Perutz [22] suggested that the Floer homology of a compact oriented M with $\partial M = \Sigma_g$ should be an object in $\mathcal{F}(\text{Sym}^g(\Sigma_g \setminus z))$. In particular, Auroux showed that if \mathcal{P} is a parametrization of ∂M (in other words, an identification of ∂M with a specific genus g surface F equipped with a handle body decomposition), the bordered Floer homology $\widehat{CFA}(M, \mathcal{P})$ defines an object $L(M, \mathcal{P})$ in the partially wrapped Fukaya category $\mathcal{F}(\text{Sym}^g(F \setminus z))$, and that the pairing in bordered Floer homology is given by the Hom pairing. However it is unclear from this construction whether $L(M, \mathcal{P})$ should be compactly supported.

Auroux's construction is conceptually very useful but for general g we don't have any way of making calculations in $\mathcal{F}(\text{Sym}^g(F \setminus z))$ other than the one provided by bordered Floer homology. The one obvious exception is the case $g = 1$ where, naively, one might expect that objects in $\mathcal{F}(T^2 \setminus z)$ are given by curves in the punctured torus. In fact, the situation is somewhat more complicated. The Fukaya category is triangulated, so a typical object actually has the form of an iterated mapping cone built out of geometric curves. In [12], Haiden, Katzarkov and Kontsevich give an especially nice algebraic model for the partially wrapped Fukaya category of a punctured surface Σ ; in the case of $T^2 \setminus z$, objects of $\mathcal{F}(T^2 \setminus z)$ correspond to chain complexes over the algebra \mathcal{A} or, equivalently, with Type D structures.

One of the main results of [12] is a structure theorem for objects of $\mathcal{F}(\Sigma)$, which says that any object can be expressed as a direct sum of immersed, possibly noncompact curves. Theorem 5 was motivated by this result but our proof is quite different. In particular, the condition that the type D structure is extendable implies that the curves are all compactly supported. More generally, if Σ is a punctured surface with stops on each boundary component, objects of $\mathcal{F}(\Sigma)$ correspond to type D structures over an appropriate algebra. Our proof of Theorem 5 generalizes to show that if the type D structure is extendable, it is isomorphic to a disjoint union of compactly supported curves equipped with local systems. This gives a new proof of the structure theorem of Haiden, Katzarkov, and Kontsevich in the compactly supported case (see Theorem 33), which is constructive and stays internal to the language of bordered Floer homology (namely, type D structures). This constructive approach has a key advantage: we obtain new information about Heegaard Floer theory and applications to 3-manifolds, as described below.

1.5. Gradings. There is a refined version of the invariant which takes spin^c structures and the absolute $\mathbb{Z}/2\mathbb{Z}$ grading on Heegaard Floer homology into account.

Definition 6. If M is as in Theorem 1, let \bar{T}_M be the covering space of T_M whose fundamental group is the kernel of the composition

$$\pi_1(T_M) \rightarrow \pi_1(\partial M) \rightarrow H_1(\partial M) \rightarrow H_1(M)$$

Equivalently, if $\lambda \in H_1(M; \mathbb{Z})$ generates the kernel of the inclusion $j_*: H_1(\partial M; \mathbb{Z}) \rightarrow H_1(M; \mathbb{Z})$ \bar{T}_M is homeomorphic to the quotient $((H_1(M; \mathbb{R}) \setminus H_1(M; \mathbb{Z}))/\langle \lambda \rangle)$. We let $p: \bar{T}_M \rightarrow T_M$ be the covering map.

The set of spin^c structures on M can be identified with $H^2(M) \simeq H_1(M, \partial M) \simeq \text{coker } j_*$. We have:

Theorem 7. *For each $\mathfrak{s} \in \text{Spin}^c(M)$, there is an invariant $\widehat{HF}(M, \mathfrak{s})$ which is a collection of oriented immersed closed curves equipped with local systems in \bar{T}_M . Moreover, $\widehat{HF}(M, \mathfrak{s})$ is well-defined up*

to the action of translation by the deck group of p , and

$$\widehat{HF}(M) = \bigcup_{\mathfrak{s} \in \text{Spin}^c(M)} p(\widehat{HF}(M, \mathfrak{s})).$$

There is an analog of Theorem 2 which recovers the spin^c decomposition of $\widehat{HF}(M_0 \cup_h M_1)$ from $\widehat{HF}(M_0, \mathfrak{s}_0)$ and $\widehat{HF}(M_1, \mathfrak{s}_1)$, where \mathfrak{s}_i runs over spin^c structures on M_i . (See Proposition 46 for a precise statement.) The $\mathbb{Z}/\mathbb{Z}2$ grading on $\widehat{HF}(M_0 \cup_h M_1)$ is determined by the sign of the intersections between the oriented curves $\widehat{HF}(M_0)$ and $\widehat{HF}(M_1)$.

1.6. Immediate consequences. The geometric interpretation of bordered Floer invariants described above has several applications. For instance:

Theorem 8. *Let Y be a closed, orientable three-manifold. If Y contains a separating essential torus then $\dim \widehat{HF}(Y) \geq 5$.*

This follows quickly from Theorem 2. Indeed, a simple geometric argument shows that any two sufficiently non-trivial immersed curves in the punctured torus intersect in at least 5 points (a specific example realizing $\dim \widehat{HF}(Y) = 5$ is illustrated in Figure 53; see also Theorem 57). Theorem 8 gives rise to an interesting geometric statement:

Corollary 9. *If Y is a prime rational homology sphere with $\dim \widehat{HF}(Y) < 5$ then Y is geometric.*

Proof. Note that any essential torus in a rational homology sphere must be separating. Thus, if $\dim \widehat{HF}(Y) < 5$ then Y is atoroidal and we may appeal to Perelman's resolution of Thurston's geometrization conjecture to conclude that Y admits a geometric structure. \square

Note that, more precisely, the geometric structure in question is either hyperbolic or it is one of 6 Seifert fibered geometries; see Scott [32], for example. As another immediate corollary of Theorem 8, we obtain a new proof of a theorem of Eftekhary [8]:

Corollary 10. *L-space integer homology spheres are atoroidal.* \square

Recall that an L-space is a rational homology sphere for which $\dim \widehat{HF}(Y) = |H_1(Y)|$. Corollary 10 is a part of a conjecture of Ozsváth and Szabó; it implies that prime integer homology sphere L-spaces with infinite fundamental group – should examples exist – are hyperbolic.

In another direction, we can establish strong behaviour for Heegaard Floer homology in the presence of certain degree one maps. Consider an integer homology sphere Y containing an essential torus, and write $Y = M_0 \cup_h M_1$ where the M_i are (necessarily) integer homology solid tori. Following our conventions above, $h(\lambda)$ must be a meridian in ∂M_0 when λ is the longitude of M_1 . The Dehn filling $Y_0 = M_0(h(\lambda))$ is the result of replacing M_1 with a solid torus (called a *pinch*); there is a degree one map $Y \rightarrow Y_0$.

Theorem 11. *If Y is a toroidal integer homology sphere and Y_0 is the result of a pinch on Y then $\dim \widehat{HF}(Y) \geq \dim \widehat{HF}(Y_0)$.*

This follows from a more general statement about pinching along tori in rational homology spheres; see Theorem 52. In particular, to the best of the authors' knowledge, this is the only result concretely treating the following:

Question 12. *If $Y \rightarrow Y_0$ is a degree one map between closed, connected, orientable three-manifolds, is it the case that $\dim \widehat{HF}(Y) \geq \dim \widehat{HF}(Y_0)$?*

1.7. The L-space gluing theorem. The geometric invariants defined in this paper can also be applied to the classification of L-spaces; in particular, we prove a complete characterization of when gluing along a torus produces an L-space. Again, an L-space is a rational homology sphere Y for which $\dim \widehat{HF}(Y) = |H_1(Y)|$. For a manifold with torus boundary M , the set of L-space slopes of M is given by

$$\mathcal{L}_M = \{\alpha \mid \dim \widehat{HF}(M(\alpha)) = |H_1(Y)|\} \subset \mathbb{Q}P^1$$

where $M(\alpha)$ denotes Dehn filling along the slope α . We denote the interior of \mathcal{L}_M by \mathcal{L}_M° .

The set \mathcal{L}_M is encoded by and easily extracted from the invariant $\widehat{HF}(M)$. In particular, a necessary condition for $|\mathcal{L}_M| > 1$ is that the associated local system be trivial. The complement of \mathcal{L}_M is obtained by considering the minimal set of tangent lines to $\widehat{HF}(M)$; see Theorem 54 for a precise statement. This provides a satisfying solution to a problem posed by Boyer and Clay [6, Problem 1.9]. Toroidal L-spaces are then characterized as follows.

Theorem 13. *Let $Y = M_0 \cup_h M_1$ be a 3-manifold where M_i are boundary incompressible manifolds and $h: \partial M_1 \rightarrow \partial M_0$ is an orientation reversing homeomorphism between torus boundaries. Then Y is an L-space if and only if $\mathcal{L}_{M_0}^\circ \cup h(\mathcal{L}_{M_1}^\circ) = \mathbb{Q}P^1$.*

This confirms a conjecture due to the first author [13], and strengthens results in [14, 15, 17, 18, 30]. In addition to the applications discussed below, the L-space gluing theorem plays a key role in the program to understand L-spaces arising as cyclic branched covers of knots in the three-sphere; see Gordon and Lidman [10, 11] and Boileau, Boyer, and Gordon [5]. A weaker version of the L-space gluing theorem was the key ingredient, along with work of Boyer and Clay [6], in proving the L-space conjecture for graph manifolds [15] (an alternate, constructive, proof is given in [31]). We note that, in light of the L-space conjecture [7], the L-space gluing theorem makes some striking predictions about the behaviour of foliations on manifolds with torus boundary, as well as the behaviour of left-orderes on the fundamental groups of these manifolds. Another notable application is given in the work of Némethi on links of rational singularities [27].

Theorem 13 allows us to refine Theorem 8 in the case that Y is a toroidal L-space. In addition to ruling out $|H_1(Y)| \leq 4$, we can easily enumerate all examples with $|H_1(Y)| < 8$; see Theorem 57. Note that this leads to another proof of Corollary 10. Another quick consequence of Theorem 13 is the following:

Theorem 14. *Suppose that K is a satellite knot in S^3 . If K is an L-space knot (that is, K admits non-trivial L-space surgeries) then both the pattern knot and the companion knot are L-space knots as well.*

This confirms a conjecture of Hom, Lidman, and Vafaee [20, Conjecture 1.7]. It has subsequently been used by Baker and Motegi [4] to show that the pattern knot must be a braid in the solid torus (see also Hom [19]).

Organization. This paper is a substantially revised version of our earlier preprint of the same name, which dealt only with loop-type manifolds. A subsequent paper [16] will discuss further properties of the invariant and give some examples. The current paper is laid out as follows.

Section 2 summarizes the relevant background from bordered Floer homology (in the case of manifolds with torus boundary) and describes a geometric representation for these invariants in terms of immersed train tracks. The main new content in this section is a graphical interpretation of the box tensor product – the chain complex $\widehat{CFA}(M_0, \alpha_0, \beta_0) \boxtimes \widehat{CFD}(M_1, \alpha_1, \beta_1)$ – in terms of intersection between train tracks; see Theorem 16. For train tracks that are immersed curves, this has a clear connection to Lagrangian intersection Floer theory. In general, however, the naive intersection of train tracks is not an invariant in any sense. Extracting invariants is the principal aim of the remaining sections.

Section 3 is devoted to algebraic issues concerning a well-behaved class of type D structures: we prove a structure theorem (Theorem 5) for extendable type D structures in two steps. We first reduce train tracks in this class to train tracks satisfying certain nice properties (Section 3.3, particularly Proposition 23), and then show that such train tracks can be manipulated and ultimately interpreted in terms of immersed curves and local systems (Section 3.7, particularly Proposition 29). Indeed, the class of train tracks considered ultimately gives a geometric interpretation of the relevant local systems. The section concludes with Theorem 33, which extends our techniques to surfaces of higher genus.

Section 4 establishes the equivalence between, and independence of choices made in the construction of, extendable type D structures and immersed curved with local systems. We note that, while only the existence of an extension is required for our purposes, it follows from the work in this section that extendable type D structures have essentially unique extensions; see Proposition 38.

Section 5 returns the focus to three-manifolds, completing the proof of Theorem 1 and Theorem 2, while Section 6 explains the modifications to the invariant needed to recover the spin^c and $\mathbb{Z}/2\mathbb{Z}$ gradings on \widehat{HF} , as described in Theorem 7.

Section 7 is devoted to the applications described above, and the paper concludes with a short Appendix containing the proof of Theorem 4.

Conventions and coefficients. All three-manifolds arising in this work are compact, connected, smooth, and orientable. Consistent with the set-up in bordered Floer homology [25], all Floer invariants in this work take coefficients in the two element field \mathbb{F} . We expect that the results we describe here should work over other fields (and perhaps over \mathbb{Z} as well) but setting it up would require defining the bordered Floer homology of a manifold with torus boundary over \mathbb{Z} . Unless explicitly stated otherwise, (singular) homology groups of manifolds should be assumed to take coefficients in \mathbb{Z} .

Acknowledgements. The authors would like to thank Peter Kronheimer, Yankı Lekili, Tye Lidman, Robert Lipshitz, Sarah Rasmussen, Ivan Smith, and Claudius Zibrowius for helpful discussions (some of them dating back a very long time). Part of this work was carried out while the third author was visiting Montréal as CIRGET research fellow, and part was carried out while the second and third authors were participants in the program *Homology Theories in Low Dimensions* at the Isaac Newton Institute.

2. BORDERED INVARIANTS AS TRAIN TRACKS

This section gives a geometric interpretation of bordered invariants in terms of immersed train tracks for manifolds with torus boundary. We begin with a brief review of the relevant notions from bordered Floer homology [25]. A less terse intro, with essentially the same notation used here, is given in [17].

2.1. Modules over the torus algebra. Let M be an orientable three-manifold with torus boundary, and choose oriented essential simple closed curves α, β in ∂M with $\beta \cdot \alpha = 1$. The ordered triple (M, α, β) is called a bordered three-manifold; the pair (α, β) may be regarded as a parametrization of the torus boundary, in the sense that $\langle \alpha, \beta \rangle$ specifies the peripheral subgroup $\pi_1(\partial M)$.

We focus on two (equivalent) bordered invariants assigned to a bordered manifold (M, α, β) . These will take the form of certain modules over the torus algebra \mathcal{A} . Various descriptions of this algebra are given by Lipshitz, Ozsváth and Thurston [25], but for our purposes, recall that \mathcal{A} is generated, as an algebra over the two-element field \mathbb{F} , by elements ρ_1, ρ_2 and ρ_3 and idempotents ι_0 and ι_1 . Multiplication in \mathcal{A} is described by the quiver depicted in Figure 4 together with the relations $\rho_2\rho_1 = \rho_3\rho_2 = 0$. The shorthand $\rho_{12} = \rho_1\rho_2$, $\rho_{23} = \rho_2\rho_3$, $\rho_{123} = \rho_1\rho_2\rho_3$ is standard. Let \mathcal{I} denote the subring of idempotents, and write $\mathbf{1} = \iota_0 + \iota_1$ for the unit in \mathcal{A} .

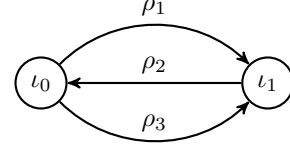


Figure 4. A quiver for the torus algebra, with relations $\rho_2\rho_1 = \rho_3\rho_2 = 0$.

The relevant bordered invariants are $\widehat{CFA}(M, \alpha, \beta)$ and $\widehat{CFD}(M, \alpha, \beta)$; both are invariants of the underlying bordered manifold up to homotopy [25]. The former is a type A structure, that is, a right A_∞ -module over \mathcal{A} . The latter is a type D structure, which consists of (1) a vector space V (over \mathbb{F}) together with a splitting as a direct sum over a left action of the idempotents $V \cong \iota_0 V \oplus \iota_1 V$; and (2) a map $\delta^1: V \rightarrow \mathcal{A} \otimes_{\mathcal{I}} V$ satisfying a compatibility condition ensuring that $\partial(a \otimes x) = a \cdot \delta(x)$ is a differential on $\mathcal{A} \otimes_{\mathcal{I}} V$ (with left \mathcal{A} -action specified by $a \cdot (b \otimes x) = ab \otimes x$). In particular, $\mathcal{A} \otimes_{\mathcal{I}} V$ has the structure of a left differential module over \mathcal{A} . We will sometimes confuse the type D structure $\widehat{CFD}(M, \alpha, \beta)$ (consisting of V and δ^1) and this associated differential module. Given any type D structure there is a collection of recursively defined maps $\delta^k: V \rightarrow \mathcal{A}^{\otimes k} \otimes V$ where $\delta^0: V \rightarrow V$ is the identity and $\delta^k = (\text{id}_{\mathcal{A}^{\otimes k-1}} \otimes \delta^1) \circ \delta^{k-1}$. The type D structure $\widehat{CFD}(M, \alpha, \beta)$ is bounded if δ^k vanishes for all sufficiently large integers k .

Given a bordered manifold (M, α, β) the associated type A and type D structures are related. In particular, according to [26, Corollary 1.1], $\widehat{CFA}(M, \alpha, \beta)$ is dual (in an appropriate sense) to $\widehat{CFD}(M, \alpha, \beta)$. However, the utility of the two structures, taken together, is a computable model for the A_∞ tensor product: Given bordered manifolds (M_0, α_0, β_0) and (M_1, α_1, β_1) consider the chain complex $\widehat{CFA}(M_0, \alpha_0, \beta_0) \boxtimes \widehat{CFD}(M_1, \alpha_1, \beta_1)$ obtained from $\widehat{CFA}(M_0, \alpha_0, \beta_0) \otimes_{\mathcal{I}} \widehat{CFD}(M_1, \alpha_1, \beta_1)$ with differential defined by

$$\partial^{\boxtimes}(x \otimes y) = \sum_{k=0}^{\infty} (m_{k+1} \otimes \text{id})(x \otimes \delta^k(y))$$

and the requirement that $\widehat{CFD}(M_1, \alpha_1, \beta_1)$ is bounded (this ensures that the above sum is finite). Then the pairing theorem of Lipshitz, Ozsváth and Thurston asserts that the homology of $\widehat{CFA}(M_0, \alpha_0, \beta_0) \boxtimes \widehat{CFD}(M_1, \alpha_1, \beta_1)$ is isomorphic to the Heegaard Floer homology $\widehat{HF}(M_0 \cup_h M_1)$ of the closed manifold obtained from the homeomorphism $h: \partial M_1 \rightarrow \partial M_0$ specified by $h(\alpha_1) = \beta_0$ and $h(\beta_1) = \alpha_0$ [25, Theorem 1.3].

2.2. Conventions for bordered manifolds. In the framework given by Lipshitz, Ozsváth and Thurston [25], the boundary parametrization of M is recorded by specifying a diffeomorphism $\phi: F \rightarrow \partial M$ where F is a torus with a fixed handle decomposition. The image of the cores of the one-handles in F correspond to the pair of α -arcs (α_1^a, α_2^a) in a bordered Heegaard diagram; completing this pair to curves in ∂M gives a pair corresponding to our parametrizing curves α and β . To relate the two notations, we must specify which curve corresponds to each α -arc in a bordered Heegaard diagram. We orient the arcs α_1^a and α_2^a so that, starting at the basepoint and following the boundary of the Heegaard surface, we pass the initial point of α_1^a , the initial point of α_2^a , the final point of α_1^a , and the final point of α_2^a . With this labelling, α in our notation corresponds to $-\alpha_1^a$ and β corresponds to α_2^a . Note that when gluing two bordered manifolds together by an orientation reversing diffeomorphism taking basepoint to basepoint, α_1^a must glue to $-\alpha_2^a$ and α_2^a must glue to $-\alpha_1^a$; thus in our notation, α glues to β and β glues to α . Finally, the arcs defined above in a Heegaard diagram seem to satisfy $(-\alpha_1) \cdot \alpha_2 = 1$, which would imply that $\alpha \cdot \beta = 1$. However, the orientation of the Heegaard surface agrees with the opposite of the orientation on ∂M . Said another

way, the surface in a bordered Heegaard diagram for M should be interpreted as being viewed from *inside* M , but we will generally look at ∂M from *outside* M so that $\beta \cdot \alpha = 1$.

2.3. Decorated graphs. There is a convenient graph-theoretic shorthand for describing these bordered invariants (see, for instance, [17, 18]). Let Γ be a directed graph with vertex set \mathcal{V}_Γ and edge set \mathcal{E}_Γ . A decorated graph has the property that every $v \in \mathcal{V}_\Gamma$ is labelled with exactly one element from $\{\bullet, \circ\}$ and every $e \in \mathcal{E}_\Gamma$ is labelled with exactly one element from $\{\emptyset, 1, 2, 3, 12, 23, 123\}$. Moreover, the edge orientations are compatible with the idempotents so that $\bullet \xrightarrow{1} \circ$, $\circ \xrightarrow{2} \bullet$, $\bullet \xrightarrow{3} \circ$, $\bullet \xrightarrow{12} \bullet$, $\circ \xrightarrow{23} \circ$, and $\bullet \xrightarrow{123} \circ$.

A decorated graph Γ describes a type D structure as follows. The underlying vector space is generated by \mathcal{V}_Γ , with the idempotent splitting specified by \bullet labels identifying the ι_0 generators and \circ labels identifying the ι_1 generators. The map δ^1 is determined by the edge labels: Given $e \in \mathcal{E}_\Gamma$ with label $I \in \{\emptyset, 1, 2, 3, 12, 23, 123\}$ consider the source x and target y in \mathcal{V}_Γ . Then $\rho_I \otimes y$ is a summand of $\delta^1(x)$, with the interpretation that $\rho_\emptyset = 1$. A decorated graph (and its associated type D structure) is reduced if none of the edges is labelled by \emptyset . An example is shown in Figure 5, describing the bordered invariant $\widehat{CFD}(M, \mu, \lambda)$ when M is the complement of the right-hand trefoil, μ is the knot meridian and λ is the Seifert longitude (see [25]). Notice that the higher δ^k are determined by directed paths in Γ ; for the example shown, there exist generators x and y such that $\delta^3(x) = \rho_3 \otimes \rho_2 \otimes \rho_1 \otimes y$ corresponding to the unique directed path of length 3. Clearly, the associated type D structure is bounded if and only if the decorated graph contains no directed cycles.

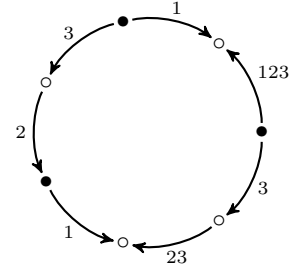


Figure 5. A decorated graph.

In the reduced case, the duality between type D and type A structures is encoded in the decorated graphs following an algorithm described by Hedden and Levine [18]. This takes the same interpretation for the underlying vector space (that is, the idempotent splitting according to vertex labels) but requires a different interpretation of the edge labels. First, one re-writes/re-interprets the edge labels according to the bijection $1 \leftrightarrow 3$, $2 \leftrightarrow 2$, $3 \leftrightarrow 1$. Next, given any length n directed path in Γ with source vertex x and target vertex y we construct a sequence $I = I_1, \dots, I_k$ and assign a multiplication $m_{k+1}(x \otimes \rho_{I_1} \otimes \dots \otimes \rho_{I_k}) = y$. The sequence I is constructed by forming a word in $\{1, 2, 3\}$ determined according to the labels of the directed edge read in order, and then regrouping to find the minimum k such that each I_j (for $1 \leq j \leq k$) is an element of $\{1, 2, 3, 12, 23, 123\}$. Thus, in our example, to the length 3 directed path we assign the label sequence $I = \{123\}$ so that $m_2(x, \rho_{123}) = y$ while the edge label 321 (formerly 123 in the original decorated graph) gives rise to a sequence $I = \{3, 2, 1\}$ and the product $m_4(x', \rho_3, \rho_2, \rho_1) = y'$.

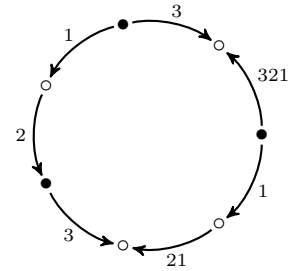


Figure 6. Relabelling by $1 \leftrightarrow 3$, $2 \leftrightarrow 2$, $3 \leftrightarrow 1$ to extract a type A structure from a decorated graph.

2.4. Train tracks. Given a reduced decorated graph Γ as in the previous section, we can immerse Γ in the torus, as described below. First, we fix a specific model for the punctured torus.

Definition 15. The *marked torus* T is the oriented surface $T = \mathbb{R}^2/\mathbb{Z}^2$ punctured at $z = (1-\epsilon, 1-\epsilon)$. The images of the y and x -axes in T will be referred to as α and β respectively.

We embed the vertices of Γ into T so that the vertices corresponding to $V_0 = \iota_0 V$ generators (the \bullet vertices) lie on α in the interval $0 \times [\frac{1}{4}, \frac{3}{4}]$ and the vertices corresponding to $V_1 = \iota_1 V$ generators (the \circ vertices) lie on β in the interval $[\frac{1}{4}, \frac{3}{4}] \times 0$. Finally, we embed each edge in T according to its label, as shown in Figure 7.

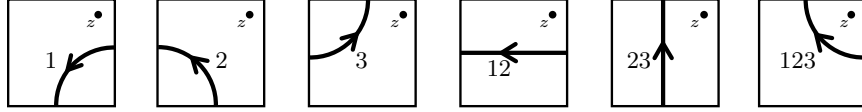


Figure 7. Assigning edges in a reduced decorated graph Γ to directed edges in the marked torus T . Notice that, by labelling corners of the (bordered) marked torus clockwise from the base point, the labels and orientations on edges may be suppressed without ambiguity.

We require that (1) all intersections between edges are transverse and away from the bordered curves α and β and (2) near a vertex, all edges are orthogonal to the curve (α or β) that the vertex lies on. The image of Γ is an *immersed train-track* which we will denote by ϑ . A concrete example is shown in Figure 8.

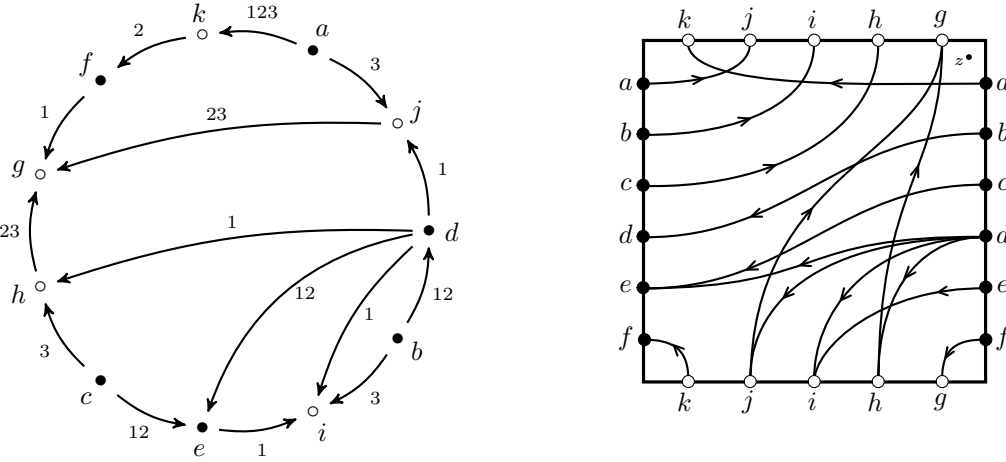


Figure 8. The train track ϑ (right) associated with the decorated graph Γ shown on the left. All train track switches occur at the vertices on the α and β curves; intersection points between edges of the graph are not (new) vertices of the graph. Note that the type D structure described is not known to come from a three-manifold.

When Γ describes $\widehat{CFD}(M, \alpha, \beta)$ for some M , the marked torus should be identified with the parametrized boundary of M , that is, $(T, \alpha, \beta) \simeq (\partial M, \alpha, \beta)$. In this case, we will write $\vartheta(M)$ or $\vartheta(M, \alpha, \beta)$. Note that $\vartheta(M)$ is not an invariant of M in any obvious sense though it does encode $\widehat{CFD}(M, \alpha, \beta)$ in the same way that a decorated graph does.

An important point is that, just as Γ need not be connected as a graph, the immersed train track ϑ , constituting equivalent data, may consist of a union of a collection of immersed train tracks. There is an interesting special case in which ϑ is simply a (collection of) immersed curves in T corresponding to the case when Γ is a valence 2 graph. In the case where $\widehat{CFD}(M, \alpha, \beta)$ admits a representative that may be described by a valence 2 decorated graph, M is called *loop-type*; compare [17]. As an example, the trefoil exterior is loop-type; see Figure 5 and compare Figure 17. It is a surprising fact that a great many classes of manifolds with torus boundary are loop-type, including any manifold admitting multiple L-space fillings [15, 30]; this class of manifolds is considered in detail in a companion paper [16]. Indeed, we have no explicit example of a manifold that is not loop-type.

2.5. Pairing train tracks. Just as a decorated graph encodes both a type D structure and a type A structure, we now establish our conventions for train tracks with respect to this duality. Fix a standard marked torus T and divide it into 4 quadrants. The type A realization $A(\vartheta)$ is obtained by including ϑ into the first quadrant and extending vertically/horizontally; the type D realization

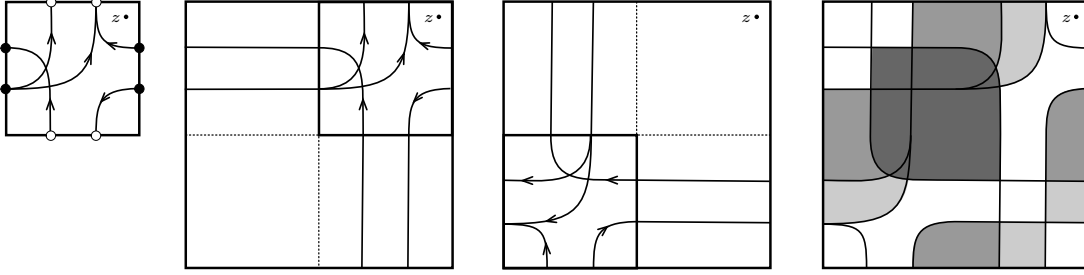


Figure 9. From left to right: a sample train track ϑ , its type A realization $A(\vartheta)$, its type D realization $D(\vartheta)$, and the pairing complex $\mathcal{C}(\vartheta, \vartheta)$ between the two. The 5 bigons contributing to the map d^ϑ in this case have been shaded.

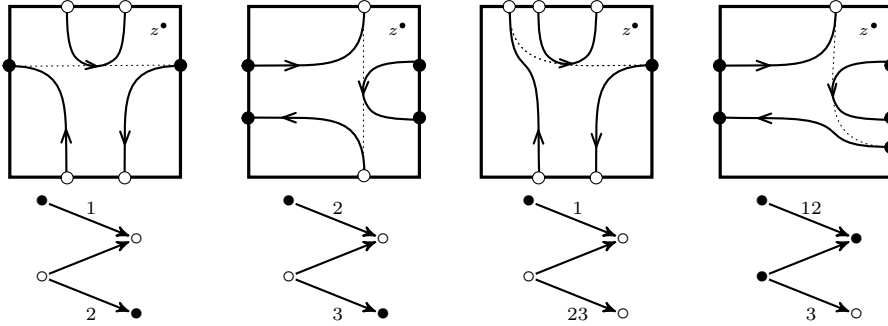


Figure 10. Modifications permitted in almost reduced train tracks.

$D(\vartheta)$ is obtained by reflecting ϑ in the anti-diagonal $y = -x$, including into the third quadrant, and extending vertically and horizontally. See Figure 9.

Now consider a pair of train tracks ϑ_0 and ϑ_1 . We define $\mathcal{C}(\vartheta_0, \vartheta_1)$ to be the vector space over \mathbb{F} generated by the intersection points between $A(\vartheta_0)$ and $D(\vartheta_1)$. Note that these intersection points are confined to the second and fourth quadrants in T , by construction.

There is a linear map $d^\vartheta: \mathcal{C}(\vartheta_0, \vartheta_1) \rightarrow \mathcal{C}(\vartheta_0, \vartheta_1)$ defined by counting bigons. Specifically, if x and y are two intersection points between $A(\vartheta_0)$ and $D(\vartheta_1)$ then the coefficient on y in $d^\vartheta(x)$ is given by a count (modulo 2) of homotopy classes of maps $f: D^2 \rightarrow T$ where $f(-i) = x$, $f(i) = y$, the positive real part of the boundary maps to $A(\vartheta_0)$, and the negative part of the boundary maps to $D(\vartheta_1)$. We say that such a bigon is carried by the train tracks ϑ_0 and ϑ_1 (or, simply, carried by $(\vartheta_0, \vartheta_1)$). See Figure 9 for an illustration of bigons carried by train tracks; note that such bigons are immersed in general. For a bigon carried by $(\vartheta_0, \vartheta_1)$ to contribute to d^ϑ , we will further require that the real part of the boundary maps to an oriented path in $A(\vartheta_0)$ (that is, the orientations on all oriented segments traversed by the path are consistent) with orientation corresponding to the boundary orientation on D^2 , and that the negative real part of the boundary maps to an oriented path in $D(\vartheta_1)$ with orientation corresponding to the opposite of the boundary orientation on D^2 ; thus both sides of the bigon $f(D^2)$ are oriented paths from x to y in either $A(\vartheta_0)$ or $D(\vartheta_1)$. Note that this requirement is automatically satisfied in the present setting, since by construction all oriented segments in $A(\vartheta_0)$ pass the puncture to their right and all oriented segments in $D(\vartheta_1)$ pass the puncture to their right; it follows that any bigon in the torus with the wrong orientation on the boundary covers z .

Under mild hypotheses, the vector space $\mathcal{C}(\vartheta_0, \vartheta_1)$ with linear map d^ϑ is, in fact, a chain complex: it may be identified with the box tensor product of the associated bordered invariants. To explain this, we need to introduce some variants of our train tracks (this will coincide with a notion of admissibility when we return our focus to three-manifold invariants later). Recall that, to this point, we have described reduced train tracks, as these have come from decorated graphs for which no edges are labelled with \emptyset .

A train track is bounded if the underlying decorated graph contains no oriented cycle. A graph is almost reduced if the only edges labelled \emptyset begin and end on valence 2 vertices and occur in one of precisely 4 configurations as shown in Figure 10. Finally, a train track is special bounded if it is bounded and almost reduced. Said another way, we are interested in bounded train tracks or, more generally, those train tracks that can be made bounded by passing (via homotopy of associated modules) to an almost reduced train track.

Theorem 16. *Fix train tracks ϑ_0 and ϑ_1 , where ϑ_0 is reduced and ϑ_1 is special bounded. Let N_0^A denote the type A structure associated with ϑ_0 and let ${}^A N_1$ denote the type D structure associated with ϑ_1 . Then d^ϑ may be identified with ∂^\boxtimes and there is an isomorphism of chain complexes*

$$\mathcal{C}(\vartheta_0, \vartheta_1) \cong N_0^A \boxtimes {}^A N_1.$$

Proof. First observe that there is an identification of the generating sets for $\mathcal{C}(\vartheta_0, \vartheta_1)$ and $N_0^A \boxtimes {}^A N_1$, since each vertical (respectively horizontal) segment in $A(\vartheta_0)$ intersects each horizontal (respectively vertical) segment of $D(\vartheta_1)$ and there are no other intersection points. Note that the horizontal segments in $A(\vartheta_0)$ correspond directly to the ι_0 generators of N_0^A , while the vertical segments correspond to the ι_1 generators. Similarly, the vertical segments of $D(\vartheta_1)$ correspond directly to the ι_0 generators N_1 , while the horizontal segments correspond to the ι_1 generators.

Since ϑ_1 is bounded, the associated type D structure ${}^A N_1$ is bounded and hence ∂^\boxtimes gives a well-defined differential on $N_0^A \boxtimes {}^A N_1$. We aim to identify the linear map d^ϑ with the differential ∂^\boxtimes ; in particular, we will show that each bigon contributing to d^ϑ is uniquely associated with a pairing between type D and type A operations contributing to ∂^\boxtimes .

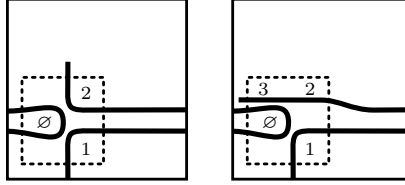
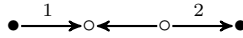
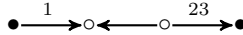


Figure 11. Portions of $D(\vartheta_1)$ where a \emptyset edge has been added to achieve special boundedness.

To begin, consider all operations from ${}^A N_1$ of the form $\delta^1(x) = \mathbf{1} \otimes y$ corresponding to edges decorated by \emptyset in the associated graph Γ ; compare Figure 10. We separate the case where special boundedness has been achieved by replacing a 12 labelled edge with



or by replacing a 123 labelled edge with



With the convention for the type D realization of ϑ_1 in mind, the relevant portion of each of these two situations is illustrated in Figure 11 where a dashed box is used to emphasise the behaviour of ϑ_1 in the third quadrant. We will refer to the parts of a train track interacting with this dashed box as *corners*.

To see the contribution to the differential, first consider a bigon that contains a corner of \mathfrak{v}_1 with the label \emptyset . This corner connects the right ends of two parallel horizontal segments; let the upper (respectively lower) segment correspond to a generator x (respectively y) in $\iota_1(\mathcal{A}N_1)$. Moreover, the left end of the segment corresponding to y is attached to a 1 labelled corner. If there is a bigon that fills in the space between the two horizontal segments, it must not extend to contain the whole horizontal segment since then the bigon would cover the base point; see Figure 12. Thus there must be a vertical segment in $A(\mathfrak{v}_0)$, corresponding to some generator w in $N_0^{\mathcal{A}}$, and the bigon does not extend to the left of this vertical segment. A bigon of this form gives a map between (the intersection point corresponding to) $w \otimes x$ and (the intersection point corresponding to) $w \otimes y$. The \emptyset -labeled corner in \mathfrak{v}_1 arises from a differential of the form $\delta^1(x) = \mathbf{1} \otimes y$ in $\mathcal{A}N_1$, so the corresponding differential is counted in the box tensor product as well.

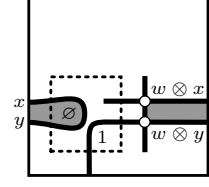


Figure 12. The bigon for $\delta^1(x) = \mathbf{1} \otimes y$.

The other case (again containing two sub-cases) involving a \emptyset edge is similar and left to the reader.

The remaining operations involve non-trivial algebra elements, for which we now set a graphical convention for corners. The corners (in the first quadrant) for the train track $A(\mathfrak{v}_0)$ are shown in Figure 13 and the corners (in the third quadrant) for the train track $D(\mathfrak{v}_1)$ are shown in Figure 14. The essential piece of data in this formalism is the following: for any bigon carried by $(\mathfrak{v}_0, \mathfrak{v}_1)$ there is a list of algebra elements for each train track that is encoded by the shaded part of each corner.

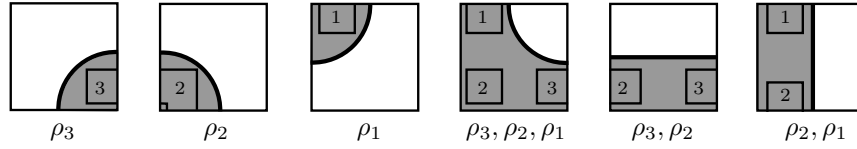


Figure 13. Corner labels for $A(\mathfrak{v}_0)$ (in the first quadrant) consistent with the type A structure for \mathfrak{v}_0 .

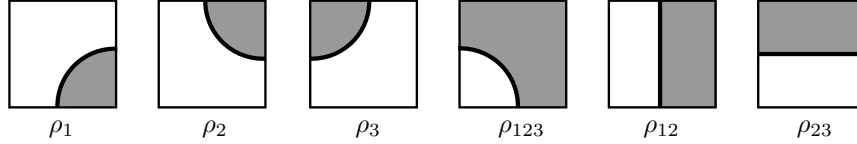


Figure 14. Corner labels for $D(\mathfrak{v}_1)$ (in the third quadrant) consistent with the type D structure for \mathfrak{v}_1 .

For instance, the only bigon that does not intersect the boundary of $[0, 1] \times [0, 1]$ is shown in Figure 15. Let \tilde{x}_0 denote the relevant vertical segment in $A(\mathfrak{v}_0)$ corresponding to some $x_0 \in \iota_1(N_0^{\mathcal{A}})$. Let \tilde{x}_1 denote the relevant horizontal segment in $D(\mathfrak{v}_1)$ corresponding to some generator $x_1 \in \iota_1(\mathcal{A}N_1)$. Similarly, let \tilde{y}_0 and \tilde{y}_1 denote the relevant horizontal segment in $A(\mathfrak{v}_0)$ and vertical segment in $D(\mathfrak{v}_1)$, respectively, and let y_0 and y_1 denote the corresponding generators in $N_0^{\mathcal{A}}$ and $\mathcal{A}N_1$. A bigon of this form gives a map from $\tilde{x}_0 \cap \tilde{x}_1$ to $\tilde{y}_0 \cap \tilde{y}_1$. The left side of the bigon is a path in $D(\mathfrak{v}_1)$ from \tilde{x}_1 to \tilde{y}_1 with a single corner labeled 2. This corresponds to a path of arrows (of length one) from x_2 to y_2 labeled by 2, which, in turn, encodes the operation $\delta^1(x_1) = \rho_2 \otimes y_1$ in $\mathcal{A}N_1$. The right edge of the bigon is a path in $A(\mathfrak{v}_0)$ with a corner labeled by the sequence 2; this in turn corresponds to a map $m_2(x_0, \rho_2) = y_0$ in $N_0^{\mathcal{A}}$. These operations pair in the box tensor product, so there is a differential from $x_0 \otimes x_1$ to $y_0 \otimes y_1$ in the complex $N_0^{\mathcal{A}} \boxtimes \mathcal{A}N_1$.

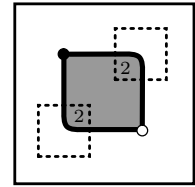
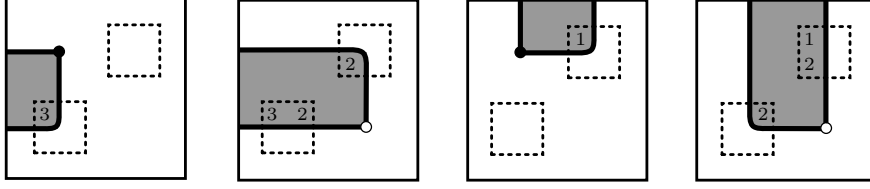


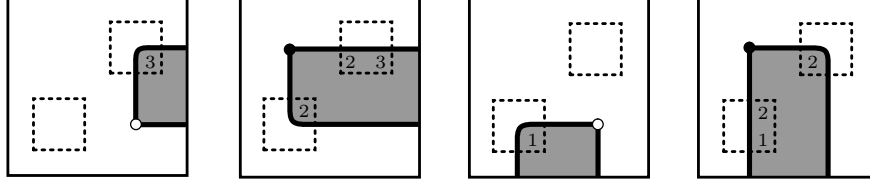
Figure 15. Bigon compatible with $m_2(x_0, \rho_2) = y_0$ and $\delta^1(x_1) = \rho_2 \otimes y_1$.

More generally, consider any immersed bigon D which gives rise to a map between $\tilde{x}_0 \cap \tilde{x}_1$ and $\tilde{y}_0 \cap \tilde{y}_1$ in $\mathcal{C}(\mathfrak{v}_0, \mathfrak{v}_1)$. The boundary of D determines a path from \tilde{x}_0 to \tilde{y}_0 in \mathfrak{v}_0 , and the corner decorations along this path determines an \mathcal{A}_∞ operation from x_0 to y_0 in $N_0^{\mathcal{A}}$. The boundary of

Starting pieces:



Ending pieces:



Connecting pieces:

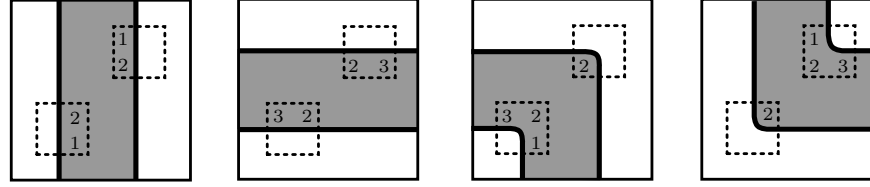


Figure 16. Decomposing a bigon into tiles: Any bigon carried by $(\vartheta_0, \vartheta_1)$ consists of one starting piece, some number of connecting pieces, and one ending piece. Note that any immersed annulus consists of a collection of connecting pieces only, but these have been ruled out by requiring ϑ_1 to be special bounded.

D also determines a path \tilde{x}_1 to \tilde{y}_1 in $D(\vartheta_1)$ and the corner decorations along this path determines a sequence of operations from x_1 to y_1 in $\mathcal{A}N_1$. We will show that these operations always pair in the box tensor product, producing a differential from $x_0 \otimes x_1$ to $y_0 \otimes y_1$. If D is not one of the bigons considered in the preceding paragraphs, then it can be cut along the lattice curves $\{0\} \times [0, 1]$ and $[0, 1] \times \{0\}$ into pieces of the form listed in Figure 16. As illustrated, the corner decorations can be recorded with sequences of the integers 1, 2, and 3; with this notation, each path from $\tilde{x}_0 \cap \tilde{x}_1$ to $\tilde{y}_0 \cap \tilde{y}_1$ determines a sequence in $\{1, 2, 3\}$. To recover a sequence of type D operations from the path in $D(\vartheta_1)$, we break this sequence of integers into increasing subsequences (this is how the integers are already grouped by the division of the bigon into pieces) and interpret, say, the increasing sequence 23 as a ρ_{23} operation. To recover a type A operation from the path in $A(\vartheta_0)$, we also divide the sequence in $\{1, 2, 3\}$ into increasing subsequences which determine the inputs to the type A operation. Consider, for example, the bigon pictured in Figure 17: Both paths determine the sequence 123. The path in $D(\vartheta_1)$ corresponds to the map $\delta^1(x_1) = \rho_{123} \otimes y_1$ while the path in $A(\vartheta_0)$ corresponds to the operation $m_2(x_0, \rho_{123}) = y_0$.

To see that the type A operation determined by a bigon always pairs with the sequence of type D operations determined by that bigon, we simply need to check that the two sequences determined by the corner decorations agree. To see this, start with bigon pieces labeled as in Figure 16. We then slide any 3 label on the ϑ_0 portion of the boundary to the right into the adjacent piece of the bigon, and we slide any 1 label on ϑ_0 upward into the adjacent piece of the bigon. It is clear from Figure 16 that, after this modification in a given bigon, the labeling on both curves is the same within each piece.

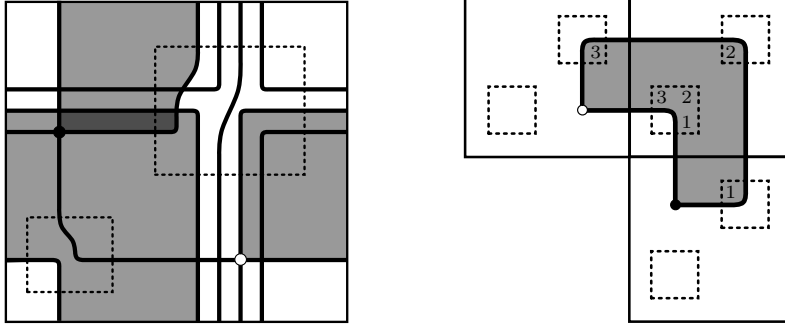


Figure 17. The chain complex arising from -1 surgery on the right-hand trefoil. The shaded region highlights a bigon with edges corresponding to $m_2(x_0, \rho_{123}) = y_0$ and $\delta^1(x_1) = \rho_{123} \otimes y_1$ so that $y_0 \otimes y_1$ is a summand of $\partial^{\boxtimes}(x_0 \otimes x_1)$.

This establishes a bijection between bigons contributing to the linear map d^θ in $\mathcal{C}(\vartheta_0, \vartheta_1)$ and the differential ∂^{\boxtimes} on $N_0^{\mathcal{A}} \boxtimes^{\mathcal{A}} N_1$, completing the proof. \square

3. CLASSIFYING EXTENDABLE TYPE D STRUCTURES

This section proves Theorem 5, our structure theorem for type D structures under the hypothesis that the module in question is extendable. While this is a purely algebraic result, it is of interest in the present context owing to the fact that the three-manifold invariants that we wish to study all satisfy this additional hypothesis; compare Theorem 4. As such, the ultimate outcome of this section will be the existence part of Theorem 1

Broadly, we establish the structure theorem in two steps: First, we give a partial characterization in terms of matrices over the ring $\mathbb{F}[U]/U^2$. And, second, we give a combinatorial algorithm that simplifies the train tracks resulting from this partial characterization.

3.1. Extended type D structures. The torus algebra \mathcal{A} admits an extension, denoted by $\tilde{\mathcal{A}}$, which plays a key role. The algebra $\tilde{\mathcal{A}}$ is a quiver algebra over the quiver shown in Figure 18 with relations $\rho_i \rho_{i-1} = 0$, where the indices are to be interpreted mod 4, along with the relation $\rho_0 \rho_1 \rho_2 \rho_3 \rho_0 = 0$. As a vector space over \mathbb{F} it is spanned by the idempotents ι_0 and ι_1 , along with elements $\rho_I = \rho_{i_1} \rho_{i_2} \cdots \rho_{i_k}$ for each sequence $I = i_1 \dots i_k$ of indices in $\mathbb{Z}/4\mathbb{Z}$ containing at most one 0 such that $i_{j+1} \equiv i_j + 1$ for each j .

The torus algebra may be recovered from $\tilde{\mathcal{A}}$ by setting $\rho_0 = 0$. More precisely, if \mathcal{J} is the ideal generated by ρ_0 then $\mathcal{A} = \tilde{\mathcal{A}}/\mathcal{J}$. As with \mathcal{A} , write $\mathbf{1} = \iota_0 + \iota_1$ and use the convention $\rho_\emptyset = \mathbf{1}$. We distinguish the element $U = \rho_{1230} + \rho_{2301} + \rho_{3012} + \rho_{0123}$ and note that U is central in $\tilde{\mathcal{A}}$.

Definition 17. An *extended type D structure* is an \mathcal{I} module $V = \iota_0 V \oplus \iota_1 V$ equipped with a map $\tilde{\delta}^1 : V \rightarrow \tilde{\mathcal{A}} \otimes_{\mathcal{I}} V$ such that the map $\tilde{\partial} : \tilde{\mathcal{A}} \otimes_{\mathcal{I}} V \rightarrow \tilde{\mathcal{A}} \otimes_{\mathcal{I}} V$ defined by $\tilde{\partial}(a \otimes x) = a \cdot \tilde{\delta}^1 x$ satisfies $\tilde{\partial}^2(x) = Ux$ for all $x \in V$. The module $\tilde{N} = \tilde{\mathcal{A}} \otimes_{\mathcal{I}} V$ is the *extended type D module* associated with V and $\tilde{\delta}^1$.

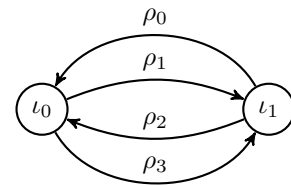


Figure 18. A quiver for the extended torus algebra

Equivalently, \tilde{N} is an extension of N if $\mathcal{A} \otimes_{\tilde{\mathcal{A}}} \tilde{N}$ is isomorphic to N as a differential \mathcal{A} module. In particular, the condition that N has an extension only depends on N and not on the type D

structure we choose to represent it. We say that a type D module N is *extendable* if it has an extension \tilde{N} , and we say that $N = \mathcal{A} \otimes_{\tilde{\mathcal{A}}} \tilde{N}$ is the underlying type D module of N .

We remark that, though it is not clear *a priori*, we will show in Proposition 38 that any two extensions of a type D structure N must be homotopy equivalent. In other words, an extended type D structure contains no more information than its underlying type D structure. Thus the chief advantage to working with extended type D structures is not the extension that we choose, but simply the fact that an extension exists. Being extendable is a rather strong algebraic constraint and, by restricting to extendable modules (as we will do for the rest of the paper), the geometric description of type D modules over \mathcal{A} can be simplified considerably.

3.2. Train tracks and matrices. Just as a type D structure can be represented by a decorated graph, an extended type D structure can be represented by a decorated graph with an extended label set. That is, the decorated graph associated with an extended module has the set of possible edge labels extended to include all sequences $I = i_1 \dots i_k$ of elements of $\mathbb{Z}/4\mathbb{Z}$ with $i_\ell \equiv i_{\ell-1} + 1$ and with at most one $i_\ell = 0$. The method for constructing an (extended) type D structure from a graph is the same. Vertices labeled by \bullet and \circ correspond to ι_0 -generators and ι_1 -generators, respectively, and an arrow labeled by I from x to y contributes a $\rho_I \otimes y$ term to $\tilde{\delta}^1(x)$.

In Section 2 we realized the decorated graph Γ representing a reduced or almost reduced type D structure N geometrically by immersing it in the parametrized torus T . This construction extends immediately to decorated graphs associated with extensions, where the arcs corresponding to the additional edge labels are determined by Figure 19. Note that all edges of the corresponding train track are oriented, but a pair of vertices may be connected by a pair of parallel but oppositely oriented edges; in this case, for convenience, we adopt the convention that the two opposing oriented edges are replaced with a single unoriented edge. For example, consider the type D module in Figure 8; a choice of extension is illustrated in Figure 20 together with the corresponding train track.

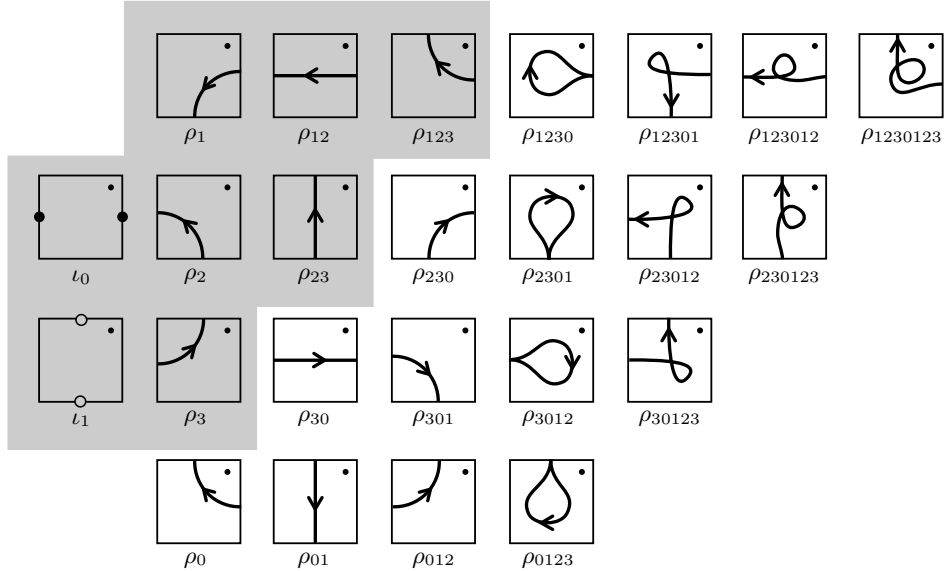


Figure 19. Train track edges corresponding to elements of the extended algebra $\tilde{\mathcal{A}}$. These can also be interpreted as homotopy classes of clockwise moving paths (or constant paths, in the case of ι_0 and ι_1) connecting sides of a square and passing the top right corner at most once, and $\tilde{\mathcal{A}}$ is generated as an \mathbb{F} -vector space by these homotopy classes; algebra multiplication is concatenation of paths, where the product is zero if the concatenation does not exist or passes the top right corner twice. The shaded elements generate \mathcal{A} .

The train tracks constructed in this way have a very particular form; for instance, all switches lie on the curves α and β . We will work with a slightly larger class of train tracks, which we now formalize.

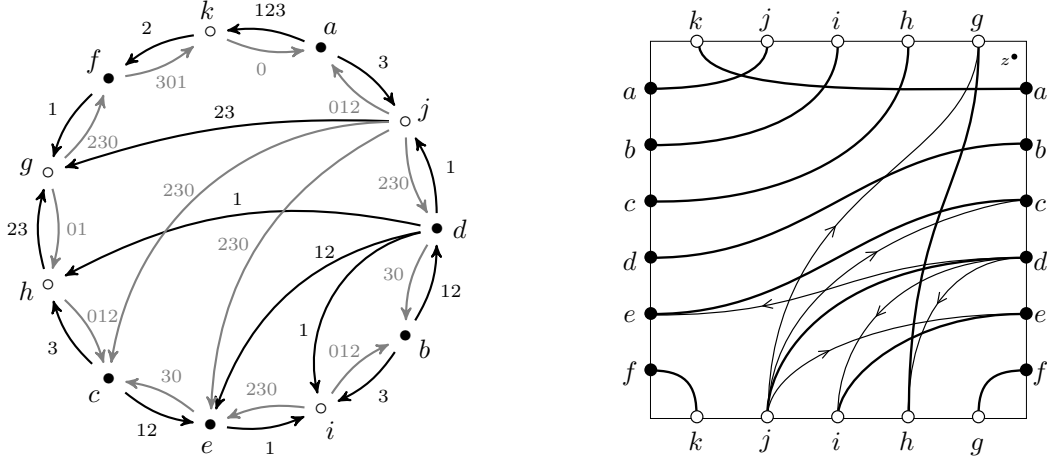


Figure 20. The train track (right) associated with an extended type D structure (left). This extended type D structure is an extension of the type D structure in Figure 8; the extended coefficient maps are shown in gray.

Definition 18. An \mathcal{A} -train track in the marked torus T is an oriented train track ϑ with the following properties: (1) ϑ is disjoint from the basepoint in T and transverse to α and β ; (2) every intersection of ϑ with $\alpha \cup \beta$ is a switch and called *primary switch* of ϑ ; and (3) no oriented path carried by ϑ contains a counterclockwise fishtail (see Figure 21).

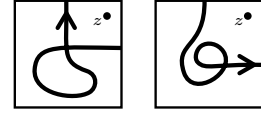


Figure 21. Examples of counterclockwise fishtails. These never appear in an \mathcal{A} -train track.

Given an \mathcal{A} -train track ϑ with n primary switches, we can construct a $2n \times 2n$ matrix M_ϑ encoding the most essential information of ϑ . We cut T open along α and β to form a square, with our usual convention that β is horizontal (oriented rightward), α is vertical (oriented upward), and the basepoint is in the top right corner of the square. The primary switches give $2n$ marked points on the edges of the square, which we label v_1, \dots, v_{2n} clockwise, starting from the top right corner. We let k denote the number of primary switches of ϑ on α , so that v_i is on the right side of the square if $1 \leq i \leq k$, the bottom side if $k + 1 \leq i \leq n$, the left side if $n + 1 \leq i \leq n + k$, and the top side if $n + k + 1 \leq i \leq 2n$. The (i, j) entry of M_ϑ counts immersed oriented paths in ϑ through the square from v_i to v_j . Such a path can be given a label recording to how many times it passes the base point on its left. More precisely, any immersed path through the square can be projected to a path in the boundary of the square by sending each point in the path to the boundary following the path’s leftward pointing normal vector. The assumption that ϑ has no counterclockwise fishtails ensures that this left projection will have net clockwise movement around the boundary. We weight each path by U^m , where m is the number of times (counted with sign) that the left projection passes the top right corner of the square. We set $U^2 = 0$ and count paths modulo 2, so M_ϑ has coefficients in $\mathbb{F}[U]/U^2$.

We will say that two \mathcal{A} -train tracks ϑ_1 and ϑ_2 are *equivalent* if $M_{\vartheta_1} = M_{\vartheta_2}$. An \mathcal{A} -train track ϑ is said to be *reduced* if no immersed oriented paths through the square $T \setminus (\alpha \cup \beta)$ begin and end on the same side of the square unless they are weighted by a positive power of U . An \mathcal{A} -train track ϑ is *valid* if $M_\vartheta^2 = UI_{2n}$, where I_{2n} is the $2n \times 2n$ identity matrix. The significance of these restrictions on train tracks is found in the following proposition:

Proposition 19. *The following are equivalent:*

- (i) *Reduced extended type D structures with a chosen (ordered) set of generators.*
- (ii) *Equivalence classes of valid, reduced \mathcal{A} -train tracks.*
- (iii) *$2n \times 2n$ matrices M over $\mathbb{F}[U]/U^2$, together with an integer $0 \leq k \leq n$, such that $M^2 = UI_{2n}$ and M is strictly block upper triangular modulo U with respect to blocks of size $k, n - k, k,$ and $n - k$.*

Before proving this proposition it is worth pausing to consider a simple example. The pair of \mathcal{A} -train tracks in Figure 22 are equivalent; the reader should construct the associated four-by-four matrix in each case and observe that these are equal, as required. The key feature here is that the additional path in the train track on the right carries the label U^2 , which is set to zero in the matrix. On the other hand, an inequivalent \mathcal{A} -train track is obtained

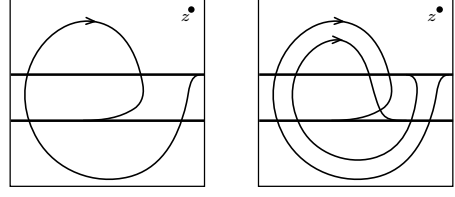


Figure 22. Equivalent valid \mathcal{A} -train tracks.

by considering only the horizontal two-way tracks of this example. Although this train track is inequivalent to the ones given, it represents an isomorphic module. For generators x and y such that $D_{123012}(x) = y$ there is an isomorphism of modules over $\tilde{\mathcal{A}}$ given by $x' = x + \rho_{1230} \otimes y$ and $y' = y$, so that $D_{123012}(x') = 0$. Note that this is an isomorphism between two different choices of extension (of a fixed type D structure) as $\tilde{\mathcal{A}}$ modules but not an isomorphism as \mathbb{F} vector spaces. That is, this train track is weakly equivalent to those of Figure 22 in the sense of Definition 20 below.

Proof of Proposition 19. Any extended type D structure \tilde{N} determines an \mathcal{A} -train track ϑ as described above, and it is immediate from the construction that if \tilde{N} is reduced then so is ϑ . This particular train track determines an equivalence class of train tracks.

Any reduced train track ϑ determines a matrix M_ϑ as described above. This is a $2n \times 2n$ matrix, where each row or column corresponds to primary switches on the boundary of the square $T \setminus (\alpha \cup \beta)$. These may be split into blocks according to which side each primary switch is on. The fact that paths in ϑ have net clockwise rotation ensures that any path labelled by 1 contributes to an entry above the diagonal in M_ϑ ; the fact that ϑ is reduced further ensures that no 1 appears in the blocks along the diagonal of M_ϑ .

Let x be an ι_0 generator of \tilde{N} , and let v_i and v_j be the marked points on the right and left side of the square $T \setminus (\alpha \cup \beta)$ corresponding to x . The terms of $\tilde{\delta}^2(x) = \rho_{1230} \otimes x + \rho_{3012} \otimes x$ are counted by the i and j rows of M_ϑ^2 , with the row determined by the start of the Reeb chord in that term. These two terms correspond to entries $(M_\vartheta^2)_{ii} = U$ and $(M_\vartheta^2)_{jj} = U$, respectively. Since there are no other terms in $\tilde{\delta}^2(x)$, there are no other nonzero entries in the i th or j th row of M_ϑ^2 (recall that matrix entries are taken modulo U^2). If x is instead an ι_1 generator of \tilde{N} , let v_i and v_j be the corresponding points on the bottom and top side of the square, respectively. The $\rho_{2301} \otimes x$ term in $\partial^2(x)$ corresponds to the entry $(M_\vartheta^2)_{ii} = U$, while the $\rho_{0123} \otimes x$ term corresponds to the entry $(M_\vartheta^2)_{jj} = U$, and there are no other nonzero entries (modulo U^2) in the i and j rows. Thus the $\tilde{\delta}^2(x) = Ux$ condition for an extended module implies that $M_\vartheta^2 = UI_{2n}$, which by definition means that ϑ is valid.

Finally, the extended type D module \tilde{N} can be extracted from the corresponding matrix M_ϑ , together with the integer k , as follows: $\iota_0 \tilde{N}$ has generators x_1, \dots, x_k and $\iota_1 \tilde{N}$ has generators x_{k+1}, \dots, x_n . Each generator x_i corresponds to a pair of indices i and $t(i)$, where

$$t(i) = \begin{cases} n + k + 1 - i & \text{if } i \leq k \\ 2n + k - i + 1 & \text{if } i > k. \end{cases}$$

An entry in the j or $t(j)$ column and the i or $t(i)$ row of M_ϑ contributes an x_j term to the coefficient map $D_I(x_i)$, where I is determined by the position in the matrix with respect to the block decomposition $M_\vartheta = M_\vartheta^1 + M_\vartheta^U$ (as described in (1), above). \square

The block decomposition on a matrix M_ϑ can be understood in terms of the coefficient maps for the corresponding extended type D structure. First, recall that a reduced type D structure may be specified by its coefficient maps $D_I: \iota_i V \rightarrow \iota_j V$ where $I \in \{1, 2, 3, 12, 23, 123\}$. In the same way, an extended type D structure has coefficient maps corresponding to the associated extended set of subscripts. Indeed, an ordinary type D module N has an extension \tilde{N} if \tilde{N} is an extended type D

module whose coefficient maps agree with those of N for $I \in \{1, 2, 3, 12, 23, 123\}$. These coefficient maps appear from a block decomposition of $M_{\mathfrak{g}}$. Precisely, write $M_{\mathfrak{g}} = M_{\mathfrak{g}}^1 + M_{\mathfrak{g}}^U$ where $M_{\mathfrak{g}}^1$ has entries that are 1 or 0 while $M_{\mathfrak{g}}^U$ has entries that are U or 0. Then there are block decompositions

$$(1) \quad M_{\mathfrak{g}}^1 = \left[\begin{array}{c|c|c|c} 0 & D_1 & D_{12} & D_{123} \\ \hline 0 & 0 & D_2 & D_{23} \\ \hline 0 & 0 & 0 & D_3 \\ \hline 0 & 0 & 0 & 0 \end{array} \right] \quad \text{and} \quad M_{\mathfrak{g}}^U = \left[\begin{array}{c|c|c|c} D_{1230} & D_{12301} & D_{123012} & D_{1230123} \\ \hline D_{230} & D_{2301} & D_{23012} & D_{230123} \\ \hline D_{30} & D_{301} & D_{3012} & D_{30123} \\ \hline D_0 & D_{01} & D_{012} & D_{0123} \end{array} \right]$$

with respect to blocks of size k , $n - k$, k , and $n - k$.

To restrict an extended type D module \tilde{N} to its underlying type D module N , we simply set $\rho_0 = 0$ in the algebra, and thus ignore all coefficient maps D_I for which I contains 0. It is clear that the analogous operation for the corresponding matrix is setting $U = 0$ (namely, setting $M_{\mathfrak{g}}^U = 0$ in $M_{\mathfrak{g}} = M_{\mathfrak{g}}^1 + M_{\mathfrak{g}}^U$), resulting in a matrix with coefficients in \mathbb{F} . This motivates the following definitions:

Definition 20. An \mathcal{A} -train track \mathfrak{g} is *weakly valid* if the corresponding matrix $M_{\mathfrak{g}}$ squares to 0 modulo U . Two \mathcal{A} train tracks \mathfrak{g}_1 and \mathfrak{g}_2 are *weakly equivalent* if the matrices $M_{\mathfrak{g}_1}$ and $M_{\mathfrak{g}_2}$ agree modulo U .

The following equivalence is immediate from that of Proposition 19.

Proposition 21. *The following are equivalent:*

- (i) *Reduced type D structures over \mathcal{A} , up to isomorphism as \mathbb{F} vector spaces, with a chosen (ordered) set of generators.*
- (ii) *Weak equivalence classes of weakly valid, reduced \mathcal{A} train tracks.*
- (ii) *$2n \times 2n$ matrices M over \mathbb{F} , together with an integer $0 \leq k \leq n$, such that $M^2 = 0$ and M is strictly block upper triangular with respect to blocks of size k , $n - k$, k , and $n - k$. \square*

Although we are mostly interested in reduced train tracks, we observe that we can define valid almost reduced train tracks as those which correspond to almost reduced type D structures over \mathcal{A} .

We pause briefly to discuss pairing of \mathcal{A} -train tracks, which is defined just as in Section 2.5. A pair $(\mathfrak{g}_0, \mathfrak{g}_1)$ is admissible if there are no immersed annuli cobounded by $A(\mathfrak{g}_0)$ and $D(\mathfrak{g}_1)$, where $A(\mathfrak{g})$ denotes the result of including \mathfrak{g} into the first quadrant and extending vertically/horizontally and $D(\mathfrak{g})$ is the reflection of $A(\mathfrak{g})$ across the anti-diagonal. $\mathcal{C}(\mathfrak{g}_0, \mathfrak{g}_1)$ is the vector space generated by intersection points of $A(\mathfrak{g}_0)$ and $D(\mathfrak{g}_1)$, equipped with a linear map $d^{\mathfrak{g}}$ which counts bigons not covering the basepoint with boundary carried by the pair $(\mathfrak{g}_0, \mathfrak{g}_1)$, with the requirement that both sides of the bigon are oriented paths from the initial intersection point to the terminal intersection point. Note that the orientation requirement is meaningful for an arbitrary \mathcal{A} -train track, unlike for those described in Section 2. Defining $\mathcal{C}(\mathfrak{g}_0, \mathfrak{g}_1)$ does not require all the information in \mathfrak{g}_1 and \mathfrak{g}_2 , it is in fact determined only by their weak equivalence classes.

Proposition 22. *Let $\mathfrak{g}_0, \mathfrak{g}'_0$ be reduced train tracks and $\mathfrak{g}_1, \mathfrak{g}'_1$ be almost reduced train tracks such that the pairs $(\mathfrak{g}_0, \mathfrak{g}_1)$ and $(\mathfrak{g}'_0, \mathfrak{g}'_1)$ are admissible. If \mathfrak{g}_0 is weakly equivalent to \mathfrak{g}'_0 and \mathfrak{g}_1 is weakly equivalent to \mathfrak{g}'_1 , then $\mathcal{C}(\mathfrak{g}_0, \mathfrak{g}_1) = \mathcal{C}(\mathfrak{g}'_0, \mathfrak{g}'_1)$.*

Proof. Note that to count bigons connecting two intersection points, one only needs to know the count of paths connecting each pair of primary vertices in each train track. The orientation requirement implies that we can ignore any path in \mathfrak{g}_0 or \mathfrak{g}_1 which has the puncture on the left side of the path; these are precisely the paths weighted by U in $M_{\mathfrak{g}_1}$ and $M_{\mathfrak{g}_1}$. Thus the map $d^{\mathfrak{g}}$ is determined by the weak equivalence class of \mathfrak{g}_1 and \mathfrak{g}_2 . \square

Note that under the hypotheses above d^ϑ is a differential, making $\mathcal{C}(\vartheta_0, \vartheta_1)$ a chain complex. Indeed, if ϑ_0 and ϑ_1 correspond to type D structures N_0 and N_1 , respectively, it follows from Theorem 16 that $\mathcal{C}(\vartheta_0, \vartheta_1)$ is isomorphic as a chain complex to $N_0^A \boxtimes N_1$.

3.3. Simplifying valid train tracks. Consider our running example and the train track in Figure 20. We observe that this train track has two special properties. First, there are exactly two unoriented edges, one from each direction, incident to each switch. It follows that if the oriented edges are ignored, the unoriented edges form a collection of immersed curves. Second, the extra unoriented edges can be grouped in pairs, where each pair connects the same two sections of the immersed curve, oriented the same way but turning opposite directions at each end and crossing once. We can slide the endpoints of each pair of oriented segments near each other along the unoriented segments, without changing the equivalence class of the train track, as shown in Figure 23(a). The resulting X shaped pairs of oriented arrows will be called *crossover arrows*, and to simplify diagrams these pairs will be replaced by a bold arrow (Figure 23(b)).

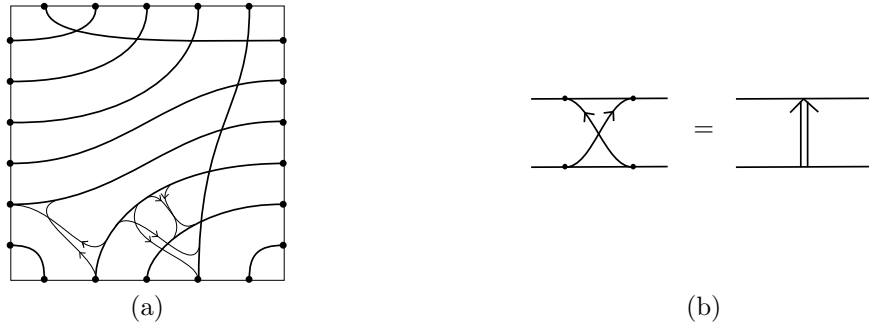


Figure 23. (a) The train track from Figure 20 homotoped so that the unoriented edges form crossover arrows. (b) Diagrammatic shorthand for crossover arrows.

The goal of the present subsection is to prove that these features are not unique to this example, but indeed hold for (some representative of) every equivalence class of valid reduced train tracks.

Proposition 23. *Any valid reduced \mathcal{A} -train track is equivalent to a train track ϑ with the following form:*

- Every switch of ϑ has exactly one unoriented edge on each side, so that ϑ is a collection of (unoriented) immersed curves along with additional oriented edges connecting points on the immersed curves;
- the immersed curves restrict to horizontal and vertical segments outside of the square $[\frac{1}{4}, \frac{3}{4}] \times [\frac{1}{4}, \frac{3}{4}]$, which we call the corner box;
- within the corner box, the immersed curves restrict to embedded arcs which connect different sides of the corner box;
- the oriented edges appear in pairs which form crossover arrows (as in Figure 23);
- the crossover arrows appear outside the corner box, and they move clockwise around the corner box.

Conversely, any train track of this form is a valid, reduced type D train track.

See Figure 26(c) for an example of a train track of this form.

Before proving Proposition 23, we review some linear algebra of matrices over $\mathbb{F}[U]/U^2$. Any invertible matrix over $\mathbb{F}[U]/U^2$ can be written as the product of elementary matrices of the following

$\{\iota_0, \dots, \iota_{m-1}\}$ placed on the boundary of the disk and m edges $\{\rho_0, \dots, \rho_{m-1}\}$ oriented clockwise along the boundary. Assuming the marked point is sufficiently close to the boundary of the disk, this point singles out the edge ρ_0 . (Take as the target of ρ_i the point i .) We follow the usual convention of writing ρ_I for the product associated with a cyclically-ordered string I from $\{1, 2, \dots, m-1, 0\}$. The path algebra of this quiver determines two algebras that are of interest to us: $\tilde{\mathcal{B}}$ is the result of quotienting by $\rho_I = 0$ for any string I containing more than one 0 (where $U = \sum_{|I|=m} \rho_I$), while \mathcal{B} is the result of quotienting by $\rho_I = 0$ for any string I containing a single 0. Clearly, when $m = 4$, there is close relationship between \mathcal{A} and \mathcal{B} (similarly, $\tilde{\mathcal{A}}$ and $\tilde{\mathcal{B}}$) which comes from attaching handles to form a punctured torus and identifying idempotents $\iota_\bullet = \iota_0 = \iota_2$ and $\iota_\circ = \iota_1 = \iota_3$. More generally, for $m = 4g$ and a specified handle attachment, we can define an algebra associated with a genus g surface (this is the one-moving-strand algebra; see [25]). The algebra, from this point of view, is built up as follows. Let ι_i and ι_j be idempotents of \mathcal{B} corresponding to points $i < j$ in the boundary of the disk. Adding a 1-handle $[-\epsilon, \epsilon] \times I$ to the disk so that $(0, 0)$ is identified with i and $(0, 1)$ is identified with j gives rise to a modified quiver and a new algebra $\mathcal{B}/\mathcal{I}_h$, where the ideal \mathcal{I}_h is determined by the handle attachment setting $\iota_i = \iota_j$, $\rho_i \rho_{j+1} = 0$, and $\rho_j \rho_{i+1} = 0$. In words: the relevant idempotents are identified in the quotient, while any and all possible *new* paths created are set to zero. Notice that these account for the familiar $\rho_3 \rho_2 = \rho_2 \rho_1 = 0$ in the definition of \mathcal{A} from Section 2.1, having made two handle attachments. The one-moving-strand algebra is obtained after $2g$ handles have been attached, though we remark that ensuring a once-punctured surface is obtained requires some additional restrictions on the handle attachments. (The reader may recognize the geometric significance of the idempotent subring in general: the Grothendieck group of the appropriate associated category of modules is completely determined by this ring; see [21].) An identical construction can be carried out for $\tilde{\mathcal{B}}$.

In the same way, we can work with other surfaces F admitting a prescribed (finite) 0- and 1- handle decomposition, whenever each 0-handle carries a marked point (i.e. there is a distinguished ρ_0 for each 0-handle). We begin with the algebra $\bigoplus_{i=1}^n \mathcal{B}^i$ associated with the collection of 0-handles, and for each 1-handle attachment identifying $\iota_i^a \in \mathcal{B}^a$ with $\iota_i^b \in \mathcal{B}^b$ we set $\bigoplus_{i=1}^n \mathcal{B}^i / \mathcal{I}_h$ where the quotient sets $\iota_i^a = \iota_i^b$, $\rho_i^a \rho_{j+1}^b$, and $\rho_j^b \rho_i^a$ (as in the case of a single 0-handle). Having attached all of the handles in the description of F , and appropriately quotienting the associated algebra for each, we arrive at an algebra \mathcal{A}_F (see Figure 25 for an explicit example). A similar construction gives $\tilde{\mathcal{A}}_F$, and when F is a once-punctured torus we drop it from the notation, recovering \mathcal{A} and $\tilde{\mathcal{A}}$ as usual.

Now a type D structure over \mathcal{B} may be defined as in Section 2.1, given a vector space V together with a left-action of the idempotent subring $\mathcal{I}(\mathcal{B})$. These have extensions (to modules over $\tilde{\mathcal{B}}$) and \mathcal{B} train tracks defined analogously; an example is shown in Figure 24 (where, as usual, two-way track segments are recorded as unoriented edges). As such, in this setting, the type D structure and a choice of extension for it can be represented by a matrix M over $\mathbb{F}[U]/U^2$ satisfying the hypotheses of Lemma 24, and hence may be expressed as $M = P\bar{M}P^{-1}$ where P is composition of elementary matrices of the form $A_{i,j}^U$ or of the form $A_{i,j}$ with $i < j$. This new form may be interpreted in terms of the associated \mathcal{B} train tracks as follows: Up to equivalence, all train tracks for which $M^2 = UI_{2n}$ can be represented by (1) a collection of unoriented track segments connecting primary switches in the boundary of the disk; and (2) a collection of clockwise-moving crossover arrows confined to a small collar neighborhood of the boundary of the disk. To see this, let c_i denote the arc segment across the collar neighborhood of the boundary corresponding to a generator/vertex x_i , for each i . Suppose we modify ϑ by adding a crossover arrow from c_i to c_j within the collar neighborhood, obtaining a new train track ϑ' . For each corner path from x_j to x_ℓ , we have added a new corner path from x_i to x_ℓ , and for each corner path from x_ℓ to x_i we have added a corner path from x_ℓ to x_j . If the crossover arrow does not pass the basepoint, $M_{\vartheta'}$

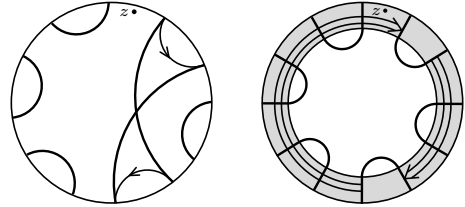


Figure 24. Equivalent train tracks in the marked disk, according to Lemma 24.

is obtained from $M_{\mathfrak{g}}$ by adding the i th column to the j th column and adding the j th row to the i th row; that is by conjugating with $A_{i,j}$. If the crossover arrow moves clockwise and passes the basepoint once, then the new corner paths are weighted with an extra U and $M_{\mathfrak{g}'}$ is obtained from $M_{\mathfrak{g}}$ by conjugating with $A_{i,j}^U$. For the example in Figure 24, the reader can check that conjugation by $A_{6,1}^U A_{2,5}$ does the trick (where determining M and \bar{M} is left as an exercise).

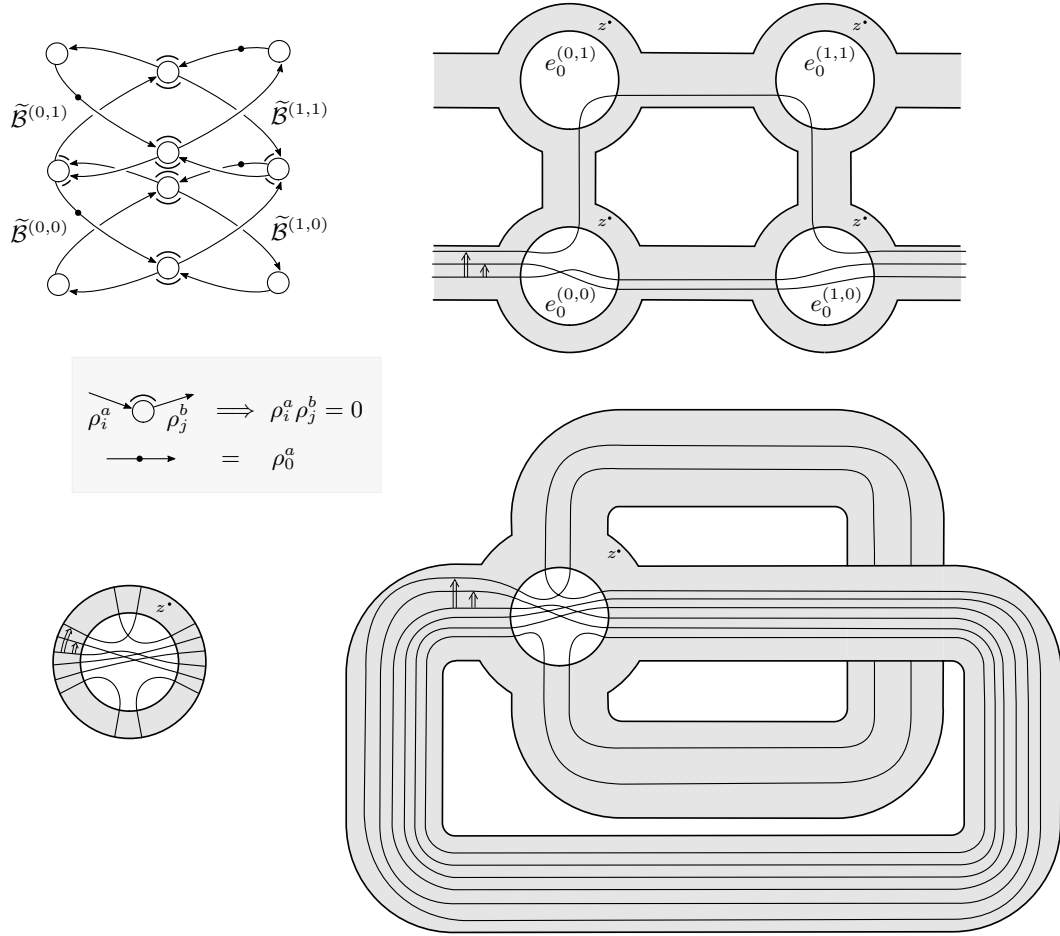
More generally, given a surface F described in terms of a finite number of 0- and 1-handles, we can first describe a type D structure over $\bigoplus_{i=1}^n \mathcal{B}^i$: the underlying vector space $\bigoplus_{i=1}^n V^i$ has left-action by the idempotents $\mathcal{I}(\bigoplus_{i=1}^n \mathcal{B}^i) = \bigoplus_{i=1}^n \mathcal{I}(\mathcal{B}^i)$ so that V^i is a type D structure associated with the i th 0-handle. The essential observation is that any quotient identifying $\iota_i^a V^a = \iota_j^b V^b$ is compatible with a left-action of the idempotents $\mathcal{I}(\bigoplus_{i=1}^n \mathcal{B}^i / \mathcal{I}_h)$, and hence gives a well-defined type D structure over $\bigoplus_{i=1}^n \mathcal{B}^i / \mathcal{I}_h$. Notice that the matrices M^i describing this type D structure are data that remains associated with the 0-handles in the decomposition of F . In particular, while the type D structures change (the underlying vector space changes, as well as the algebra), the M_i are unchanged at every stage. We emphasise that, in the course of this construction, the relevant type D structures are *not* obtained by a sequence of quotients as differential modules, rather, the vector spaces are quotiented in a way compatible with an idempotent quotient of the algebra. Geometrically, the relevant train tracks extend over the 1-handles as parallel lines connecting the relevant generators in the quotient; see Figure 25. This is the key observation required in order to establish Theorem 33, below, treating type D structures associated with general surfaces.

3.5. The proof of Proposition 23. Let \mathfrak{g}' be a valid reduced \mathcal{A} -train track and let $M = M_{\mathfrak{g}'}$ be the corresponding matrix. Set $\bar{M} = PMP^{-1}$ as in Lemma 24; the matrix \bar{M} corresponds to an extended type D structure, from which we can construct an \mathcal{A} -train track $\bar{\mathfrak{g}}$. To construct $\bar{\mathfrak{g}}$, let $\bar{\mathfrak{g}}$ have the same primary vertices as \mathfrak{g} , labelled x_1, \dots, x_{2n} as described above, and add oriented corner edges from x_i to x_j if the (i, j) entry of \bar{M} is nonzero. The form of \bar{M} implies that there will be exactly one incoming and one outgoing corner edge at each primary vertex, and that for each corner edge from x_i to x_j there is an oppositely oriented edge from x_j to x_i . Replacing the pairs of oppositely oriented corner edges with single unoriented corner edges as usual, observe that there is exactly one unoriented corner edge at each primary vertex. It follows that $\bar{\mathfrak{g}}$ is an immersed multicurve.

We observed that M is obtained from \bar{M} by conjugating with a sequence of elementary matrices of the form $A_{i,j}$ with $i < j$ or $A_{i,j}^U$. Each conjugation corresponds to adding a crossover arrow to $\bar{\mathfrak{g}}$ near the boundary of the square (i.e. the disk to which handles are attached). That is, adding the appropriate sequence of crossover arrows to $\bar{\mathfrak{g}}$ produces a train track \mathfrak{g} whose corresponding matrix is M . Since we only use type $A_{i,j}$ matrices if $i < j$, all the crossover arrows added move clockwise. Up to regular homotopy, we can assume that $\bar{\mathfrak{g}}$ is horizontal or vertical outside of the corner box $[\frac{1}{4}, \frac{3}{4}] \times [\frac{1}{4}, \frac{3}{4}]$ and that the crossover arrows added lie outside the corner box. Since \mathfrak{g} is reduced, the arcs within the corner box connect different sides of the square. Thus \mathfrak{g} has the form claimed and \mathfrak{g} is equivalent to \mathfrak{g}' since the matrix associated to each is M .

Conversely, given any train track \mathfrak{g} of this form, there is a reduced train track $\bar{\mathfrak{g}}$ obtained by removing the crossover arrows. $\bar{\mathfrak{g}}$ is clearly valid and $M_{\mathfrak{g}}$ is obtained from $M_{\bar{\mathfrak{g}}}$ by conjugating with elementary matrices, which preserves the property that the matrix squares to UI_{2n} . It follows that \mathfrak{g} is valid as well as reduced. \square

3.6. Crossover arrow calculus. In practice, any track representing an extended type D structure can be modified to a train track of the form given in Proposition 23 using regular homotopies together with some local geometric moves; this is often easier than the matrix manipulations described above. First, after replacing pairs of oppositely oriented corner edges with unoriented edges, the ∂^2 condition implies that there is an odd number of unoriented corner edges leaving each side of each primary switch. Typically, there will be exactly one at each side of each vertex and the train track will



$$\begin{array}{l}
 \begin{array}{c} \rho_i^a \curvearrowright \rho_j^b \\ \longrightarrow \end{array} \implies \rho_i^a \rho_j^b = 0 \\
 \begin{array}{c} \longrightarrow \\ \bullet \longrightarrow \end{array} = \rho_0^a
 \end{array}$$

Figure 25. Three (related) extended type D structures: over $\tilde{\mathcal{B}}$ (lower left) where $m = 4$ has been omitted from the notation; over $\tilde{\mathcal{A}}$ (lower right); and over the algebra described by the quiver in the top left (upper right). The associated surface in this last example is made up of four 0-handles and six 1-handles (it should be viewed in the cylinder $S^1 \times \mathbb{R}$), and each 1-handle attachment gives rise to a quotient of the algebra $\tilde{\mathcal{B}}^{(0,0)} \oplus \tilde{\mathcal{B}}^{(1,0)} \oplus \tilde{\mathcal{B}}^{(0,1)} \oplus \tilde{\mathcal{B}}^{(1,1)}$ (as described by the key in the shaded box). This last example covers the example associated with the torus. The reader can check that the matrices underlying the first two examples are identical, while the last example requires 4 matrices (one for each 0-handle).

immediately have the form of an immersed multicurve along with some additional corner edges (see Figure 20); if this is not the case it can be achieved by a change of basis in the (extended) type D structure. We then slide the additional unoriented corner edges along the immersed curve part of the train track, allowing regular homotopies which do not change the underlying train track. Homotopies which slide ends of corner edges past each other are also allowed, with the condition that sliding the terminal end of one edge past the initial end of another edge introduces a new edge, the composition of the two. These moves preserve the equivalence class of the type D train track. In this way, the unoriented corner edges can be grouped into crossover arrows. For example, the naive train track in Figure 20 is regular homotopic to the train track in Figure 26(a).

We now have a train track with the form of an immersed multicurve along with crossover arrows. We are allowed to slide arrows along the multicurve within the square without changing the equivalence class of the train track, as long as ends of arrows do not slide past each other. Moreover, the local moves shown in Figure 27 produce equivalent train tracks. To see this, note that the mod 2 count of oriented paths between any pair of endpoints is the same on both sides of each replacement. Making use of these local moves, we can push all crossover arrows out of the corner box and further ensure

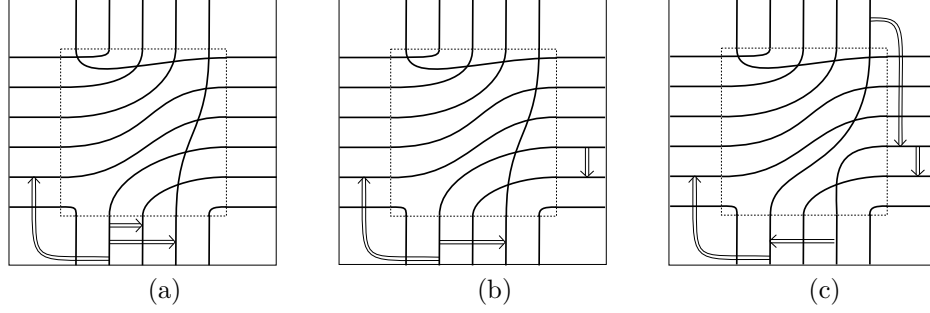


Figure 26. (a) A train track equivalent to the one in Figure 23, after a slight homotopy. This has the form specified in Proposition 23 except that two crossover arrows move counterclockwise. (b) The innermost counterclockwise arrow can be replaced by a clockwise arrow by pushing it through the corner region. (c) The remaining counterclockwise arrow can be replaced with two clockwise arrows by pushing through the corner region and resolving a crossing. Note that this train track is in the form guaranteed by Proposition 23.

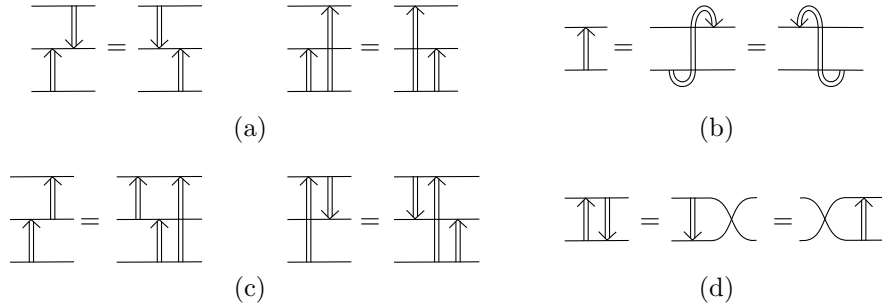


Figure 27. Local moves of crossover arrows which produce equivalent train tracks: (a) beginnings or ends of arrows slide past each other freely; (b) U-turns can be added at the start and end of an arrow if they turn opposite directions; (c) if the start of one arrow slides past the end of another arrow, we add a new arrow which is the composition of the two; (d) opposing arrows can be replaced with one arrow and a crossing.

that they all move clockwise, resulting in a train track satisfying the form in Proposition 23 (see Figure 26(b)-(c)).

Having arrived at the form predicted by Proposition 23, we will make use of two additional moves to modify the train tracks:

- (M1) add or remove a clockwise crossover arrow (near the boundary of the zero-handle) that passes at least one corner;
- (M2) slide a crossover arrow over a one handle.

In contrast with the local moves described in Figure 27, the moves (M1) and (M2) change the equivalence class of the train track. However, these moves induce isomorphisms between the associated extended type D structures.

Proposition 25. *Suppose ϑ' is obtained from ϑ by an application of a sequence of the moves (M1) and (M2) together with the local moves depicted in Figure 27. If \tilde{N}' and \tilde{N} are the extended type D structures associated with ϑ' and ϑ , respectively, then there is an isomorphism $\tilde{N}' \cong \tilde{N}$ as $\tilde{\mathcal{A}}$ modules.*

Proof. As observed, all local moves produce equivalent train tracks, and hence equality on the associated extended type D structures. To prove the proposition then, we need to establish changes of basis for each of the moves (M1) and (M2) that induce the desired isomorphisms.

Suppose first that ϑ' is obtained from ϑ by an application of (M1), removing a crossover arrow from horizontal or vertical edge representing a generator x of \tilde{N} to an edge representing a generator y . We claim that \tilde{N}' is related to \tilde{N} by the change of basis replacing x with $x + \rho_I \otimes y$, where I is the sequence of corners passed by the crossover arrow being removed.

Consider the case where x has idempotent ι_0 , y has idempotent ι_1 , and we add a crossover arrow from the left end of the horizontal segment corresponding to x , which we will call v_x , to the top end of the vertical segment corresponding to y , which we will call v_y (other cases of clockwise arrows are similar). Adding the crossover arrow adds a new corner path starting at v_x for each corner path starting at v_y , and a new corner path ending at v_y for each one ending at v_x . The corner paths starting at v_y correspond to $\rho_I \otimes z$ terms in $\tilde{\partial}(y)$ where the sequence I begins with 2. The new corner paths starting from v_x pass one extra corner, so they correspond to terms $(\rho_1 \rho_I) \otimes z$ in $\tilde{\partial}(x)$. In other words, we add $\rho_1 \tilde{\partial}(y)$ to $\tilde{\partial}(x)$ (note that multiplying $\tilde{\partial}(y)$ on the left by ρ_1 picks out exactly the terms for which the Reeb chord interval starts with 2). Similarly, each corner path ending at v_x corresponds to a term $\rho_I \otimes x$ in $\tilde{\partial}(z)$ for some z and some I ending in 0, and for each the new corner path added corresponds to a $(\rho_I \rho_1) \otimes y$ term in $\tilde{\partial}(z)$. This is precisely the effect of the change of basis (over $\tilde{\mathcal{A}}$) replacing x with $x + \rho_1 \otimes y$.

Now suppose that ϑ' is obtained from ϑ by an application of (M2), where the crossover arrows slides between two horizontal or two vertical edges representing generators x and y of \tilde{N} and the crossover arrow is oriented from the edge representing x to the edge representing y . In this setting, we claim that \tilde{N}' is obtained from \tilde{N} by the change of basis that replaces x with $x + y$.

Consider an \mathcal{A} -train track ϑ with associated extended type D structure \tilde{N} . Let x and y be generators of \tilde{N} , and suppose that x and y both have idempotent ι_0 (the case where x and y both have idempotent ι_1 is identical). Let v_{i_x} and v_{j_x} be the marked points on the right and left boundary, respectively, of the square $T \setminus (\alpha \cup \beta)$, and let v_{i_y} and v_{j_y} be marked points on the right and left boundary of the square associated to y . Suppose ϑ' is obtained by connecting the horizontal segments by crossover arrows at each end, one from v_{i_x} to v_{i_y} and one from v_{j_x} to v_{j_y} ; note that this is equivalent to move (M2), since we could equivalently add two cancelling arrows at one end of the horizontal strands and then slide one to the other end. The effect of this move on M_ϑ is conjugation by $A_{i_x, i_y} A_{j_x, j_y}$. For each corner path out of v_{i_y} or v_{j_y} we add the corresponding corner path out of v_{i_x} or v_{j_x} , and for each corner path into v_{i_x} or v_{j_x} we add the corresponding corner path into v_{i_y} or v_{j_y} . Each corner path out of v_{i_y} or v_{j_y} corresponds to a term z in $D_I(y)$ for some $I \in \{1, 2, 3, 12, 23, 123\}$, and the new corner path added corresponds to the same term in $D_I(x)$. Thus we add each term in $\partial(y)$ to $\partial(x)$. Each corner path into v_{i_x} or v_{j_x} corresponds to an x term in $D_I(z)$ for some generator in z and some $I \in \{1, 2, 3, 12, 23, 123\}$, so for each such term we add the term y to $D_I(z)$. This is exactly the effect of the change of basis on \tilde{N} which replaces x with $x + y$. This shows that move (M2) corresponds to a change of basis in the extended the D structure \tilde{N} , as claimed. \square

Remark 26. We note that the move (M1), along with the local moves, apply in precisely the same way to \mathcal{B} train tracks. As such, it follows that the train tracks produced by Proposition 23 can typically be immediately simplified by removing all arrows that pass at least one corner (consider, for example, the resulting simplification on Figure 24 which removes both arrows). In view of Proposition 25, we will liberally drop such arrows in the sequel without explicit reference to the change of basis required. On the other hand, since the move (M2) requires an identification of idempotents (corresponding to handle attachments), this change only makes sense for \mathcal{A} train tracks. Taken together, however, the reader will note that all of the forgoing applies to arbitrary punctured surfaces (having fixed a handle decomposition), and not simply the punctured torus.

With these observations in place, our goal is to simplify a given \mathcal{A} -train track and produce an immersed curve. This is achieved by systematically removing all of the crossover arrows, and we

give an algorithm that does this in the next section. In practice this is easy to carry out by hand, and towards motivating the algorithm we will expand on this assertion somewhat.

Definition 27. A curve (or curve segment) γ' is carried by γ if $\gamma' \subset \gamma \times [-\epsilon, \epsilon]$ for arbitrarily small values of $\epsilon > 0$. If γ_1 and γ_2 are simultaneously carried by γ then we call γ_1 and γ_2 parallel.

Note that this definition allows for both a local and global notion of parallel curves. A collection of curves may run parallel for some length before diverging; in this case the parallel segments are carried by a curve segment γ . We say the segments lie on parallel curves if they remain parallel when extended arbitrarily in either direction; in this case, the collection of curves is carried by a closed curve γ . Note also that two (locally) parallel segments may lie on the same immersed curve in the torus, and these can also be parallel in the global sense. This happens when the immersed curve is $\gamma_1 \cup \dots \cup \gamma_n$, where each γ_i is a segment parallel to a carrying curve γ ; in other words the immersed curve wraps around γ n times. In this case, we will still say that the parallel segments lie on parallel curves (even though they in fact lie on different parts of the same self-parallel curve). Now consider an \mathcal{A} -train track and choose a given crossover arrow between two parallel track segments. There are two cases to consider: the segments are only locally parallel (that is, they eventually diverge in each direction), or they lie on parallel curves. When the former occurs, we can push the chosen arrow to the point where the tracks diverge using the moves in the previous section; note that this may involve several applications of (M2). The result is an arrow which connects two diverging strands; that is, which passes a corner. If it is clockwise moving, the arrow can be removed using (M2); if not, we slide the arrow between the parallel segments in the opposite direction until they diverge and again remove it if it runs clockwise. If the arrow is counterclockwise on both ends, then there must be (and odd number of) crossings between the parallel segments (see Figure 28); resolving a crossing using the local move in Figure 27(d) results in two arrows which can both be removed when pushed until the strands diverge. In this way, any given arrow can be removed using the moves (M1), (M2), and the local moves in Figure 27, unless the arrow connects parallel curves.

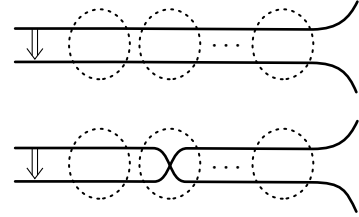


Figure 28. A schematic for pushing an arrow through the zero handle past and even (top) or an odd (bottom) number of crossings.

The key potential issue here is that removing any given arrow may involve sliding past others and thus create more arrows. We need to control the number of new arrows added to ensure that the process of removing arrows one at a time eventually terminates. To deal with this, we introduce a bookkeeping tool in the form of a weight system for arrows, which measure how far an arrow needs to be pushed before the strands diverge. The strategy is to deal with the easiest to remove arrows (i.e. those with smallest weights) first. These weights will be infinite for crossover arrows connecting (globally) parallel curves, and we will show that there is an inductive algorithm that, at each step, increases the smallest weight (taken over all arrows) by one while controlling the number of arrows added in the process. By compactness of the underlying curves, after a finite number of steps the only remaining arrows can be weighted by ∞ . Figure 29 shows the outcome of this process applied to the train track in Figure 26(c). Note that when performing this procedure by hand, it may not be necessary to explicitly specify this weight system.

3.7. Arrow sliding algorithm. Having reduced a given \mathcal{A} -train track to a configuration of curves and crossover arrows via Proposition 23, the aim of this section is to show that all crossover arrows can be eliminated unless they connect parallel curves. Recall that two parallel curve segments may be members of the same curve; see Definition 27 and compare Figure 29.

It will now be useful to make explicit the handle decomposition associated with the punctured torus T , in which the corner box corresponds to a 0-handle; see Figure 30. The corner box contains an arbitrary configuration of embedded arcs (possibly intersecting one another). Boxes σ_\bullet and σ_\circ are permutation boxes; they contain a braid-like immersed curve diagram. The boxes labeled A are

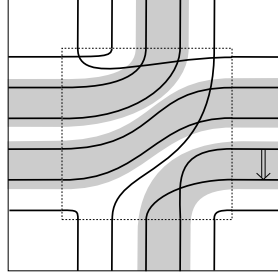


Figure 29. The running example: Starting with the train track of Figure 26(c), three applications of the move (M1) results in the configuration above. The remaining crossover arrow cannot be removed, but since the strands are (necessarily) homotopic we can replace this with a local system over a single curve γ (where $\gamma \times [-\epsilon, \epsilon]$ is shaded).

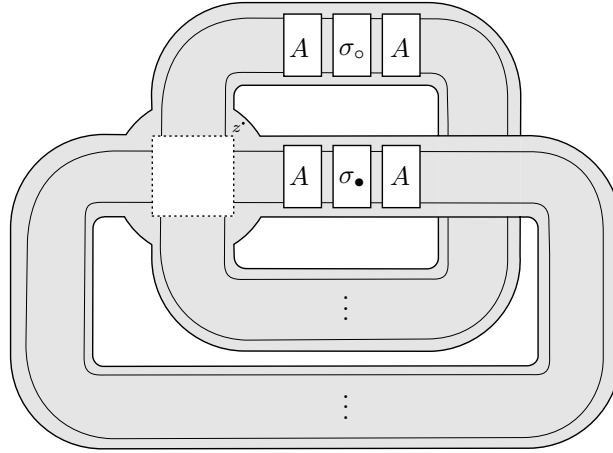


Figure 30. The anatomy of an \mathcal{A} train track, according to Proposition 23: After applying (M1) moves to remove each of the (clockwise) crossover arrows covering a corner, all of the crossover arrows can be moved into the 1-handles (these are contained in the four boxes labeled A . Each one handle contains a permutation box (labelled σ_\bullet and σ_\circ to agree with the notation for idempotents) containing an immersed collection of track segments encoding the permutation. Finally, following previous sections, the dashed box in the 0-handle corresponds to the corner box.

arrow boxes; they contain parallel curve segments joined by an arbitrary configuration of crossover arrows. (All of the crossover arrows are contained in these arrow boxes.) Each strand in an arrow box has two directions: towards the cornerbox and away from the cornerbox (to the permutation box). A specific example is shown in Figure 31.

Weights. Every crossover arrow in an arrow box can be assigned a weight, which is a value in the set $(\mathbb{Z} \setminus \{0\})^2 \cup \{\infty\}$. If the strands the arrow ends on are parallel, the weight is ∞ . Otherwise, the weight is a pair (\tilde{w}, \hat{w}) , where the integer \tilde{w} (w -to) is defined as follows. Follow the strands on which the arrow begins and ends, starting by moving towards the cornerbox; at some point, the two strands will diverge (that is, leave the corner box through different edges). The non-zero integer \tilde{w} indicates that the arrow enters the corner box $|\tilde{w}|$ times before the strands diverge; the sign of \tilde{w} records whether the arrow runs clockwise (+) or counterclockwise (−) around the corner box when this happens. The non-zero integer \hat{w} (w -from) is defined similarly by following the strands in the opposite direction, initially traveling away from the corner box, until they diverge.

Definition 28. The depth of an arrow is defined to be $\min\{|\tilde{w}|, |\hat{w}|\}$, or ∞ if the weight is ∞ . The depth of a curve configuration is the minimum depth of all its crossover arrows.

By compactness of the curves, if an arrow has finite depth, then there is an absolute bound on that depth which depends only on the number of strands in the configuration. Our aim is to prove:

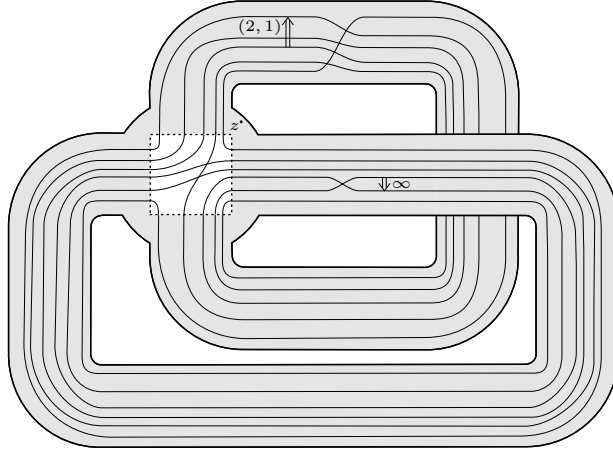


Figure 31. An equivalent view of the train track from Figure 26(c), where the two crossover arrows that passed corners have been removed by a change of basis using (M1) moves. Notice that, in each handle, the arrows and permutations satisfy Lemma 31. The crossover arrows have been labelled by their respective weights; comparing Figure 29 shows that the arrow with finite depth $(\tilde{w}, \hat{w}) = (2, 1)$ can be removed by applications of the moves (M1) and (M2), while the infinite depth arrow persists.

Proposition 29. *A curve configuration of depth m is equivalent to another curve configuration with the same number of strands and depth no less than $m + 1$.*

By induction, it will follow that any curve configuration is equivalent to an infinite depth curve configuration, that is, one in which the only crossover arrows run between parallel strands. Some additional structures and preliminary lemmas are required before proving Proposition 29.

Colors and orders. We now define a partial order on the set of strands in an arrow box. To do this, observe that any strand a in the box lifts to a quasi-geodesic in the universal cover of T . By following the lift of a in the positive direction, we get a ray γ_a in the cover. More explicitly, the universal cover of T is a ribbon graph, homotopy equivalent to a regular 4-valent tree, which we view as embedded in the hyperbolic plane \mathbb{H}^2 . The path γ_a takes in this tree can be described by a string in the letters n, e, s, w which records which edge of the corner box the strand exits through each time it passes through the corner box, as illustrated in Figure 32. By compactness of the curves in the configuration, this string is clearly periodic. Such a string associated with a is called a coloring of a , and the word-length of the string is the depth of the color. Said another way, retracting the universal cover of T to the Caley graph for $\pi_1(T) \cong \langle n, e \rangle$, these colors corresponds to reduced words in the free group where $s = n^{-1}$ and $w = e^{-1}$.

The Gromov boundary of the tree can be naturally identified with a Cantor set $C \subset S^1 = \partial\mathbb{H}^2$. Since γ_a does not pass through the initial branch of the tree corresponding to the arrowbox it starts in, the set of possible endpoints of γ_a is the intersection of C with an interval $I \subset S^1$ of length $3\pi/2$. Thus there is a natural order on the set of possible endpoints defined by declaring $x < y$ if we can go counterclockwise from x to y in I . We define $a < b$ if $\gamma_a(\infty) < \gamma_b(\infty)$. Equivalently, $a < b$ means that if we take a crossover arrow from a to b and push it in the positive direction until the strands diverge, the arrow will point in a counterclockwise direction when the strands diverge. This coincides with the lexicographic order on strands, noting that the order on the letters differs in each arrow box; see Figure 32.

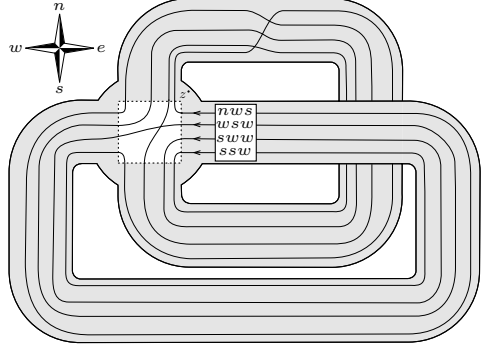


Figure 32. A depth 3 coloring in an arrow box; these strands are (lexicographically) ordered top-to-bottom since $n < w < s$ for this arrow box.

In the same way, we can define a sequence of partial orders $<_m$ on the set of strands in an arrow box. Let $\gamma_a(m)$ be the m th vertex the ray γ_a passes through. The set of possible values of $\gamma_a(m)$ is a finite approximation to the Cantor set $C \cap I$, and can be ordered in the same way as $C \cap I$. We define $a <_m b$ if $\gamma_a(m) < \gamma_b(m)$. It is easy to see that $a <_m b$ implies $a <_{m+1} b$ and that $<_m$ agrees with $<$ for sufficiently large m . More explicitly, we can think of the vertex $\gamma_a(m)$ as being given by the first m letters of the string associated with γ_a , which we refer to as the *depth m coloring* of a . (Figure 32 contains a depth 3 coloring that is ordered.) By a slight abuse of notation, we write $a \leq_m b$ to mean $\gamma_a(m) \leq \gamma_b(m)$, noting that $a \leq_m b$ does not imply $a <_m b$ or $a = b$.

Ordering crossover arrows in an arrowbox. In an arrowbox, where all strands are parallel, crossover arrows have a well-defined length, measured by how many strands they cross. A collection of arrows that point in the same direction can be sorted by length, as follows:

Lemma 30. *A configuration of crossover arrows which all point up is equivalent to a new configuration in which all the arrows point up and are sorted by length, in the sense that shorter arrows lie to the left of longer arrows.*

Proof. Let $n + 1$ be the total number of strands in the arrowbox. We say a configuration is k -sorted if all arrows of length n appear on the right, followed by all arrows of length $n - 1$, then all arrows of length $n - 2$, etc. up to arrows of length $n - k$. The length $< n - k$ part of a configuration is the configuration obtained by deleting all arrows of length greater or equal to $n - k$.

We prove by induction on k that any configuration is equivalent to k -sorted configuration whose length $< n - k$ part is the same as the length $< n - k$ part of the original configuration. The base case $k = 0$ is clear, since an arrow of length n slides freely past any other arrow. For the general case, given a configuration C_0 , we first apply the induction hypothesis to find a k sorted configuration C_1 whose length $< n - k$ part agrees with C_0 . Choose the length $n - k - 1$ arrow which is farthest to the right among those arrows of C_1 which are out of order, and slide it to the right, past the first arrow it encounters, to obtain a new configuration C_2 .

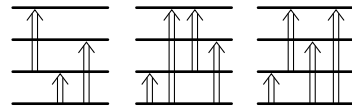


Figure 33. Ordering arrows from left to right, following the steps used in the proof of Lemma 30.

If this slide did not create a new arrow (as in Figure 27(a)) C_2 is still k sorted and the same length $< n - k - 1$ part as C_1 . If the slide created a new arrow (as in Figure 27(c)) C_2 has the same length $< n - k - 1$ part as C_1 but is not sorted. In this case, we apply the induction hypothesis to find a configuration C_3 which is k sorted and has the same length $< n - k$ part as C_2 . (In particular, the position of the length $n - k - 1$ arrow has been switched, and we have not added any arrows

of length $n - k - 1$). Repeating this process, we eventually arrive at a $(k + 1)$ -sorted configuration whose length $< n - k - 1$ part agrees with that of C_0 . \square

On a one-handle, the curve configuration consists of two arrowboxes and one permutation box, as shown in Figure 30. We introduce the notational shorthand $[A_1, \sigma, A_2]$ to specify this data so that, if τ is some other permutation, the equality

$$[A_1, \sigma, A_2] = [A_1^\tau, \tau^{-1}\sigma, A_2]$$

should be interpreted as conjugating the arrow box A_1 by τ . This has the effect of altering $\sigma \mapsto \tau^{-1}\sigma$, potentially altering the arrows (as suggested by A_1^τ), and adding the permutation τ among strands on the left, so that there is no net change to the overall handle (or, indeed, the equivalence class of the train track). Fix an ordering \leq on the strands in each arrowbox. We say that the arrow boxes are sorted with respect to \leq if $a \geq_m b$ whenever there is a crossover arrow from a to b .

Lemma 31. *Any configuration $[A_1, \sigma, A_2]$ in a 1-handle is equivalent to a configuration $[A'_1, \sigma', A'_2]$, where the arrow boxes A'_1 and A'_2 are sorted with respect to the fixed ordering \leq . Moreover, if the original configuration had depth m , then the depth m colorings on the old and new configurations are the same, and the new configuration has depth $\geq m$.*

If \leq was the color ordering for the old configuration, it is probably not the same as the color ordering for the new configuration. But the last part of the lemma implies that the ordering \leq_m is the same for both configurations. Notice also that σ' need not be equal to σ , nor is the outcome of this process unique. An example of this phenomena, which comes up repeatedly in the proof of the lemma, can be seen on a two-strand bundle with a pair of opposite arrows.



Figure 34. Three equivalent configurations; the pair on the right both satisfy Lemma 31.

Proof of Lemma 31. We begin by making some simplifications. First, if the original configuration has depth m , we divide the strands into equivalence classes (bundles). Two strands belong to the same equivalence class if they run parallel for $m - 1$ steps in both directions. The hypothesis that the configuration has depth m means that two strands joined by a crossover arrow are in the same equivalence class. Crossover arrows from one bundle do not interact with stands from a different bundle, so we can operate on each bundle separately; thus we assume without loss of generality that we are operating on a single bundle of strands.

Next, we observe that it suffices to prove the statement under the assumption that the strands in the bundle are ordered from top to bottom in A_1 , and bottom to top in A_2 , so that we are aiming to have all arrows in A'_1 pointing up, and all arrows in A'_2 pointing down. The general case follows easily from this special case by an appropriate conjugation (in each arrow box) of $[A_1, \sigma, A_2]$, as described above.

Begin by arranging the bundle so that all crossings between strands are on the right and all crossover arrows are on the left. It is enough to show that the right-most down arrow can be moved past every up arrow, and to the other side of the crossings (at the expense of possible altering the permutation between strands). An example is shown in Figure 35. Using Lemma 30, arrange the collection of up arrows so that the shortest arrows appear first. We will induct on the the length of the down arrow immediately to the left of the collection of up arrows.

Suppose then that the right-most down arrow has length 1. This arrow slides past all length 1 up arrows, with the exception of the possibility illustrated in Figure 34, namely, the length 1 down arrow meets a length one up arrow. If this occurs, we replace the pair with a single up arrow and a new crossing between the strands. Effectively, the down arrow is replaced by a crossing and this new crossing slides to the right to compose with (and alter) the permutation. Notice that this will, in general, have a non-trivial effect on the remaining up arrows encountered, however this can only

increase their length (if a starting or ending point is on one of the strands in question) and not, in particular, switch their direction.

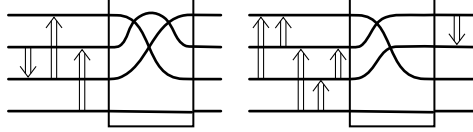


Figure 35. Two equivalent views of the same bundle. The configuration on the left is in the form desired at the beginning of the algorithm; the configuration on the right shows the result of an application of the base case in the induction.

If the length 1 down arrow does not meet a length 1 up arrow between the same strands, it slides freely past all remaining length $k > 1$ arrows. New arrows may be produced in the process by composition, but these will have length $k - 1$ and be (additional) up arrows; compare Figure 35. Finally, we slide the arrow through the crossings specified by the permutation σ . There are two cases: Either the arrow remains a down arrow on the other side of these crossings and we are done, or the arrow switches to an up arrow. In the latter case there must be a crossing between the strands that caused the switch, which we resolve (see, for example, Figure 35). The result alters the permutation but produces an up arrow on the left and a down arrow on the right. This completes the base case for induction.

Now suppose that the right-most down arrow has length n ; our induction hypothesis is that arrows of length less than n can be moved to the right of the up arrows. As before, the up arrows collected to the right are ordered by length. There are three groups in this collection: the short arrows (those of length less than n), the length n arrows, and the long arrows (those of length greater than n). Sliding the down arrow past the short arrows may produce compositions (see Figure 36), but these new down arrows have length less than n and are dealt with by the induction hypothesis. To pass the length n arrows, we proceed as in the base case. That is, the arrow passes freely unless it meets an up arrow joining the same strands. In this case the arrow is replaced by a crossing, which slides to the right; no new down arrows are created as the remaining arrows are all long. Finally, if the arrow passes to the long arrows the arrow proceeds to the permutation (again without producing new down arrows, compare Figure 36) and we resolve a crossing in the permutation if needed.

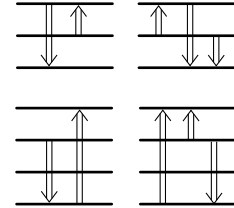


Figure 36. Compositions with short (above) and long (below) arrows.

Finally, we consider the effect of the operations we have performed on the weights of crossover arrows and orderings of strands. In the course of the proof, we have added transpositions between strands belonging to the same bundle. Strands belonging to the same bundle have the same depth $m - 1$ coloring, and any strand must pass at least once through the corner box before it goes over one of the new transpositions. Thus the depth m coloring of all strands is unchanged. From this, it follows that any arrow with depth $\geq m$ in the old configuration has depth $\geq m$ in the new configuration as well. In the course of the proof, we may have created many new crossover arrows, but these all run between strands in the same bundle, so they have complexity $\geq m$ as well. \square

Proof of Proposition 29. The argument is divided into four steps.

Step 1: Remove arrows with $\tilde{w} = -m$. Order to depth m by applying Lemma 31 to each one-handle, with respect to the ordering \leq_m . Notice that, since the original configuration has depth m , depth less than or equal to m is unaffected by this operation and so it does not matter which one we do first. The new configuration has depth m and is sorted with respect to \leq_m . This means that if we take an arrow with $|\tilde{w}| = m$ and push it m steps in the direction towards the corner box (to where

its endpoints diverge), it will remain positively oriented. Thus there are no arrows with $\tilde{w} = -m$ in the new configuration.

Step 2: Remove arrows with $\tilde{w} = m$. Fix an arrow box. If it contains any arrows with $\tilde{w} = m$, choose the one among them which is closest to the corner box. We can remove this arrow by pushing it in the positive direction until its ends diverge. As we do so, we may encounter other arrows with ends on one of the strands which our arrow runs between. We claim that these arrows can be pushed along in front of our chosen arrow (like a pile of snow accumulating in front of a snowplow) without their ends diverging until the chosen arrow reaches the point where its ends diverge. To see this, note that every arrow in the arrow box which lies between the corner box and our chosen arrow has $|\tilde{w}| > m$, so it can be pushed along m steps without its ends diverging. Similarly, arrows which we encounter in any subsequent arrow box have complexity at least m , so they can be pushed $m - 1$ steps in any direction without diverging. Other arrows which these arrows would have to pass can likewise be pushed along (they need to move at most $m - 1$ steps). At the end of the process, we can remove the chosen arrow, and then just push all other arrows back to where they started. The net result is that we have removed the chosen arrow without making any other changes to the curve configuration. Repeating this process removes all arrows with $\tilde{w} = m$.

Step 3: Remove arrows with $\hat{w} = -m$. For a given arrow box A , we will change the configuration so as to eliminate all arrows with $\hat{w} = -m$ from A . To do this, we first apply Lemma 31 to the region consisting of the arrow box and its adjacent permutation with ordering \leq_{m+1} . This region is shown in Figure 37.

By Lemma 31, the depth m colorings in the old and new configurations agree. Moreover, the depth $m + 1$ colorings on A are the same in both configurations. To see this, consider the number of steps a strand leaving the arrowbox towards the corner box takes to return to it. If it returns after one step through the corner box, it must re-enter through the right-hand side of the figure and exit through the left. Since all crossover arrows in the original arrowbox have $|\tilde{w}| \geq m + 1$ (Steps 1 and 2), any new transpositions we added in the course of applying the lemma will not change the next m labels in the coloring. Thus the first $m + 1$ labels in the original coloring will remain unchanged. A similar argument applies if the strand takes two or more steps to return to the arrowbox.

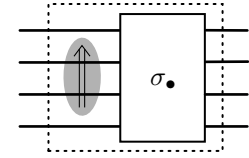


Figure 37. Lemma 31 applied to the dashed region; arrows have $|\tilde{w}| \geq m + 1$ and $|\hat{w}| \geq m$.

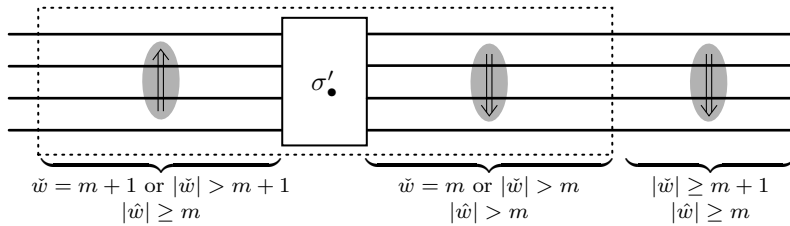


Figure 38. A summary of weights after Lemma 31 is applied to the region of the horizontal strands in the dashed box. Weights outside the dashed box are inherited from the previous step.

At this point, the configuration is as shown in Figure 38. It is sorted to depth $m + 1$ on the left, and to depth m on the right. It follows from Lemma 31 that every arrow in the dashed box has depth greater or equal to m . In fact, every arrow in the dashed box has $\tilde{w} \geq m + 1$ on the left of the permutation, and $\hat{w} \geq m + 1$ on the right. To see this, note that when we apply Lemma 31, the strands in each bundle used in the proof run parallel for m steps to the left. Finally, since the configuration is sorted, we see that $\tilde{w} \neq -(m + 1)$ for arrows on the left, and $\tilde{w} \neq -m$ for arrows on the right. In summary, the weights in the new configuration are as shown in the figure.

In the process of applying Lemma 31, we may have created some new arrows with $\tilde{w} = m$ in the right-hand side of the dashed region. Since the right-hand arrowbox in the 1-handle is sorted to depth m , these can now be removed just as in Step 1.

Consider the arrow in A which is closest to the cornerbox. This arrow has $|\tilde{w}| \geq m + 1 \geq 2$, so we can slide it through the cornerbox to obtain a new configuration. In its old position, the arrow had $|\hat{w}| \geq m$, so the new arrow will have $|\tilde{w}| \geq m + 1$. Similarly, the old arrow had $\tilde{w} = m + 1$ or $|\tilde{w}| > m + 1$, so the new arrow will have $\hat{w} = m$ or $|\hat{w}| > m$. Repeating this operation for each arrow in A , we eventually arrive at a depth m configuration in which we have slid every arrow out of A .

Summarising our progress to this point: we have removed all arrows with $\tilde{w} = -m$ or $\hat{w} = -m$ from our chosen arrowbox A without adding any new arrows with $\tilde{w} = -m$ or $\hat{w} = -m$ in any of the other arrowboxes. Therefore, by repeating this sequence of steps on each arrowbox, we arrive at a depth m configuration of curves in which there are no crossover arrows with $\tilde{w} = -m$ or $\hat{w} = -m$.

Step 4: Remove arrows with $\hat{w} = m$. There may remain arrows for which $\hat{w} = m$; the last step in the proof of Proposition 29 is to show that we can eliminate all arrows with weight of depth n without changing the rest of the configuration. This proceeds in exactly the same way as in Step 2. Fix a 1-handle, choose a direction \rightarrow on it, and consider all crossover arrows which have weight $w_{\rightarrow} = m$ when sliding in this direction. All the other arrows in the 1-handle have $|w_{\rightarrow}| \geq m + 1$, so we can slide the arrows with $w_{\rightarrow} = m$ off one at a time without changing the weights of any other arrow, just as we did in Step 2. Repeating this operation for each 1-handle and each direction, we arrive at a configuration in which every arrow has depth greater or equal to $m + 1$. \square

3.8. The proof of Theorem 5. We are now positioned to prove the theorem that is the focus of the section.

Fix a reduced, extendable type D structure and express it as an immersed train track. By Proposition 23 this may be expressed as a curve configuration, a schematic for which is given in Figure 30. Then the algorithm detailed in Section 3.7 ensures that this curve configuration can be simplified to one in which the only crossover arrows connect parallel-running curves in the marked torus. Indeed, the original type D structure is isomorphic as an \mathcal{A} -module to the type D structure determined by this simplified curve configuration. It is convenient to introduce terminology for a train track of this form.

Definition 32. A *curve-like train track* is an \mathcal{A} -train track which has the form of immersed curves together with crossover arrows which connect parallel curves.

It remains to associate a local system with any collection of parallel curves that arise. Consider such a collection of n parallel curves, and notice that we can replace, without loss of generality, any crossings between two curves with a triple of alternating crossover arrows as in Figure 39; compare Figure 27(d). Moreover, by applying the move (M2) we may assume that all of the arrows are contained in the 0-handle and run between curves whose endpoints are on two different sides of the corner box.



Figure 39. Equivalent configurations.

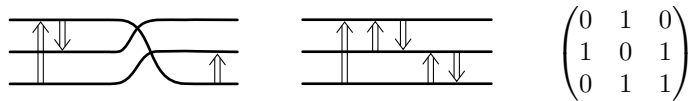


Figure 40. Extracting a local system from a bundle of curves, where the generators run from top to bottom.

Interpreting this configuration as (part of) a train track, we take the segments on each side of the collection of arrows as generators and form a $n \times n$ matrix (x_{ij}) where the entry x_{ij} is the mod 2

count of oriented paths from x_i to x_j . The result is a local system of dimension n over the immersed curve γ carrying the bundle of curves. Note that to define this local system we must choose an orientation on γ (for the example in Figure 40 we count paths oriented left to right); choosing the opposite orientation corresponds to inverting the matrix. \square

3.9. A remark on surfaces of higher genus. We conclude by observing that everything in this section may be applied to any surface F equipped with a decomposition into finitely many 0- and 1-handles (with appropriate marked points in each 0-handle). Indeed, given such a handle structure there is a naturally associated algebra \mathcal{A}_F (constructed in Section 3.4), and an extendable type D structure may be realised as a \mathcal{A}_F train track in the surface. Note that, in the case of a once-punctured surface of genus g , this algebra coincides with the 1-moving-strand algebra (and not the full dg algebra) defined by Lipshitz, Ozsváth, and Thurston [26]. The linear-algebraic Lemma 24 goes through as before (as explained in Section 3.4, this is local information about the 0-handles), as does the arrow-reduction algorithm from Proposition 29. So, while we are primarily interested in the torus algebra for this work, we have in fact shown:

Theorem 33. *Let \mathcal{A}_F be the algebra associated with a marked surface F equipped with a decomposition into finitely many 0- and 1-handles. Then any extendable type D structure over \mathcal{A}_F may be realised as a collection of immersed curves in F decorated with local systems.*

This recovers a result due to Haiden, Katzarkov, and Kontsevitch [12] via rather different techniques.

4. DECORATED IMMERSED CURVES AS TYPE D STRUCTURES

The previous section shows how an extended type D structure over $\tilde{\mathcal{A}}$ can be interpreted as a collection of immersed curves decorated by local systems in the marked torus T . The goal of this section is to show that this in fact gives a bijection between the set of homotopy equivalence classes of extendable type D structures and the set of decorated immersed multicurves in the marked torus. Moreover, we show that the pairing on extendable type D structures coming from the box tensor product corresponds to a geometric pairing of decorated immersed curves.

4.1. The bijection. Let \mathcal{D} denote the set of extendable type D structures over \mathcal{A} , up to homotopy equivalence. \mathcal{C} will denote the set of collections of oriented immersed curves decorated with local systems in the marked torus; recall that by marked torus we mean the punctured torus T with a choice of parametrizing curves α and β . Each decorated curve is a triple (γ, k, A) , where γ is an oriented immersed curve (up to regular homotopy), k is a positive integer, and A is a similarity class of $k \times k$ matrices over \mathbb{F} . The orientation on γ can be reversed at the expense of inverting A ; that is, (γ, k, A) is equivalent to $(-\gamma, k, A^{-1})$. Moreover, a pair (γ, k_1, A_1) and (γ, k_2, A_2) is equivalent to the single curve $(\gamma, k_1 + k_2, A_1 \oplus A_2)$, and if γ is homotopic to m times γ' then (γ, k, A) is equivalent to (γ', mk, A') , where A' is the matrix

$$\left[\begin{array}{c|c|c|c} 0 & 0 & 0 & A \\ \hline I_k & 0 & 0 & 0 \\ \hline 0 & I_k & 0 & 0 \\ \hline 0 & 0 & I_k & 0 \end{array} \right].$$

To remove this ambiguity, we will assume that collections of decorated curves in \mathcal{C} are minimal in the sense that each underlying curve appears only once and no curve is periodic (i.e. can be written as $k \cdot \gamma'$ for some immersed curve γ' and integer $k > 1$).

We define a bijection $f : \mathcal{D} \rightarrow \mathcal{C}$ as follows: given an object in \mathcal{D} , we choose a reduced representative N and an extension \tilde{N} of N , and then realize \tilde{N} as a collection of decorated immersed curves as in Section 3. It remains to prove that f is well defined and that it has an inverse. We will defer the proof of well-definedness until after pairing has been discussed in the next subsection.

The inverse of f is easy to describe. Given a decorated immersed curve (γ, k, A) in the marked torus, we construct a train track by replacing γ with k parallel copies of γ , writing A as a product of elementary matrices $P_1 \cdots P_\ell$, and adding a crossover arrow between copies of γ for each elementary matrix, where an elementary matrix of type A_{ij} corresponds to an arrow connecting the i th copy of γ to the j th copy of γ and the arrows corresponding to $P_\ell, P_{\ell-1}, \dots, P_1$ appear in order according to the orientation of γ . We assume that γ is homotoped so that it has minimal intersection with $\alpha \cup \beta$, and we take care that no crossover arrows intersect α or β . The result is a valid reduced \mathcal{A} -train track; this corresponds to an extended type D structure \tilde{N} , which has an underlying (extendable) type D structure N . Clearly this is the reverse of the procedure defining f , so $f(N) = (\gamma, k, A)$. The inverse function extends to collections of immersed curves by taking direct sum of modules. Note that the choices involved in defining $f^{-1}((\gamma, k, A))$ are a matrix representing the similarity class A and an elementary decomposition of that matrix. Changing either choice corresponds to sliding crossover arrows around γ by moves which preserve the homotopy equivalence class of the corresponding extended type D module; thus f^{-1} is well-defined.

4.2. Pairing. The set \mathcal{D} , as a subset of ${}^A\text{Mod}$, is equipped with a pairing given by the box tensor product: Given objects N_1 and N_2 in \mathcal{D} , their pairing is the homology of $N_1^A \boxtimes N_2$, where N_1^A is the \mathcal{A}_∞ module corresponding to N_1 under the duality described in Section 2.3. The pairing on the set \mathcal{C} will be defined in terms of the intersection Floer homology of immersed curves with local systems in the marked torus.

Definition 34. Let $\gamma_1 = (\gamma_1, k_1, A_1)$ and $\gamma_2 = (\gamma_2, k_2, A_2)$ be two decorated immersed curves in the marked torus. The intersection Floer homology of γ_1 and γ_2 , written $HF(\gamma_1, \gamma_2)$ is defined to be the \mathbb{F} -vector space of dimension $k_1 k_2 \#(\gamma_1 \cap \gamma_2) + 2n(k_1 k_2 - \text{rk}(A_1 \otimes A_2 + I))$, where $\#(\gamma_1 \cap \gamma_2)$ is the geometric intersection number and n is the number of immersed annuli bounded by γ_1 and γ_2 . Note that under the assumption that γ_1 and γ_2 are not periodic, n is 1 if $\gamma_1 \sim \gamma_2$ or 0 otherwise; in particular, if γ_1 and γ_2 are not parallel, HF simply counts the minimal intersection of k_1 copies of γ_1 and k_2 copies of γ_2 . HF is extended to collections of decorated curves by direct sum.

Given objects Γ_1 and Γ_2 of \mathcal{C} , we define their pairing to be $HF(\Gamma_1, r(\Gamma_2))$, where r denotes the orientation reversing diffeomorphism of the marked torus which exchanges α and $-\beta$.

For $i = 1, 2$, let N_i be (a reduced representative of) an object in \mathcal{D} , and choose an extension \tilde{N}_i . Let ϑ_i be a valid reduced \mathcal{A} train track constructed from \tilde{N}_i as described in Section 3.2. By the algorithm in Section 3.3, ϑ_i can be modified by a sequence of train track equivalences and the arrow slide moves (M1) and (M2) to a valid reduced \mathcal{A} train track ϑ'_i which has the form of immersed curves with crossover arrows and for which all crossover arrows connect parallel curves. Let \tilde{N}'_i be the extended type D structure corresponding to ϑ'_i and let N'_i be the underlying type D structure. Since the moves (M1) and (M2) correspond to homotopy equivalences, N'_i is homotopy equivalent to N_i . Let Γ_i be the collection of decorated immersed curves representing ϑ'_i , so that $f(N_i) = \Gamma_i$. We want to show that $H_*(N_1^A \boxtimes N_2) = HF(\Gamma_1, r(\Gamma_2))$.

We will consider the complex $\mathcal{C}(\vartheta'_1, \vartheta'_2)$ defined in Section 3.2. $\mathcal{C}(\vartheta'_1, \vartheta'_2)$ is the intersection Floer chain complex of $A(\vartheta'_1)$ and $D(\vartheta'_2)$. Recall that $D(\vartheta'_2)$ is obtained by reflecting $A(\vartheta'_2)$ across the anti-diagonal, so if Γ_2 represents ϑ'_2 in type A position then $r(\Gamma_2)$ represents ϑ'_2 in type D position.

In order for $\mathcal{C}(\vartheta'_1, \vartheta'_2)$ to be defined, we need the pair to be admissible—there can be no immersed annuli carried by $A(\vartheta'_1)$ and $D(\vartheta'_2)$. To ensure this, we will modify ϑ'_2 so that it has no component for which the underlying curve consists only of the following four types of segments:

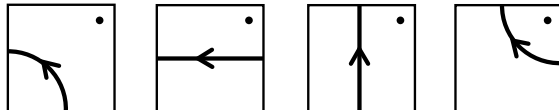




Figure 41. Local moves which preserve the Floer homology of immersed train tracks.

This ensures that the pair is admissible, since any immersed annulus, when cut by α and β , consists only of the connecting pieces shown on the bottom row of Figure 16. If any component of \mathfrak{v}'_2 does contain only the four segment types above, we choose one of the latter three types of segments and modify \mathfrak{v}'_2 by applying a finger-move isotopy to the given segment across either α or β , as in Figure 10; if \mathfrak{v}'_2 has parallel copies of the relevant segment we apply the isotopy to each copy, keeping them parallel, and ensure that the finger-move avoids any crossover arrows. Let \mathfrak{v}''_2 denote the result of applying these finger-moves, if necessary, to \mathfrak{v}'_2 . Note that \mathfrak{v}''_2 is an almost reduced train track whose corresponding type D structure N''_2 is homotopy equivalent to N'_2 , where the homotopy equivalence replaces certain ρ_{12} , ρ_{23} , or ρ_{123} arrows with zig-zags as in Figure 10. N''_2 is both bounded and almost reduced.

By Theorem 16, $\mathcal{C}(\mathfrak{v}'_1, \mathfrak{v}''_2)$ is isomorphic to $(N'_1)^A \boxtimes N''_2$, which is quasi-isomorphic to $N_1^A \boxtimes N_2$. It remains to show that the homology of $\mathcal{C}(\mathfrak{v}'_1, \mathfrak{v}''_2)$ agrees with $HF(\Gamma_1, r(\Gamma_2))$, as defined in Definition 34. Recall that $\mathcal{C}(\mathfrak{v}'_1, \mathfrak{v}''_2)$ is the Floer chain complex of the immersed train tracks \mathfrak{v}'_1 and $r(\mathfrak{v}''_2)$, when each is put in a particular position. The particular position is required because, in general, Floer homology of immersed train tracks in the punctured torus T is not preserved by homotopies of the train tracks. However, in this case we may homotope the underlying curves of each train track:

Lemma 35. *Let \mathfrak{v}_1 and \mathfrak{v}_2 be an admissible pair of curve-like train tracks in T , and assume that all crossover arrows in each train track are outside a neighborhood of the other train track. The Floer homology of \mathfrak{v}_1 and \mathfrak{v}_2 is preserved by regular homotopies of the underlying curves of \mathfrak{v}_1 and \mathfrak{v}_2 .*

Proof. This follows immediately from the fact that Floer homology of train tracks is preserved by the local moves in Figure 41. Invariance under (a), bigon removal, is standard. For (b), let x and y denote the bottom and top intersection points, respectively, for the arrangement of curves on the left, and let x' and y' denote the bottom and top generators in the configuration on the right. We will assume the train tracks are paired so that the Floer differential counts bigons whose right boundary follows the gray train track; the argument is similar if the roles of the two train tracks are reversed. We first consider possible immersed bigons counted in the Floer differential with x as the initial or final point. Based on local behavior near x , bigons whose initial point is x have three types as shown in Figure 42: bigons which cover the fourth quadrant, bigons which cover the second quadrant whose boundary does not traverse the crossover arrow, and bigons which cover the second quadrant near x and whose boundary does traverse the crossover arrow.

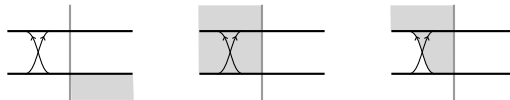


Figure 42. Three bigon types.

Bigons of the first two types are unaffected by sliding the crossover arrow to the right; that is, there are corresponding bigons starting at x' . The third type of bigon is destroyed by sliding the crossover arrow, so there is no corresponding bigon starting at x' . Note, however, that for any bigon of this type connecting x to another intersection point z , there is also a bigon from y to z . We also note that there are no bigons starting from x' which do not arise in this way. Bigons ending at x cover

the first or third quadrants and never involve the crossover arrow, and are thus unaffected by sliding the arrow; the bigons into x correspond exactly to the bigons into x' .

Similarly, we consider bigons in and out of y . Bigons starting at y cover either the second or fourth quadrant and correspond exactly to bigons starting at y' . Bigons ending at y cover the first or third quadrants and do not involve the crossover arrow. Each of these bigons gives rise to a corresponding bigon ending at y' after the crossover arrow is slid rightward, but there is an additional type of bigon ending at y' , covering the fourth quadrant and traversing the arrow, which do not arise in this way; for each such bigon, there is a nearly identical bigon ending at x' (and thus one ending at x).

Observe that the differential of the Floer chain complex is unchanged by the arrow slide in (b) except that for each term starting at y we add or remove a corresponding term starting at x , and for each term ending at x we add or remove a corresponding term ending at y . This is precisely the effect of the change of basis given by $x' = x + y$, $y' = y$. It follows that the homology of the complex is unchanged. \square

By the Lemma, to compute $\mathcal{C}(\vartheta'_1, \vartheta''_2)$ we may first homotope both train tracks so that the underlying curves are in minimal position before taking the intersection Floer homology. For simplicity, assume that ϑ'_1 and ϑ''_2 each have one component, corresponding to the decorated immersed curves (γ_1, k_1, A_1) and (γ_2, k_2, A_2) , respectively. Since γ_1 and γ_2 are in minimal position, there are no bigons carried by the pair of train tracks ϑ'_1 and ϑ''_2 . If γ_1 and γ_2 do not cobound an immersed annulus, then neither do ϑ'_1 and ϑ''_2 , and the pair of train tracks is admissible. In this case, the Floer complex (and the Floer homology) is generated by the intersection points of k_1 parallel copies of γ_1 with k_2 parallel copies of γ_2 ; the number of such intersection points is $k_1 k_2 \#(\gamma_1 \cap \gamma_2)$. If γ_1 and γ_2 cobound an immersed annulus, then we must perform a finger move as shown in Figure 43 to achieve admissibility.

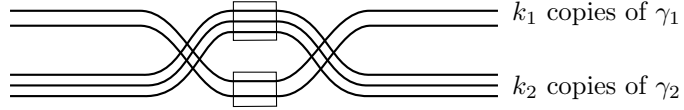


Figure 43. Performing a finger move.

We may assume that all crossover arrows are concentrated in the boxes shown, and we assume that the curves are oriented right to left. This adds $2k_1 k_2$ intersection points, but these points are connected by bigons. Each of the two clusters of added intersection points can be indexed by a pair (i, j) , where the intersection is between the i th copy of γ_1 and the j th copy of γ_2 . Each point on the right is connected to the corresponding point on the left by a bigon which wraps around the annulus, avoiding the middle region in the figure above. Additionally, there is a bigon through the middle region of the figure from the (i, j) intersection point on the right to the (i', j') intersection point on the left if and only if the ii' entry of A_1 and the jj' entry of A_2 are both 1. Thus the bigons connecting the two sets of $k_1 k_2$ intersection points are encoded by the $k_1 k_2 \times k_1 k_2$ matrix $A_1 \otimes A_2 + I$. The rank of this matrix determines how many pairs of generators cancel when taking homology of the resulting complex, so the contribution of this finger move to the Floer homology of the train tracks is $2(k_1 k_2 - \text{rk}(A_1 \otimes A_2 + I))$. It follows that the homology of $\mathcal{C}(\vartheta'_1, \vartheta''_2)$ agrees with $HF(\Gamma_1, r(\Gamma_2))$, as desired.

4.3. Well-definedness. It remains to show that the bijection $f : \mathcal{D} \rightarrow \mathcal{C}$ is well-defined. In principle applying f as defined above involves several choices, including the representative N of the homotopy equivalence class, the extension \tilde{N} of N , and the sequence of arrow slides used to reduce the train track corresponding to \tilde{N} to immersed curves with local systems. We will prove invariance under these choices by considering the pairing of immersed train tracks.

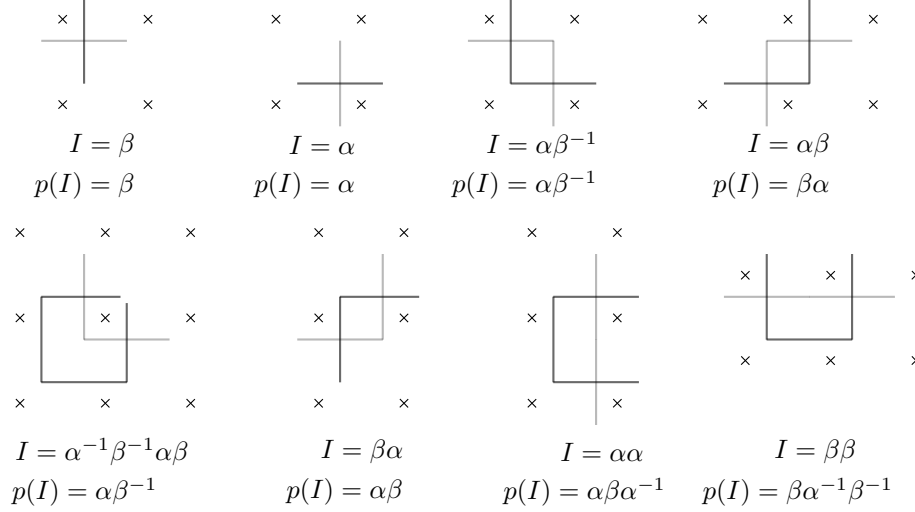


Figure 44. Examples of ϑ_I in type A position (light) and $\vartheta_{p(I)}$ in type D position (dark) for various choices of I . The train tracks are in the marked torus but are shown in the covering space $\mathbb{R}^2 \setminus \mathbb{Z}^2$ for clarity.

Let N_1 and N_2 be two extendable type D structures that are homotopy equivalent to each other. Since N_1 and N_2 are homotopy equivalent, they have the same pairing behavior; that is,

$$H_*(N_1^A \boxtimes \bar{N}) \cong H_*(N_2^A \boxtimes \bar{N})$$

for any reduced type D structure N . For $i = 1, 2$, let ϑ_i be a curve-like train track in T which represents a type D structure homotopy equivalent to N_i . For instance, ϑ_i could be the result of applying the algorithm in section 3. It follows from Theorem 16 that $H_*(\mathcal{C}(\vartheta_1, \bar{\vartheta})) \cong H_*(\mathcal{C}(\vartheta_2, \bar{\vartheta}))$ for any reduced weakly valid \mathcal{A} train track $\bar{\vartheta}$. We will show that the decorated immersed curves representing ϑ_i are determined, up to regular homotopy of the underlying curves, by its pairing behavior; thus ϑ_1 and ϑ_2 determine the same element of \mathcal{C} .

Let ϑ be a curve-like train track. A component of ϑ consists of the following data: an immersed curve γ in the punctured torus which intersects $\alpha \cup \beta$ minimally, an integer determining how many parallel copies of the curve there are, and a collection of crossover arrows between parallel copies of γ . The curve γ may be represented as a cyclic word in $\{\alpha^\pm, \beta^\pm\}$ by viewing it as an element of the fundamental group of the punctured torus, which is the free group generated by two elements α and β (this requires choosing a basepoint on γ , but choosing a different basepoint simply cyclically permutes the letters in the word). We first claim that the underlying curves of ϑ_i are determined by the results of pairing ϑ_i with certain immersed line segments. More precisely, for any reduced word I in $\{\alpha^{\pm 1}, \beta^{\pm 1}\}$, there is a weakly valid \mathcal{A} train track ϑ_I . ϑ_I consists of a sequence of horizontal and vertical segments corresponding to the letters in I , joined end to end to form an immersed curve segment (see Figure 44 for examples). This immersed line segment is unoriented, so $\vartheta_I = \vartheta_{I^{-1}}$, where I^{-1} denotes the inverse word in the free group. For each word I with length at least two, we construct a word $p(I)$ as follows: starting with ϑ_I in type A position we apply a homotopy in the complement of the basepoint and fixing the midpoint of the initial and final segments of ϑ_I to form a new train track that is in type D position, and we choose $p(I)$ such that this train track is $D(\vartheta_{p(I)})$ (see Figure 44).

Lemma 36. *For a curve-like train track ϑ , the dimension of the homology of $\mathcal{C}(\vartheta, \vartheta_{p(I)})$ depends only on the number of times I or I^{-1} appears in the cyclic words representing the underlying curves of ϑ , counted with multiplicity, and on the number of times J or J^{-1} appears for any J for which $p(J)$ is shorter than $p(I)$.*

Proof. We demonstrate the proof in a few examples, and leave the general case to the reader. Consider $I = \alpha$, which has $p(I) = \alpha$. $\vartheta_{p(I)} = \vartheta_\alpha$ has a single vertical segment; when put in type

D position this is reflected across the anti-diagonal to produce a single horizontal segment. The chain complex $\mathcal{C}(\mathfrak{V}, \mathfrak{V}_\alpha)$ clearly has one generator for each vertical segment in \mathfrak{V} , or equivalently for each instance of α or α^{-1} in the cyclic words representing the immersed curves in \mathfrak{V} . Similarly, the homology of $\mathcal{C}(\mathfrak{V}, \mathfrak{V}_\beta)$ is precisely the number of instances of β or β^{-1} in the curves defining \mathfrak{V} .

Now consider, for example, $I = \alpha\beta$. $p(I) = \beta\alpha$, and $D(\mathfrak{V}_{\beta\alpha})$ has one horizontal and one vertical segment, as shown in Figure 44. Thus the complex $\mathcal{C}(\mathfrak{V}, \mathfrak{V}_{\beta\alpha})$ has one generator for each instance of α or α^{-1} in \mathfrak{V} and one generator for each instance of β or β^{-1} . However, there is also a differential for each instance of $\alpha\beta$ or $\beta^{-1}\alpha^{-1}$ in \mathfrak{V} , since the relevant segments of \mathfrak{V} form a bigon with $\mathfrak{V}_{\beta\alpha}$. It follows that

$$\dim H_*(\mathcal{C}(\mathfrak{V}, \mathfrak{V}_{p(\alpha\beta)})) = (\text{num. of } \alpha^{\pm 1} \text{ in } \mathfrak{V}) + (\text{num. of } \beta^{\pm 1} \text{ in } \mathfrak{V}) - (\text{num. of } (\alpha\beta)^{\pm 1} \text{ in } \mathfrak{V}).$$

Since the first two quantities on the right are already determined (by the result of pairing \mathfrak{V} with \mathfrak{V}_J for length 1 words J), the number of instances of $I^{\pm 1}$ in \mathfrak{V} is determined by the result of pairing \mathfrak{V} with $\mathfrak{V}_{p(I)}$.

For longer words I the reasoning is similar, though there will be more terms since the complex $\mathcal{C}(\mathfrak{V}, \mathfrak{V}_{p(I)})$ counts bigons formed with \mathfrak{V}_J for any subword J of $p(I)$. \square

The preceding Lemma (and induction on the length of $p(I)$) shows that if the dimension of the homology of $\mathcal{C}(\mathfrak{V}, \mathfrak{V}_J)$ is known for every word J , then the number of instances of I or I^{-1} in \mathfrak{V} can be determined for any word I . Since \mathfrak{V} has a finite number of curves which have a finite length, sufficiently long words will only occur a nonzero number of times if they repeat the entire cyclic word for one of the immersed curves in \mathfrak{V} . In this way, the underlying immersed curves in \mathfrak{V} can be determined, with multiplicity.

Finally, we claim that for a collection of parallel curves in \mathfrak{V} with crossover arrows, the corresponding local system is determined by the pairing behavior of tracks. In other words, given two tracks which have the same underlying curves but different local systems, they can be distinguished by pairing with some other immersed train track. The local system will not be seen by pairing with any of the immersed line segments \mathfrak{V}_I considered above. Instead, for each immersed curve γ in \mathfrak{V} we will pair with a train track \mathfrak{V}' which is parallel copies of $r(\gamma)$ connected by crossover arrows. We now represent \mathfrak{V} and \mathfrak{V}' by elements Γ and Γ' , and use the fact that $\mathcal{C}(\mathfrak{V}, \mathfrak{V}')$ is quasi-isomorphic to $HF(\Gamma_1, r(\Gamma_2))$, where the later is defined in Definition 34. For any component of Γ_1 with underlying curve other than γ , the pairing with Γ_2 does not depend on the local system, so we may assume that Γ_1 has a single component (γ, k, A) , while $r(\Gamma_2)$ is the single curve (γ, ℓ, B) . That the result of this pairing determines A is now an exercise in linear algebra.

Proposition 37. *If A_1 and A_2 are $k \times k$ matrices over \mathbb{F} which are not similar, then there exists a matrix B such that $\text{rk}(A_1 \otimes B - I) \neq \text{rk}(A_2 \otimes B - I)$.*

Proof. We outline the key steps but leave the details of the proof as an exercise to the reader. We assume that A_1 , A_2 , and B are written in rational canonical form, and we may choose B to have a single block, so that

$$B = \begin{bmatrix} 0 & 0 & \cdots & 0 & 1 \\ 1 & 0 & \cdots & 0 & b_1 \\ 0 & 1 & \cdots & 0 & b_2 \\ \vdots & \vdots & \ddots & \ddots & \vdots \\ 0 & 0 & \cdots & 1 & b_{n-1} \end{bmatrix}$$

It is sufficient to consider the case that A_1 and A_2 have this form as well. It follows that

$$A \otimes B + I = \begin{bmatrix} I & 0 & \cdots & 0 & A \\ A & I & \cdots & 0 & b_1 A \\ 0 & A & \cdots & 0 & b_2 A \\ \vdots & \vdots & \ddots & \ddots & \vdots \\ 0 & 0 & \cdots & 1 & I + b_{n-1} A \end{bmatrix}$$

which row reduces to

$$\begin{bmatrix} I & 0 & \cdots & 0 & M_0 \\ 0 & I & \cdots & 0 & M_1 \\ 0 & 0 & \cdots & 0 & M_2 \\ \vdots & \vdots & \ddots & \ddots & \vdots \\ 0 & 0 & \cdots & 0 & I + M_{n-1} \end{bmatrix}$$

where $M_0 = A$ and $M_i = A(b_i + M_{i-1})$ for $i > 0$. The rank of this is determined by the rank of the lower right block. We choose the coefficients in B so that $p(x) = x^n + b_1 x^{n-1} + \cdots + b_{n-1} x + 1$ is the minimal polynomial of A_1 (which we assume without loss of generality does not divide the minimal polynomial of A_2). It follows that $A_1 \otimes B + I$ has rank $k(n-1)$ and $A_2 \otimes B + I$ has rank strictly greater than $k(n-1)$. \square

We have shown that if N_1 and N_2 are extendable type D structures which are homotopy equivalent then $f(N_1) = f(N_2)$, establishing the well-definedness of f . We conclude this section with the observation that, in particular, any two extensions of an extendable type D module correspond to the same decorated immersed curve and are thus homotopy equivalence.

Proposition 38. *An extendable type D module over \mathcal{A} has a unique extension, up to homotopy equivalence.*

5. BORDERED FLOER INVARIANTS AS DECORATED IMMERSSED CURVES

We now return our attention to Floer theoretic invariants of manifolds with torus boundary. Our goal in this section is to prove Theorems 1 and 2. Suppose that (M, α, β) is a parametrized three-manifold with torus boundary. By Theorem 4 (proved in the Appendix), the type D structure $\widehat{CFD}(M, \alpha, \beta)$ is extendable. The results of the preceding two sections imply that there is a well-defined collection of immersed curves with local systems associated to $\widehat{CFD}(M, \alpha, \beta)$. This collection of curves lives in the abstract torus T , which we identify with $T(M)$ via a map which identifies the vertical edge of T with $\alpha \subset \partial M$ and the horizontal edge of T with $\beta \subset \partial M$. We denote the result by $f_{\alpha, \beta}(\widehat{CFD}(M, \alpha, \beta))$.

It remains to check that this collection of curves does not depend on the choice of parametrization (α, β) .

Proposition 39. *There are equivalences*

$$(2) \quad f_{\alpha, \beta}(\widehat{CFD}(M, \alpha, \beta)) \cong f_{\alpha, \beta \pm \alpha}(\widehat{CFD}(M, \alpha, \beta \pm \alpha))$$

$$(3) \quad f_{\alpha, \beta}(\widehat{CFD}(M, \alpha, \beta)) \cong f_{\alpha \pm \beta, \beta}(\widehat{CFD}(M, \alpha \pm \beta, \beta))$$

where \cong denotes regular homotopy of curves with local systems.

Proof. We will establish the equivalence (2); the equivalence (3) is nearly identical, and is left to the reader. To this end, we recall the bimodules associated with a Dehn twist established in [26]. These give rise to

$$\widehat{T}_\alpha^{\pm 1} \boxtimes \widehat{CFD}(M, \alpha, \beta) \cong \widehat{CFD}(M, \alpha, \beta \pm \alpha)$$

where \widehat{T}_α is the type DA bimodule denoted $\widehat{CFDA}(\tau_\mu)$ in the notation of [26, Section 10]. This bimodule, and its inverse, are shown in Figure 45. Thus we need to show that $f_{\alpha,\beta}(N) \cong f_{\alpha,\beta \pm \alpha}(\widehat{T}_\alpha^{\pm 1} \boxtimes N)$, where N is the extendable type D structure $\widehat{CFD}(M, \alpha, \beta)$.

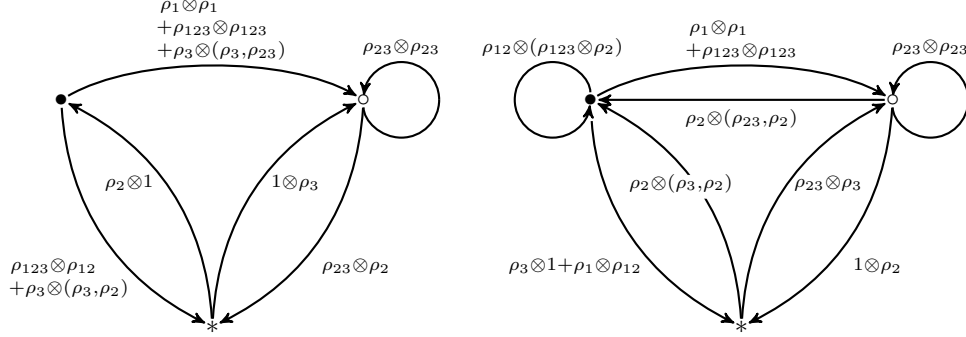


Figure 45. Graphical representations of the Dehn twist bimodules \widehat{T}_α (left) and \widehat{T}_α^{-1} (right), following [26, Section 10].

We may work with one component of $\widehat{CFD}(M, \alpha, \beta)$ at a time, so we will assume that $f_{\alpha,\beta}(N)$ consists of a single immersed curve γ decorated by a local system. Let \mathfrak{v} be the corresponding curve-like train track, consisting of parallel copies of γ connected by crossover arrows. Recall that the valid reduced train track \mathfrak{v} determines an extendable type D structure which is homotopy equivalent to N ; since we may modify N by homotopy equivalence, we will assume \mathfrak{v} corresponds directly to N . We can view the crossover arrows as all being concentrated in a single box, which slides freely along γ . By sliding this box, we can ensure that no crossover arrow has its head or tail on a segment of curve corresponding to a ρ_3 arrow.

We claim that the effect on \mathfrak{v} of tensoring N with \widehat{T}_α is easy to describe: it is applying a negative Dehn twist along α (and homotoping the result if necessary to achieve minimal intersection with β). Let \mathfrak{v}' be the train track obtained from \mathfrak{v} by applying a negative Dehn twist in a thin strip along the left edge of the square $T \setminus (\alpha \cup \beta)$ (see Figure 46). The effect of this transformation can be described as follows:

- For each intersection x with α we add a new intersection point x' with β , such that x and x' are connected by a segment connecting the bottom and left edges of the square;
- Each path from the bottom of the square to the left of the square ending at x becomes a path from the bottom to the top ending at x' ;
- Each path from the right of the square to the left ending at x becomes a path from the right to the top ending at x' ;
- Each path from the top of the square to the left ending at x becomes a path from the top edge of the square to itself ending at x' ; and
- intersection points with β and curve segments that do not meet the left edge of the square are unaffected.

We can attempt to read off a type D structure from this new train track in the usual way, although we note that the result may not be a valid type D structure (it may fail to satisfy $\partial^2 = 0$). In any case, the result is precisely what is obtained from N by tensoring with \widehat{T}_α , if we ignore the two operations in \widehat{T}_α with multiple \mathcal{A}_∞ inputs. Indeed, referring to Figure 45, this has the following effect on N :

- For each ι_0 generator x we add a new ι_1 generator x' such that x and x' are connected by a ρ_2 arrow;
- Each ρ_2 arrow ending at x becomes a ρ_{23} arrow ending at x' ;

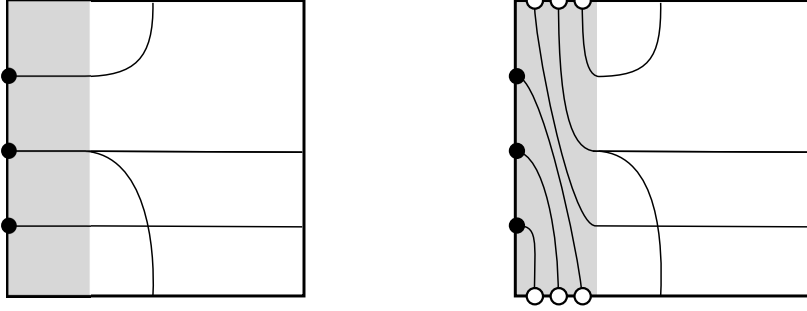


Figure 46. Applying a Dehn twist to a train track

- Each ρ_{12} arrow ending at x becomes a ρ_{123} arrow ending at x' ;
- Each path ρ_3 arrow starting at x becomes an arrow labelled by $1 = \rho_0$ starting at x' ; and
- ι_0 generators, ρ_1 , ρ_{123} and ρ_{23} arrows are unchanged.

Note that each ρ_3 in N gives rise to a ρ_0 labelled arrow in the tensor product, and a corresponding bigon between ϑ' and β . We will now use the assumption that ϑ is curve-like and that there are no crossover arrows between segments corresponding to ρ_3 arrows in N ; it follows that bigons between ϑ' and β appear in one of the three configurations shown in Figure 47. These three configurations arise from ρ_3 arrows in ϑ which are followed by, respectively, backwards ρ_1 arrows, ρ_{23} arrows, and ρ_2 arrows. Note that in the latter two configurations, adding the gray segments shown in the figure corresponds to incorporating the two operations of \widehat{T}_α that we ignored until now into the box tensor product with N —each (ρ_3, ρ_{23}) or (ρ_3, ρ_2) sequence in N gives becomes a ρ_3 in the tensor product. Let ϑ'' be the result of adding these gray lines to ϑ' . Note that ϑ'' is a valid (not necessarily reduced) train track and the corresponding type D structure is precisely $\widehat{T}_\alpha \boxtimes N$.

Now consider the effect of removing the bigons between ϑ'' and β . In the first configuration, removing the bigons by homotoping the parallel immersed curves has precisely the effect of canceling ρ_0 arrows in the underlying type D structures. Each ρ_1 arrow into a generator z for which there is a ρ_0 arrow from x' to z and a ρ_2 arrow from x' to x becomes a ρ_{12} into x . In the second two configurations, the bigons the segments of ϑ'' forming the bigon can simply be deleted. This is because in the corresponding type D structure, the terminal endpoint of the ρ_0 arrows have no other incoming arrows, so the endpoints of the ρ_0 arrows can be canceled without adding any new arrows. In all three configurations, it is clear that the result of removing the bigons from ϑ'' in the appropriate way is simply the result of homotoping ϑ' to be in minimal position with β .

We have shown that a curve-like train track associated with $\widehat{T}_\alpha \boxtimes N$ is obtained from ϑ by applying a negative Dehn twist about α . Thus, interpreting curve-like train tracks as decorated immersed curves, we have that $f_{\alpha,\beta}(\widehat{T}_\alpha \boxtimes N)$ is obtained from $f(N)$ by applying the same Dehn twist to the underlying curve γ of $f(N)$. It follows that $f_{\alpha,\beta}(N) \cong f_{\alpha,\beta+\alpha}(\widehat{T}_\alpha \boxtimes N)$, since the change of marking cancels the action of the Dehn twist.

A similar argument applies to the bimodule \widehat{T}_α^{-1} , where tensoring by this bimodule has the effect of applying a positive Dehn twist about α to the corresponding train track and to $f(N)$. However, it is easier to observe that $f_{\alpha,\beta}(N) = f_{\alpha,\beta}(\widehat{T}_\alpha \boxtimes \widehat{T}_\alpha^{-1} \boxtimes N)$ is obtained from $f_{\alpha,\beta}(\widehat{T}_\alpha^{-1} \boxtimes N)$ by applying a negative Dehn twist, so $f_{\alpha,\beta}(\widehat{T}_\alpha^{-1} \boxtimes N)$ is obtained from $f_{\alpha,\beta}(N)$ by applying a positive Dehn twist. Again, we see that $f_{\alpha,\beta}(N) \cong f_{\alpha,\beta-\alpha}(\widehat{T}_\alpha^{-1} \boxtimes N)$, since the change of marking cancels the action of the Dehn twist. \square

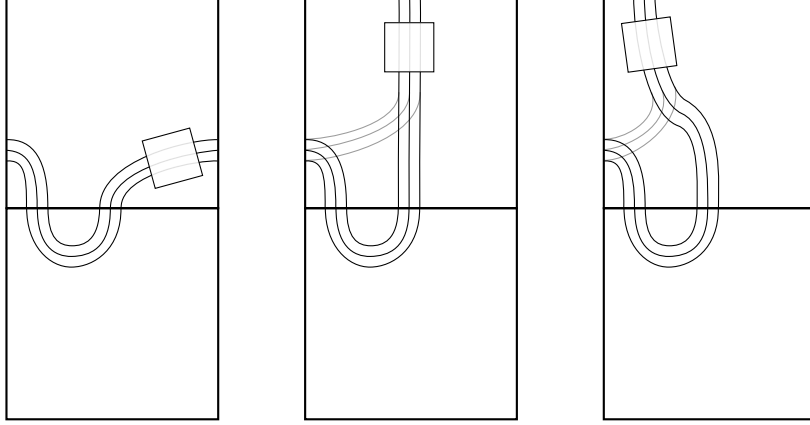


Figure 47. Possible configurations of bigons in \mathfrak{V}' corresponding to ρ_3 arrows in N that are followed by backward ρ_1 arrows, ρ_{23} arrows, and ρ_2 arrows, respectively. The assumption that \mathfrak{V} has no crossover arrows between segments corresponding to ρ_3 arrows ensures that the bigons do not involve any crossover arrows; there could be crossover arrows in the boxes shown. The black segments are part of \mathfrak{V}' and \mathfrak{V}'' is obtained from \mathfrak{V}' by adding the gray segments in the second and third configuration.

Since we can move between any two markings/bordered structures by a sequence of Dehn twists, Proposition 39 ensures that

$$f_{\alpha,\beta}(\widehat{CFD}(M, \alpha, \beta)) \cong f_{\alpha',\beta'}(\widehat{CFD}(M, \alpha', \beta'))$$

for any two pairs of parametrizing curves (α, β) and (α', β') .

We will write

$$\widehat{HF}(M) = f_{\alpha,\beta}(\widehat{CFD}(M, \alpha, \beta)).$$

As we have shown, this definition is independent of the choice of parametrization (α, β) . This completes the proof of Theorem 1.

We now turn to the proof of Theorem 2. Recalling the set-up of the theorem, suppose M_0 and M_1 are manifolds with torus boundary and $h : \partial M_1 \rightarrow \partial M_0$ is a gluing map. Chose a parametrization (α_1, β_1) for ∂M_1 and fix the parametrization (α_0, β_0) of ∂M_0 by setting $\alpha_0 = h(\beta_1)$ and $\beta_0 = h(\alpha_1)$. Following the conventions for bordered Heegaard Floer invariants (see Section 2.2), these parametrizations are consistent with the gluing map h ; that is, by the pairing theorem in [25], $\widehat{HF}(M_0 \cup_h M_1)$ is given by the homology of $\widehat{CFA}(M_0, \alpha_0, \beta_0) \boxtimes \widehat{CFD}(M_1, \alpha_1, \beta_1)$. By the equivalence of categories proved Section 4, the homology of this box tensor product agrees with the pairing of the decorated immersed curves $f(\widehat{CFD}(M_0, \alpha_0, \beta_0))$ and $f(\widehat{CFA}(M_1, \alpha_1, \beta_1))$. To pair these curves, following section 4.2, we include them in the same marked torus, reflecting one across the anti-diagonal, and take intersection Floer homology. Note that as 3-manifold invariants, we think of $\widehat{HF}(M_0) = f(\widehat{CFD}(M_0, \alpha_0, \beta_0))$ and $\widehat{HF}(M_1) = f(\widehat{CFA}(M_1, \alpha_1, \beta_1))$ as living in two different marked tori, the parametrized boundaries of M_0 and M_1 . Identifying these marked tori with a reflection across the anti-diagonal corresponds to a gluing map which takes α_1 to $-\beta_0$ and β_1 to α_0 ; this is precisely the map \bar{h} , the elliptic involution composed with h . Letting γ_0 denote $\widehat{HF}(M_0)$ and γ_1 denote the image of $\widehat{HF}(M_1)$ under \bar{h} , the pairing is given by $HF(\gamma_0, \gamma_1)$, as claimed.

6. GRADINGS

The bordered invariants of M come equipped with a mod 2 and a Spin^c grading. In this section, we explain how the invariant $\widehat{HF}(M)$ can be enhanced to capture this information, leading to a proof of Theorem 7. While this does not capture all of the graded information in the bordered Heegaard Floer

Edge type	Vertex sign	Orientation	Edge type	Vertex sign	Orientation
I_•	+	● ←	I_◦	+	◦ →
I_•	-	● →	I_◦	-	◦ ←
II_•	+	● →	II_◦	+	◦ ←
II_•	-	● ←	II_◦	-	◦ →

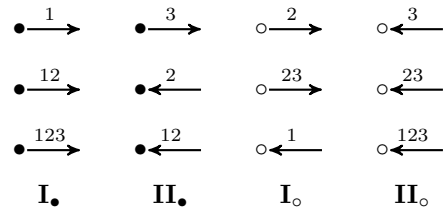
Table 1. Producing the oriented graph given a signed decorated graph Γ and the vertex types from Figure 48.

package, it is sufficient for the applications in this paper; a more thorough discussion of gradings, including the Maslov grading, will appear in the companion to this paper [16].

6.1. The $\mathbb{Z}/2\mathbb{Z}$ grading. We first recall the $\mathbb{Z}/2\mathbb{Z}$ grading in bordered Floer homology. For each spin^c structure \mathfrak{s} , $\widehat{CFD}(M, \alpha, \beta; \mathfrak{s})$ admits a relative $\mathbb{Z}/2\mathbb{Z}$ grading gr^D as defined by Petkova in [29]. (This grading may be identified with a specialization of the full grading package on the bordered invariants; see [21, Appendix A].) The relative $\mathbb{Z}/2\mathbb{Z}$ grading satisfies $\text{gr}^D(\partial x) = \text{gr}^D(x) - 1$ and $\text{gr}^D(a \otimes x) = \text{gr}^D(a) + \text{gr}^D(x)$ for $a \in \mathcal{A}$, where $\text{gr}^D(\rho_1) = \text{gr}^D(\rho_3) = 0$ and $\text{gr}^D(\rho_2) = \text{gr}^D(\rho_{123}) = \text{gr}^D(\rho_{12}) = \text{gr}^D(\rho_{23}) = 1$. Note that if $\widehat{CFD}(M, \alpha, \beta; \mathfrak{s})$ is connected (see below), the relative $\mathbb{Z}/2\mathbb{Z}$ grading is completely determined by this condition. The generators of $\widehat{CFA}(M, \alpha, \beta; \mathfrak{s})$ inherit a grading gr^A from the corresponding generators in $\widehat{CFD}(M, \alpha, \beta; \mathfrak{s})$, where the grading of generators with idempotent ι_0 is reversed. A generator $x_0 \otimes x_1$ in a box tensor product $\widehat{CFA}(M_0, \alpha_0, \beta_0) \boxtimes \widehat{CFD}(M_1, \alpha_1, \beta_1)$ inherits the grading $\text{gr}^A(x_0) + \text{gr}^D(x_1)$, which recovers the relative $\mathbb{Z}/2\mathbb{Z}$ grading on $\widehat{CF}(M_0 \cup M_1)$.

The graph representing a $\mathbb{Z}/2\mathbb{Z}$ graded type D structure can be enhanced, replacing the vertex labeling $\{\bullet, \circ\}$ with $\{\bullet^+, \bullet^-, \circ^+, \circ^-\}$, where $+$ designates grading 0 and $-$ designates grading 1.

We first observe that this data is equivalent to a choice of orientation on each edge of the underlying (undecorated) graph. To see this, it is convenient to partition vertices into 4 types, as in Figure 48. This is a natural partition to consider in the context of extendable type D structures:



Proposition 40. *Suppose that Γ is a decorated graph associated with a reduced extendable type D structure N . Then every vertex \bullet has at least one incident edge of type **I_•** and at least one incident edge of type **II_•**, and every vertex \circ has at least one incident edge of type **I_◦** and at least one incident edge of type **II_◦**.*

Figure 48. Vertex types for decorated graphs.

Proof. This is essentially [17, Proposition 3.3]. □

In particular, when Γ has valence 2 (and hence the associated train track is an immersed curve), there is exactly one of each edge type incident at every vertex.

This partition allows us to convert the system of signed vertices into an orientation on the underlying graph. The orientations on edges incident to any given vertex are assigned following the rules in Table 1. See Figure 49 for this process carried out in an example. Note that reversing the overall orientation on this graph corresponds to switching the grading of every vertex, and vice versa. For consistency with the gradings on the relevant bordered invariants, if an orientation in a given component is to be changed one must reverse orientations on every connected component corresponding to the relevant summand $\widehat{CFD}(M, \alpha, \beta; \mathfrak{s})$.

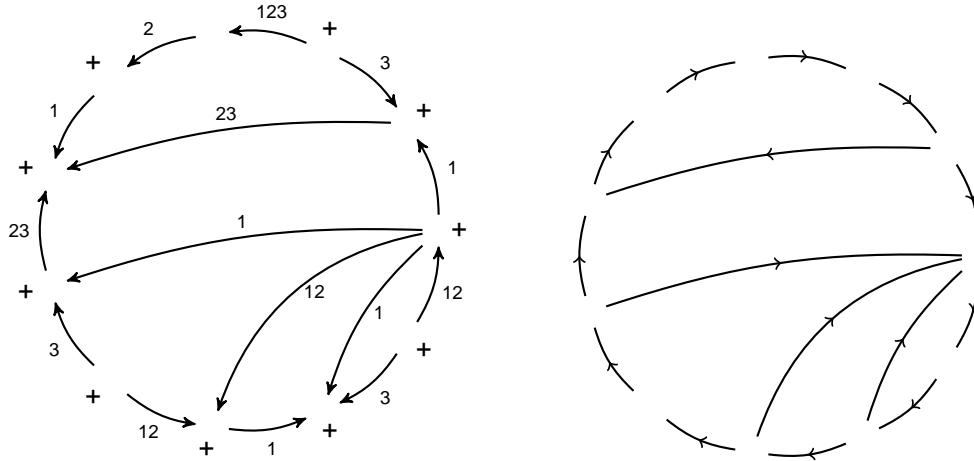


Figure 49. A $Z=2Z$ augmentation of a decorated graph (left), and the associated orientation graph (right).

Lemma 41. The conventions of Table 1 define a consistent orientation on each edge of the graph.

Proof. It is enough to check that edges labelled 2 and 123 change the grading and that all other labelings preserve it. It is easy to see from the table that the two ends of an edge have the same mod 2 grading if they are both of the same type (i.e. both I or both II). Referring to Figure 48, we see that edges labeled 2 and 123 have one end of type I and one of type II; other edges have ends of the same type.

Remark 42. The condition from Proposition 40 ensures that every vertex of the graph has both an inward pointing and an outward pointing edge. If the graph is a loop corresponding to an immersed curve in $T(M)$, it follows that the $Z=2Z$ grading is completely determined by the choice of an orientation on γ . More generally, if the graph corresponds to an immersed curve with a connected local system, all the parallel curves in the local system must carry the same orientation. Thus to specify the $Z=2Z$ grading it is again enough to specify an orientation on the underlying immersed curve.

6.2. The Spin^c grading. We first review the Spin^c grading on bordered Floer homology. Recall that each generator x of $\widehat{\text{CFD}}(M; \mathfrak{s}; \mathfrak{t})$ has an associated spin structure $s(x) \in \text{Spin}^c(M)$. The elements of $\text{Spin}^c(M)$ are homology classes of nonvanishing vector fields on M , and $\text{Spin}^c(M)$ has the structure of a finite set modeled on $H^2(M) = H_1(M; @M)$. The same decomposition holds for $\widehat{\text{CFA}}(M; \mathfrak{s}; \mathfrak{t})$, so that

$$\widehat{\text{CFD}}(M; \mathfrak{s}; \mathfrak{t}) = \bigoplus_{s \in \text{Spin}^c(M)} \widehat{\text{CFD}}(M; \mathfrak{s}; \mathfrak{t}; s) \quad \text{and} \quad \widehat{\text{CFA}}(M; \mathfrak{s}; \mathfrak{t}) = \bigoplus_{s \in \text{Spin}^c(M)} \widehat{\text{CFA}}(M; \mathfrak{s}; \mathfrak{t}; s):$$

Restricting attention to the generators in a particular idempotent \mathfrak{t} , then we can also define a refined spin^c grading $s(x) \in \text{Spin}^c(M; \mathfrak{t})$, which lives in a finite set modeled on $H^2(M; @M) = H_1(M)$. Elements of $\text{Spin}^c(M; \mathfrak{t})$ are homology classes of nonvanishing vector fields with prescribed behavior on $@M$ and $s(x)$ is the image of $s(x)$ in $\text{Spin}^c(M)$.

To compare the refined gradings of two generators, we adopt the following. Given $t \in \text{Spin}^c(M)$, let

$$\text{Spin}^c(M; \mathfrak{t}; t) = \{s \in \text{Spin}^c(M; \mathfrak{t}) \mid s = t \text{ in } \text{Spin}^c(M) \}:$$

If $j : H_1(@M) \rightarrow H_1(M)$ is the map induced by inclusion, $\text{Spin}^c(M; \mathfrak{t}; t)$ is a finite set modeled on $H_M = \text{im } j = H_1(@M) = \ker j$. When $@M$ is a torus we let $\text{Spin}^c(M; \mathfrak{t}; t) = \text{Spin}^c(M; \mathfrak{t}_0; t) \sqcup \text{Spin}^c(M; \mathfrak{t}_1; t)$ and define

$$\frac{1}{2}H_M = \{x \in H_1(@M; \mathbb{R}) \mid j(x) \in H_1(M; \mathbb{Z}) \} = \ker j$$

Labeled edge	$\mathfrak{s}(y) - \mathfrak{s}(x)$	Labeled edge	$\mathfrak{s}(y) - \mathfrak{s}(x)$
$x \xrightarrow{1} y$	$-(\alpha + \beta)/2$	$x \xrightarrow{12} y$	$-\beta$
$x \xrightarrow{2} y$	$(\alpha - \beta)/2$	$x \xrightarrow{23} y$	α
$x \xrightarrow{3} y$	$(\alpha + \beta)/2$	$x \xrightarrow{123} y$	$(\alpha - \beta)/2$

Table 2. Grading shifts in $\widehat{CFD}(M, \alpha, \beta)$ associated with labelled edges.

Given two generators x and y in $\widehat{CFD}(M, \alpha, \beta; \mathfrak{s})$ with idempotents ι_x and ι_y , respectively, we think of the grading difference $\mathfrak{s}_{\iota_x}(x) - \mathfrak{s}_{\iota_y}(y)$ as an element of $\frac{1}{2}H_M$, which is in H_M if and only if $\iota_x = \iota_y$.

Lemma 43. *We can identify $\text{Spin}^c(M, \mathfrak{t})$ with a subset of $\frac{1}{2}H_M$ in such a way that arrows in $\widehat{CFD}(M, \alpha, \beta)$ shift the Spin^c grading as shown in Table 2.*

Proof. This is just a rephrasing of [30, Lemma 3.8]; compare [25, Lemma 11.42]. Specifically, choose some identification $f: \text{Spin}^c(M, \iota_0, \mathfrak{t}) \rightarrow H_M$. For $\mathfrak{s} \in \text{Spin}^c(M, \iota_0, \mathfrak{t})$, we identify \mathfrak{s} with $f(\mathfrak{s})$, and for $\mathfrak{s} \in \text{Spin}^c(M, \iota_1, \mathfrak{t})$ we identify \mathfrak{s} with $f(i^{-1}(\mathfrak{s})) - (\alpha + \beta)/2$, where $i: \text{Spin}^c(M, \iota_0, \mathfrak{t}) \rightarrow \text{Spin}^c(M, \iota_1, \mathfrak{t})$ is the map defined in [30, Lemma 3.8]. \square

Let (M_0, α_0, β_0) and (M_1, α_1, β_1) be two bordered three-manifolds with torus boundary and consider the box tensor product $\widehat{CFA}(M_0, \alpha_0, \beta_0) \boxtimes \widehat{CFD}(M_1, \alpha_1, \beta_1)$. For x_0, y_0 in $\widehat{CFA}(M_0, \alpha_0, \beta_0; \mathfrak{s}_0)$ and x_1, y_1 in $\widehat{CFD}(M_1, \alpha_1, \beta_1; \mathfrak{s}_1)$, the grading difference $s_{\iota_{x_0}}(x_0) + s_{\iota_{x_1}}(x_1) - s_{\iota_{y_0}}(y_0) - s_{\iota_{y_1}}(y_1)$ between $x_0 \otimes x_1$ and $y_0 \otimes y_1$ is a well defined element of

$$H_1(\partial M_0) / (\ker(j_{0,*}) \oplus \ker(j_{1,*})) \cong H_1(M_0 \cup M_1),$$

where $j_{i,*}$ is the map induced by the inclusion $j_i: H_1(\partial M_i) \rightarrow H_1(M_i)$. This recovers the Spin^c decomposition of $\widehat{CF}(M_0 \cup M_1)$.

In section 2 we explained how to assign a train track $\mathfrak{v}(M, \alpha, \beta)$ in T_M to the type D structure $\widehat{CFD}(M, \alpha, \beta)$. Since the differential on $\widehat{CFD}(M, \alpha, \beta)$ respects the decomposition into Spin^c structures, $\mathfrak{v}(M, \alpha, \beta)$ decomposes as a union of train tracks $\mathfrak{v}(M, \alpha, \beta; \mathfrak{s})$, where \mathfrak{s} runs over $\text{Spin}^c(M)$.

Recall from the introduction that \overline{T}_M is the cover of T_M whose fundamental group is the kernel of the composite map $\pi_1(T_M) \rightarrow H_1(T_M) \rightarrow H_1(\partial M) \rightarrow H_1(M)$.

Proposition 44. *$\mathfrak{v}(M, \alpha, \beta; \mathfrak{s})$ lifts to a train track $\overline{\mathfrak{v}}(M, \alpha, \beta; \mathfrak{s})$ in \overline{T}_M .*

Proof. Let q_1 and q_0 be the midpoints of the α and β arcs in $T(M)$. The set of lifts of q_1 to \overline{T}_M is an H_M torsor; fix an identification of this set with $\text{Spin}^c(M, \iota_1, \mathfrak{t})$. The set of lifts of q_0 is also an H_M torsor; identify it with $\text{Spin}^c(M, \iota_0, \mathfrak{t})$ in such a way that if $q_i(\overline{\mathfrak{s}}_i)$ is the lift of q_i corresponding to $\overline{\mathfrak{s}}_i$ then $q_1(\overline{\mathfrak{s}}_1) - q_2(\overline{\mathfrak{s}}_2) = \overline{\mathfrak{s}}_1 - \overline{\mathfrak{s}}_2$, where the difference on the right-hand side is the one given by Lemma 43.

Each generator x in idempotent ι_i of $\widehat{CFD}(M, \alpha, \beta; \mathfrak{s})$ corresponds to a primary switch of $\mathfrak{v}(M, \alpha, \beta; \mathfrak{s})$ which is near to q_i . We lift the switch corresponding to x to a point near $q_i(\text{Spin}^c_{\iota_i}(x))$. Comparing the grading shifts in Table 2 with Figure 7, we see that each arc of $\mathfrak{v}(M, \alpha, \beta; \mathfrak{s})$ lifts to a unique arc in \overline{T}_M which is compatible with the lifts of its endpoints. \square

Remark 45. It is clear from the construction that $\overline{\mathfrak{v}}(M, \alpha, \beta; \mathfrak{s})$ is well-defined up to the action of the deck group H_M on the covering space T_M .

Proof of Theorem 7. Orient the track $\vartheta(M, \alpha, \beta; \mathfrak{s})$ and lift it to a collection of oriented tracks $\overline{\vartheta}(M, \alpha, \beta; \mathfrak{s})$ in \overline{T}_M . The result is a compact train track in the cover \overline{T}_M , which we now simplify as in section 3. In fact, we can simplify $\overline{\vartheta}(M, \alpha, \beta)$ using exactly the same moves as we used to simplify ϑM down in T_M . Each move we perform involves some arcs and/or crossover arrows which are supported in the 0-handle of the downstairs track. It is easy to see from the definition that all of the arcs involved lift up to a single 0-handle in the cover, so the move can be performed on the cover as well.

It is also easy to see that these moves respect the relative $\mathbb{Z}/2$ grading. For example, consider move (M1), which eliminates a clockwise running crossover arrow which runs from x to y , as in Proposition 25. Let z be the generator connected to y by the two-way arc, so that ∂y contains a term of the form $\rho_J \otimes z$. The presence of the crossover arrow implies that ∂x contains a term of the form $\rho_{IJ} \otimes z$. It follows that x and $\rho_I \otimes y$ have the same $\mathbb{Z}/2$ grading, so the change of basis in which we replace x by $x + \rho_I \otimes y$ respects the $\mathbb{Z}/2$ grading. The argument for move (M2) is very similar.

We define $\overline{\vartheta}(M, \mathfrak{s})$ to be this simplified train track; its image in T_M is the track obtained by simplifying $\vartheta(M, \mathfrak{s})$. Finally, the same argument as in section 5 shows that $\overline{\vartheta}(M, \mathfrak{s})$ does not depend on the choice of parametrization. We denote the resulting invariant by $\widehat{HF}(M, \mathfrak{s})$. \square

To sum up, $\widehat{HF}(M, \mathfrak{s})$ is a well-defined collection of curves equipped with local systems in the cover \overline{T}_M . Note that it can be dangerous to view different copies of $\widehat{HF}(M, \mathfrak{s})$ as being contained in the same copy of \overline{T}_M . When we want to emphasize the fact that we are thinking of the copy of \overline{T}_M containing $\widehat{HF}(M, \mathfrak{s})$, we will denote it by $\overline{T}_{M, \mathfrak{s}}$.

6.3. The refined pairing theorem. We conclude by giving a refined version of the pairing theorem. Suppose that $Y = M_0 \cup_h M_1$. Restriction gives a surjective map

$$\pi : \text{Spin}^c(Y) \rightarrow \text{Spin}^c(M_1) \times \text{Spin}^c(M_2).$$

If $\mathfrak{s}_i \in \text{Spin}^c(M_i)$, it is not hard to see that $\pi^{-1}(\mathfrak{s}_0 \times \mathfrak{s}_1)$ is a torsor over $H_Y = H_1(\partial M_0) / \langle \lambda_0, h_*(\lambda_1) \rangle$, where λ_i is the homological longitude of M_i . Let \overline{T}_Y be the covering space of T_{M_0} whose fundamental group is the kernel of the natural map $\pi_1(T_{M_0}) \rightarrow H_1(T_{M_0}) \rightarrow H_Y$. \overline{T}_Y is the largest covering space of T_M which is covered by both \overline{T}_{M_0} and \overline{T}_{M_1} .

Let $p_i : \overline{T}_{M_i} \rightarrow \overline{T}_Y$ be the projection, and let \overline{p}_1 be the composition with p_1 with the elliptic involution on \overline{T}_Y . (The elliptic involution is the map which descends from the map $w \mapsto -w$ on the universal cover. It is well defined up to the action of the deck group.) The images $p_0(\widehat{HF}(M_0, \mathfrak{s}_0))$ and $\overline{p}_1(\widehat{HF}(M_1, \mathfrak{s}_1))$ are well defined up to the action of the deck group H_Y .

Proposition 46. *Suppose that $\mathfrak{s} \in \text{Spin}^c(Y)$ has $\pi(\mathfrak{s}) = \mathfrak{s}_1 \times \mathfrak{s}_2$. There is some $\alpha_{\mathfrak{s}} \in H_Y$ such that $\widehat{HF}(Y, \mathfrak{s})$ is given by the pairing of $p_0(\widehat{HF}(M_0, \mathfrak{s}_0))$ with $\alpha_{\mathfrak{s}} \cdot \overline{p}_1(\widehat{HF}(M_1, \mathfrak{s}_1))$ in \overline{T}_Y . Moreover, the relative $\mathbb{Z}/2$ grading of a generator of $\widehat{HF}(Y, \mathfrak{s})$ is given by the sign of the corresponding intersection point.*

Proof. It suffices to check that the statement about Spin^c structures holds for the train tracks $\vartheta(M_0; \mathfrak{s}_0), \vartheta(M_1, \mathfrak{s}_1)$ (before simplification), since the pairings before and after simplification are the same. Suppose x_0, x_1 are generators of $\widehat{CFA}(M_0), \widehat{CFD}(M_1)$ which pair to give a generator of $\widehat{HF}(Y, \mathfrak{s})$. Then we must have $x_0 \in \widehat{CFD}(M_0, \mathfrak{s}_0)$ and $x_1 \in \widehat{CFD}(M_1, \mathfrak{s}_1)$, and we may choose $\alpha_{\mathfrak{s}}$ so that the intersection between the train tracks $p_0(\vartheta(M_0); \mathfrak{s})$ and $\alpha_{\mathfrak{s}} \cdot \overline{p}_1(\vartheta(M_1; \mathfrak{s}))$ contains the intersection between the segments corresponding to x_0 and x_1 . If y_0, y_1 are other generators of $\widehat{CFA}(M_0, \mathfrak{s}_0)$ and $\widehat{CFD}(M_1, \mathfrak{s}_1)$, $y_0 \boxtimes y_1$ will be a generator of $\widehat{CF}(Y, \mathfrak{s})$ if and only if the image of $\mathfrak{s}(x_0) - \mathfrak{s}(y_0) - \mathfrak{s}(x_1) + \mathfrak{s}(y_1)$ is 0 in $H_1(Y)$. This is equivalent to saying that $\mathfrak{s}(x_0) - \mathfrak{s}(y_0)$ and

$\mathfrak{s}(x_1) - \mathfrak{s}(y_1)$ have the same image in $H_1(Y)$, and this occurs if and only if the segments corresponding to y_0 and y_1 intersect in $p_0(\mathfrak{g}(M_0); \mathfrak{s}) \cap \alpha_{\mathfrak{s}} \cdot \bar{p}_1(\mathfrak{g}(M_1; \mathfrak{s}))$.

Next, consider the relative $\mathbb{Z}/2\mathbb{Z}$ grading. Recall that fixing the $\mathbb{Z}/2\mathbb{Z}$ grading on $\widehat{CFA}(M_0, \alpha_0, \beta_0)$ corresponds to choosing an orientation of each curve in $\gamma_0 = \widehat{HF}(M_0)$. In particular, upward (respectively downward) oriented α_0 segments in γ_0 correspond to \circ^+ (respectively \circ^-) generators of $\widehat{CFA}(M_0, \alpha_0, \beta_0)$, and rightward (respectively leftward) oriented β_0 segments in γ_0 correspond to \bullet^+ (respectively \bullet^-) generators of $\widehat{CFA}(M_0, \alpha_0, \beta_0)$. Fixing the $\mathbb{Z}/2\mathbb{Z}$ grading on $\widehat{CFD}(M_1, \alpha_1, \beta_1)$ corresponds to choosing orientations on $\gamma_1 = \widehat{HF}(M_1)$ with similar identification except that the grading is reversed on \bullet generators. Reflecting across the anti-diagonal, it follows that upward (respectively downward) oriented segments in γ_1 correspond to \bullet^+ (respectively \bullet^-) generators of $\widehat{CFD}(M_1, \alpha_1, \beta_1)$ and rightward (respectively leftward) oriented segments in γ_1 correspond to \circ^- (respectively \circ^+) generators of $\widehat{CFD}(M_1, \alpha_1, \beta_1)$. The (relative) $\mathbb{Z}/2\mathbb{Z}$ grading on $\widehat{HF}(M_0 \cup_h M_1)$ is given by $\text{gr}(x \otimes y) = \text{gr}^A(x) + \text{gr}^D(y)$, while the grading of $HF(\gamma_0, \gamma_1)$ is given by intersection signs. It is straightforward to check that generators of $\widehat{HF}(M_0 \cup_h M_1)$ of the form $\circ^+ \otimes \circ^+$, $\circ^- \otimes \circ^-$, $\bullet^+ \otimes \bullet^+$, and $\bullet^- \otimes \bullet^-$, which all have the same $\mathbb{Z}/2\mathbb{Z}$ grading, correspond exactly to positive intersection points and the remaining generators correspond to negative intersection points. \square

6.4. Longitudinal gluings. As an example, we describe in detail the case where h identifies the rational longitudes of M_0 and M_1 , so that Y contains a new closed surface. First suppose that we have a manifold M whose rational longitude λ has order k in $H_1(M)$. Choose a class $x \in H_2(M, \partial M)$ with $\partial x = k\lambda$, and a class μ in $H_1(M)$ with $\mu \cdot \lambda = 1$, so that $\mu \cdot x = k$.

Note that $\iota_0 \widehat{CFD}(M, \mu, \lambda)$ counts minimal-position intersections of $\widehat{HF}(M)$ with a copy of μ which passes through the basepoint z . On the other hand,

$$\iota_0 \widehat{CFD}(M, \mu, \lambda) \simeq SFH(M, \gamma_\mu) \simeq \widehat{HFK}(K_\mu)$$

where K_μ is the core of the Dehn filling $M(\mu)$. In summary, we can compute the knot Floer homology of K_μ by intersecting $\widehat{HF}(M)$ with a line of slope μ passing through z . (We will return to this point in [16].)

The Spin^c decomposition of $\widehat{HFK}(K_\mu)$ is determined as follows. Let $r: \text{Spin}^c(M, \partial M) \rightarrow \text{Spin}^c(M)$ be the restriction map. Given $\mathfrak{s} \in \text{Spin}^c(M)$, $r^{-1}(\mathfrak{s})$ is a $G = k\mathbb{Z} \oplus \mathbb{Z}/k$ -torsor, where G is the image of $H_1(\partial M)$ in $H_1(M)$. Let $\gamma \in \pi_1(T_M, z)$ be a path representing μ . The set of lifts of γ to \bar{T}_M is also a G -torsor. We label the set of lifts by μ_α and the elements of $r^{-1}(\mathfrak{s})$ by \mathfrak{s}_α in such a way that $\widehat{HFK}(K_\mu, \mathfrak{s}_\alpha)$ counts intersections of $\widehat{HF}(M, \mathfrak{s})$ with μ_α .

Fix $\mathfrak{s} \in \text{Spin}^c(M, \partial M)$ and consider $\widehat{HF}(M, \mathfrak{s}) \subset \bar{T}_{M, \mathfrak{s}}$. The class x determines a height function $h_x: \bar{T}_{M, \mathfrak{s}} \rightarrow \mathbb{R}$, which is constant on curves parallel to λ and evaluates to $\frac{1}{2} \langle c_1(\mathfrak{s}_\alpha), x \rangle$ at the midpoint of μ_α . In particular, if μ_α and $\mu_{\alpha'}$ are two consecutive lifts of μ , the heights of their midpoints differ by $\mu \cdot x = k$.

Now suppose that we have two manifolds M_0 and M_1 with rational longitudes λ_i of order k_i which are identified by h . Let $k = \text{gcd}(k_1, k_2)$, and define $c_i = k_i/k$. Given $x_i \in H_2(M_i, \partial M_i)$ as above, we can form a primitive class $y = c_2 x_1 - c_1 x_2 \in H_2(Y)$. Given $\mathfrak{s}_i \in \text{Spin}^c(M_i)$, let $\gamma_i = \widehat{HF}(M_i, \mathfrak{s}_i)$. Then for $\mathfrak{t} \in \pi^{-1}(\mathfrak{s}_0, \mathfrak{s}_1)$,

$$\widehat{HF}(Y, \mathfrak{t}) = \text{Hom}(p_0(\gamma_0), \alpha_{\mathfrak{t}} \cdot \bar{p}_1(\gamma_1)),$$

where $\alpha_{\mathfrak{t}} \in H_Y = H_1(\partial M_0)/\langle k_0 \lambda_0, k_1 \lambda_0 \rangle \simeq \mathbb{Z} \oplus \mathbb{Z}/k$.

The height functions h_{x_i} on \bar{T}_{M_i} induce height functions $h_{y,i}: \bar{T}_Y \rightarrow \mathbb{R}$ given by $h_{y,1}(p_1(w)) = c_2 h_{x_1}(w)$ and $h_{y,2}(p_1(w)) = -c_1 h_{x_1}(w)$. Then $\langle c_1(\mathfrak{t}), y \rangle$ measures the shift in heights induced by $\alpha_{\mathfrak{t}}$

so that

$$\langle c_1(t), y \rangle = 2(h_{y,1}(\alpha_t \cdot w) - h_{y,2}(w))$$

for all $w \in \overline{T}_Y$.

7. APPLICATIONS

With invariance (Theorem 1) and pairing (Theorem 2) for $\widehat{HF}(M)$ established, we can now provide proofs for the applications stated in the introduction. To facilitate the proofs, we will first discuss a convenient way of arranging the curves $\widehat{HF}(M)$.

7.1. Peg-board diagrams. To visualize the essential properties of the immersed curves, it is helpful to consider particular minimal representatives of $\widehat{HF}(M)$ defined as follows: Fix a metric on the torus T and a sufficiently small $\epsilon > 0$. Consider the minimal length representative of the homotopy class of $\widehat{HF}(M)$, subject to the requirement that the resulting curve is distance at least ϵ from the marked point. We call the result a *peg-board representative* for $\widehat{HF}(M)$, imagining that there is a *peg* of radius ϵ centered at the marked point. We can also discuss peg-board representatives for the lift of $\widehat{HF}(M)$ to $\mathbb{R}^2 \setminus \mathbb{Z}^2$, imagining a peg of radius ϵ centered at each lattice point. The arrangement of pegs and minimal length curves will also be referred to as a peg-board diagram. At times it is useful to consider the piecewise linear curve in the covering space \tilde{T} which results from shrinking the peg radius to 0 in a peg-board diagram. This curve, which we call the *singular peg-board representative* of $\widehat{HF}(M)$, consists of line segments connecting lattice points in \mathbb{R}^2 . See Figure 51 or Figure 54 for examples of peg-board and singular peg-board diagrams. We will say that a curve is pulled tight if it is in peg-board position.

Peg-board diagrams provide a simple way to put curves in minimal intersection position. If γ_1 and γ_2 are peg-board representatives for two curves relative to some peg radius ϵ and γ_1 intersects γ_2 transversally, then it is not difficult to see that γ_1 and γ_2 are in minimal position. Suppose, to the contrary, that there is some bigon in T connecting intersection points x and y . The corresponding segments from x to y in γ_1 and in γ_2 are homotopic to each other in T . They are not equal to each other, since γ_1 and γ_2 intersect transversally, so at most one of them can be the (unique) minimal length path connecting x to y in T with distance at least ϵ from the marked point; this contradicts the fact that both γ_1 and γ_2 have minimal length. In general, peg-board representatives for two curves relative to the same radius will not have transverse intersection, but the same principle applies after perturbing the curves slightly, as we now describe.

By a corner we will mean any time a curve passes through a lattice point in a singular peg-board diagram (even if there is no change in direction), or equivalently any time the curve touches a peg in a peg-board diagram. To ensure transverse intersection, we will think of each corner as wrapping around a peg of a different radius. More precisely, let k be the total number of corners in γ_1 and γ_2 , and let $\epsilon_1, \dots, \epsilon_k$ be k different peg radii between ϵ and $\frac{3\epsilon}{2}$. Starting with (radius ϵ) peg-board representatives for γ_1 and γ_2 , we perturb the i th corner by pushing the curve away from the marked point to a minimum distance of ϵ_i for $1 \leq i \leq k$, and we minimize the length of each curve subject to this new constraint. After this modification, γ_1 and γ_2 have transverse intersection; whether or not the intersection is minimal depends on relative sizes of the peg radii ϵ_i . Note that each corner in a peg-board includes a path in the boundary of the peg, the circle of radius ϵ_i ; this in turn determines an interval in \mathbb{R} , by mapping $(\epsilon_i \cos \theta, \epsilon_i \sin \theta)$ to θ , well defined up to shifting by 2π . We define a partial order on corners by saying $c_1 < c_2$ if the interval in \mathbb{R} corresponding to c_2 is strictly contained in the interval corresponding to c_1 , possibly after shifting by a multiple of 2π . We will require that $\epsilon_1, \dots, \epsilon_k$ above are chosen to be consistent with this partial order, in the sense that if $c_i < c_j$ then $\epsilon_i < \epsilon_j$, for any two corners c_i and c_j on opposite curves.

Moreover, if the intervals in \mathbb{R} determined by c_i and c_j are equal, the relative size of ϵ_i and ϵ_j is determined by neighboring corners. Given an orientation of γ_1 and γ_2 such that c_i and c_j wrap in the same direction, consider the corners c'_i and c'_j following c_i and c_j on γ_1 and γ_2 ; we require that the line segment connecting c_i to c'_i does not cross the segment connecting c_j to c'_j .

If two curves, or collections of curves, in a radius ϵ peg-board diagram are perturbed as described above, we say that they are in *transverse peg-board position*. The following lemma states that transverse peg-board position realizes the minimal intersection number for two homotopy classes of curves.

Lemma 47. *Suppose γ_1 and γ_2 are two curves in transverse peg-board position. Then, for sufficiently small ϵ , γ_1 intersects γ_2 transversally and γ_1 and γ_2 are in minimal position.*

Proof. It is clear that the intersection of γ_1 and γ_2 is transverse locally near each peg, since any intersection is between two line segments tangent to different concentric circles or between a circle and a line segment tangent to a different circle with the same center. As long as ϵ is sufficiently small so that line segments in the singular diagram are a minimum distance of 2ϵ from any lattice point they do not hit, the only other intersection points are between line segments connecting different pairs of lattice points, which must not be parallel.

If γ_1 and γ_2 are not in minimal position, then there is some bigon in T connecting intersection points x and y . The corresponding segments from x to y in γ_1 and in γ_2 are homotopic to each other in T . Each are perturbations of the minimal length path from x to y (given by the ϵ peg-board representative) by at most $\epsilon/2$. Thus the bigon is contained in a thin strip, an $\epsilon/2$ -neighborhood of the minimal length path. From this it is clear that x and y must be intersections between a line segment and an arc at some corner, or between two line segments coming from the same segment in an unperturbed peg-board diagram. Consider the subcurves of γ_1 and γ_2 , starting from x , forming the bigon. Both must approach the same corner (since otherwise the bigon would not be contained in a strip of width ϵ). In fact, both segments must meet the corner on the same side. Each curve traverses an arc along concentric circles before leaving the corner on a line segment. If a greater angle is covered on the inner arc, then the curves will separate by more than ϵ before intersecting at y , which contradicts that the bigon lies in a strip of width ϵ . By our choice of ordering, the outer arc does not cover a greater angle, so both arcs must have the same angle. In this case the curves approach the next corner along parallel segments, but repeating the reasoning above implies that these curves will never cross. \square

7.2. Solid torus like curves. Having introduced peg-board diagrams, we pause to discuss two key classes of immersed curves that arise. These are illustrated by the following two examples:

Example 48. (a) If M is the solid torus $S^1 \times D^2$, then $\widehat{HF}(M)$ is the longitude $\partial D^2 \times \{\text{pt}\}$ decorated with the trivial 1-dimensional local system.

(b) If M is the twisted I -bundle over the Klein bottle, then $\widehat{HF}(M)$ consists of the two immersed curves shown in Figure 51, each decorated with the trivial local system.

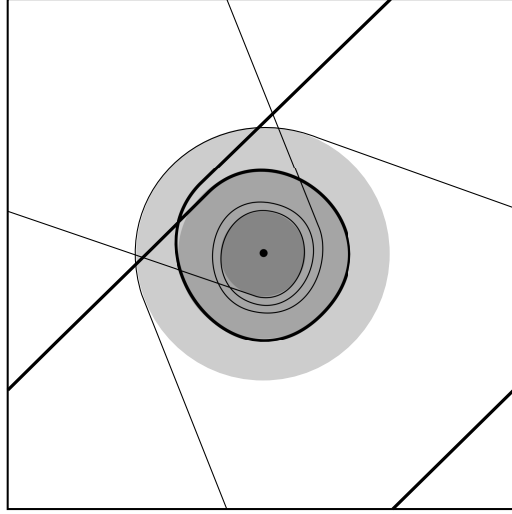


Figure 50. Two curves in T in transverse peg-board position.

Constructing these immersed curves from the corresponding type D modules (which are well known) is a simple exercise. The invariant for the solid torus is a simple closed curve on the torus; in fact the solid torus is the unique irreducible manifold with torus boundary with this property. In the invariant for the twisted I -bundle over the Klein bottle, consider the component that is away from the basepoint (the top component in Figure 51). This curve follows a simple closed curve in T but it traverses that curve more than once. We say that an immersed curve is *loose* if it is homotopic to some number of multiples of a simple closed curve in the punctured torus, or equivalently, if it can be homotoped to an arbitrarily small neighborhood of a simple closed curve in T that does not pass through the marked point. In a peg-board diagram, such a curve pulls tight to a straight line which avoids the pegs. Loose curves behave differently from other curves with respect to pairing precisely because they can be uncoupled from the pegs in this way.

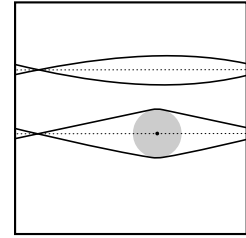


Figure 51. Pulling the invariant associated with the twisted I -bundle over the Klein bottle tight.

The remaining component of the invariant for the twisted I -bundle over the Klein bottle is not loose. However, it satisfies a slightly weaker condition: it can be homotoped to an arbitrarily small neighborhood of a simple closed curve in the torus *which passes through the basepoint*. Equivalently, it pulls tight to a straight line through the basepoint in a singular peg-board diagram. The manifolds M for which every component of $\widehat{HF}(M)$ has this form are an interesting class of manifolds.

Definition 49. A three-manifold with torus boundary M is a *Heegaard Floer homology solid torus* if each component of the immersed multicurve $\widehat{HF}(M)$ pulls tight to a straight line, possibly through the basepoint, in a singular peg-board diagram. (Note that all such curves must be parallel to the homological longitude, since each component of $\widehat{HF}(M)$ lifts to a closed curve in \overline{T}_M .)

This is equivalent to another definition of Heegaard Floer solid tori that has appeared [17, 33]: If M is a rational homology solid torus and λ is the rational longitude of M , then consulting the discussion on Dehn twisting in Section 5 (and appealing to the equivalence between $\widehat{HF}(M)$ and $\widehat{CFD}(M, \mu, \lambda)$) we observe that $\widehat{CFD}(M, \mu, \lambda) \cong \widehat{CFD}(M, \mu + \lambda, \lambda)$ as type D structures.

If $\widehat{HF}(M)$ consists of a single loose curve with trivial local system in each Spin^c structure, we say M is solid torus like. Gillespie studied such manifolds and showed that they are boundary compressible [9, Corollary 2.9]. More generally, we say $\widehat{HF}(M)$ is loose if each component of $\widehat{HF}(M)$ is a loose curve

(possibly equipped with a nontrivial local system). Since $\widehat{HF}(M)$ lifts to \overline{T}_M , all such components must be parallel. We will prove the following generalization of Gillespie's result.

Proposition 50. *If $\widehat{HF}(M)$ is loose, then M is boundary compressible.*

Before giving the proof, we recall some facts about knot Floer homology and the Thurston norm. Let λ be the rational longitude of M , and suppose that λ has order k in $H_1(M)$. Choose a meridian $\mu \in H_1(\partial M)$ with $\mu \cdot \lambda = 1$. Then μ is k times a primitive element of $H_1(M)$.

Fix a class $x \in H_2(M, \partial M)$ with $\partial x = \lambda$ and define

$$\widehat{HFK}(K_\mu, x, i) = \bigoplus_{\langle c_1(\mathfrak{t}), x \rangle = 2i} \widehat{HFK}(K_\mu, \mathfrak{t})$$

where the sum runs over $\mathfrak{t} \in \text{Spin}^c(M, \partial M)$. Then

$$2 \cdot \max\{i \mid \widehat{HFK}(K_\mu, x, i) \neq 0\} = \|x\|_\mu$$

Here $\|\cdot\|_\mu$ is the generalized Thurston norm given by

$$\|x\|_\mu = \min_{[S]=x} c_\mu(S),$$

where the minimum is taken over all properly embedded orientable surfaces representing x . If S is connected, $c_\mu(S) = \max\{-\chi(S) + |\partial S \cdot \mu|, 0\}$; otherwise $c_\mu(S) = \sum c_\mu(S_i)$, where S_i are the connected components of S .

As we described in Section 6.4, the Spin^c decomposition of $\widehat{HFK}(K_\mu)$ can be computed by intersecting $\widehat{HF}(M, \mathfrak{s})$ with lifts of μ to $\overline{T}_{M, \mathfrak{s}}$, where \mathfrak{s} runs over $\text{Spin}^c(M)$. The choice of x determines a height function on $\overline{T}_{M, \mathfrak{s}}$ such that intersections of $\widehat{HF}(M, \mathfrak{s})$ with lifts of the meridian at height i correspond to elements of $\widehat{HFK}(K_\mu, x, i)$.

Similarly, if Y is a closed manifold, and $y \in H_2(Y)$ is a primitive class, we define

$$\widehat{HF}(Y, y, i) = \bigoplus_{\langle c_1(\mathfrak{s}), [\Sigma] \rangle = 2i} \widehat{HF}(Y, \mathfrak{s}).$$

Then $\|y\| = 2 \cdot \max\{i \mid \widehat{HF}(Y, y, i) \neq 0\}$.

Proof of Proposition 50. Fix a class x as above, and choose a norm-minimizing surface S realizing x . After tubing to remove excess boundary components, we may assume that ∂S consists of precisely k parallel copies of λ . Since λ has order k in $H_1(M)$, all k boundary components lie on a single component of S . Let S_0 be the component with boundary, and consider the modified complexity $\tilde{c}(S) = -\chi(S_0) + \sum_{i>0} c(S_i)$, where the sum runs over the other components of S . Note that $\tilde{c}(S) = c(S)$ unless $k = 1$ and $S_0 = D^2$.

By hypothesis, $\widehat{HF}(M)$ is a union of loose curves in T_M . Each individual curve lifts to some $\overline{T}_{M, \mathfrak{s}}$ as a circle parallel to λ . This circle is at some height $n \in \mathbb{Z}$ with respect to the height function determined by x . Let n_+ and n_- be the heights of the highest and lowest circles in $\widehat{HF}(M)$. Then n_+ is the largest value of i for which $\widehat{HFK}(K_\mu, x, i)$ is nontrivial, and n_- is the lowest. Since knot Floer homology is conjugation-symmetric, we must have $n_- = -n_+$. The relation between \widehat{HFK} and the Thurston norm implies that $\tilde{c}(S) = 2n_+ - k$.

Now consider the closed manifold $Y = M \cup_h M$, where $h(\lambda) = -\lambda$ and $h(\mu) = \mu$, and let $y \in H_2(Y)$ be the class obtained by doubling x . Then $\widehat{HF}(Y, y, i)$ is calculated by pairing $\widehat{HF}(M, \mathfrak{s})$ with $\alpha \cdot \bar{h}(\widehat{HF}(M, \mathfrak{s}'))$, where $\mathfrak{s}, \mathfrak{s}'$ run over $\text{Spin}^c(M)$, and α runs over all deck transformations which shift height by i . The largest value of i for which $\widehat{HF}(Y, y, i)$ is potentially nontrivial is obtained by pairing the highest set of curves in $\widehat{HF}(M)$ with the lowest set of curves in $\bar{h}(\widehat{HF}(M))$. The latter

is simply the image of the highest set of curves in $\widehat{HF}(M)$ under \bar{h} , so the maximal value of i is $n_+ - n_- = 2n_+$. We can view the highest set of curves as a single local system (V, A) on S^1 , so

$$\widehat{HF}(Y, y, 2n_+) = \text{Hom}(S_{(V,A)}^1, S_{(V,A)}^1)$$

This group is nonzero, since it contains the identity element. It follows that $\widehat{HF}(Y, y, 2n_+) \neq 0$, so $\|y\| = 4n_+$.

On the other hand, the double DS of S represents y and has complexity $2c(S)$. If M is boundary incompressible, then $S_0 \neq D^2$, so $c(S) = \tilde{c}(S) = 2n_+ - k$. In this case, we would have $c(DS) = 4n_+ - 2k < \|y\|$, which is impossible. We conclude that $S_0 = D^2$ and M was boundary compressible. \square

Remark 51. The proof shows that $\widehat{HF}(M)$ is loose, then all the curves in it are at height 0. Loose manifolds with curves at other heights do not exist. One possible explanation for this would be that $\widehat{HF}(M, \mathfrak{s})$ should represent an exact Lagrangian in \overline{T}_M .

7.3. A dimension inequality for pinches. Consider the following construction: Let Y be a rational homology sphere of the form $M_0 \cup_h M_1$, so that each M_i is a rational homology solid torus. Denote by λ_i the rational longitude in each ∂M_i ; recall that this slope is characterized by the property that some number of like oriented copies of λ_i bounds a properly embedded surface in M_i . The Dehn surgery $Y_0 = M_0(h(\lambda_1))$ is the result of pinching M_1 in Y . Note that $h(\lambda_1)$ is a well defined slope in ∂M_1 . In certain settings there is an associated degree n map $Y \rightarrow Y_0$, where n is the order of $i_*([\lambda_1])$ in $H_1(M_1)$. In particular, when both M_0 and M_1 are integer homology spheres, there is always a degree one map associated with a pinch.

Theorem 52. *Given a rational homology sphere $Y = M_0 \cup_h M_1$, where M_0 and M_1 are rational homology solid tori, there is an inequality*

$$\dim \widehat{HF}(Y) \geq nm \dim \widehat{HF}(Y_0)$$

where $Y_0 = M_0(h(\lambda_1))$, n is the order of $i_*([\lambda_1])$ in $H_1(M_1)$, and $m = |\text{Spin}^c(M_1)| = |H_1(M_1, \partial M_1)|$.

The proof of Theorem 11 follows from a special case of version Theorem 52 (with $n = m = 1$).

Proof of Theorem 52. Let γ_0 and γ_1 denote the decorated curves $\widehat{HF}(M_0)$ and $\bar{h}(\widehat{HF}(M_1))$, respectively, in $T = \partial M_0 \setminus z$. By the gluing theorem, $\widehat{HF}(Y)$ is equivalent to the Floer homology $HF(\gamma_0, \gamma_1)$ and in particular, since Y is a rational homology sphere, the dimension is given by the intersection number of γ_0 and γ_1 .

Let $\hat{\gamma}_1$ be the collection of curves obtained from γ_1 by replacing any non-trivial local systems with trivial ones, deleting any curve components that are nullhomotopic in the torus ∂M_0 (ignoring the base point) and pulling the remaining curves tight (again, ignoring the base point), that is, replacing them with minimal length representatives of their homotopy class, allowing homotopies that pass the base point. Let $\frac{p}{q}$ be the slope of the curve in T determined by $h(\lambda_1)$, and let $L_{p,q}$ be the corresponding simple closed curve $p\alpha_0 + q\beta_0$.

For each spin^c -structure of M_1 , recall that $\widehat{HF}(M_1)$ is homotopic, ignoring the basepoint, to the homological longitude $n \cdot \lambda_1$. Thus for each spin^c -structure of M_1 , γ_1 contains at least one curve that is homotopic in ∂M_0 to $\bar{h}(n \cdot \lambda_1) = n \cdot L_{p,q}$ along with some number of nullhomotopic curves. It follows that $\hat{\gamma}_1$ is a collection of at least m copies of $n \cdot L_{p,q}$ so that

$$\dim HF(\gamma_0, \hat{\gamma}_1) \geq nm \dim HF(\gamma_0, L_{p,q}) = nm \widehat{HF}(Y').$$

It remains to show that $\dim HF(\gamma_0, \gamma_1) \geq \dim HF(\gamma_0, \hat{\gamma}_1)$. This follows immediately if γ_1 carries a non-trivial local system, since decreasing the dimension of any local system involved necessarily decreases the number of intersection points, so without loss of generality we may assume that all local systems are trivial.

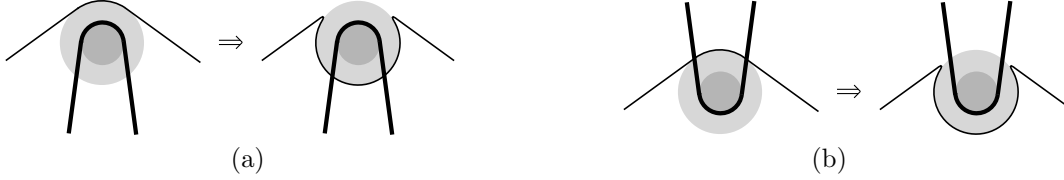


Figure 52. Sliding a component of γ_1 over a basepoint in T to produce $\hat{\gamma}_1$, as in the proof of Theorem 52: Every instance of (a) adding intersection points is balanced by an instance of (b) removing intersection points.

Note then that $\hat{\gamma}_1$ can be obtained from γ_1 by a sequence of the following moves: (i) deleting a component; (ii) resolving a self-intersection to split off a closed component; (iii) homotopy in T to put curves in transverse peg board position with γ_0 ; and (iv) passing the curve through a peg at which it changes direction in a transverse peg board diagram. We claim that none of these moves increases the intersection number with γ_0 . Indeed, (i) clearly does not increase intersection number, and (ii) does not change the number of intersections with γ_0 at all. Further, (iii) does not increase intersection number, since transverse peg board position realizes the minimal intersection for homology classes in T . It only remains to check that (iv) does not increase intersection number.

Allowing a corner of γ_1 to slide over the base point may add new intersection points with γ_0 ; this happens exactly when there is a corner of γ_0 such that the arc determined by the corner of γ_0 is contained in the arc determined by the corner of γ_1 (see Figure 52(a)). In this case, as γ_0 passes through the relevant corner, it both approaches the peg and leaves the peg on the same side of γ_1 , namely on the side that contains the peg. Sliding γ_1 across the peg adds two intersections for each such corner. However, this is balanced by the fact that intersection points are removed for other corners of γ_0 . If at a given corner γ_0 approaches and leaves the peg from the side of γ_1 not containing the peg, sliding γ_1 over the peg removes two intersection points (see Figure 52(b)). For each corner of γ_0 of the first type, there is a corner of the second type; this follows from the fact that if γ_0 leaves a corner on one side of γ_1 , it approaches the next corner on the opposite side of γ_1 . Thus, overall, (iv) does not increase intersection number. \square

7.4. Heegaard Floer homology for toroidal manifolds. As another immediate consequence of the geometric interpretation of bordered Floer invariants, we will now prove Theorem 8, which states that if Y contains an essential torus then $\dim \widehat{HF}(Y) \geq 5$.

Proof of Theorem 8. By cutting along the torus, realize Y as $M_0 \cup_h M_1$ where M_0 and M_1 are manifolds with incompressible torus boundary and $h: \partial M_1 \rightarrow \partial M_0$ is a diffeomorphism. Let $\gamma_0 = \widehat{HF}(M_0)$ and $\gamma_1 = \widehat{h}(\widehat{HF}(M_1))$ be the relevant decorated immersed multicurves in $\partial M_0 \setminus z_0$. For $i = 0, 1$, let c_i be the number of corners in a peg-board representative for γ_i . We first observe that if γ_0 and γ_1 are pulled tight in transverse peg-board position (recall that this ensures minimal intersection), then there are at least $c_0 c_1$ intersection points. To see this, note that each corner in γ_0 determines a wedge between the incoming and outgoing segments. Near each corner of γ_0 , there are 0, 1, or 2 intersection points depending on whether both, one, or neither of the segments defining the corner of γ_0 are contained in the wedge defined by the corner of γ_1 (see Figure 52 for arrangements with 0 and 2 intersections). As shown in the proof of Theorem 52, for each corner of γ_1 with 0 intersections there is a corresponding corner with 2 intersections. Thus each corner of γ_0 intersects with each corner of γ_1 on average once.

By Proposition 50, neither γ_0 nor γ_1 can be loose. Then each of γ_0, γ_1 has at least two corners, so $\#(\gamma_0 \cap \gamma_1) \geq 4$. Moreover, if we assume that $\#(\gamma_0 \cap \gamma_1) = 4$ we must have that γ_0 and γ_1 each have only one component with exactly two corners, and the singular peg-board diagram for each curve has exactly two segments. It is also clear that neither curve can carry a non-trivial local system. Now M_0 and M_1 must both be integer homology solid tori, since otherwise the corresponding curves would have multiple components; it follows that the sum of the two segments in the singular diagram,

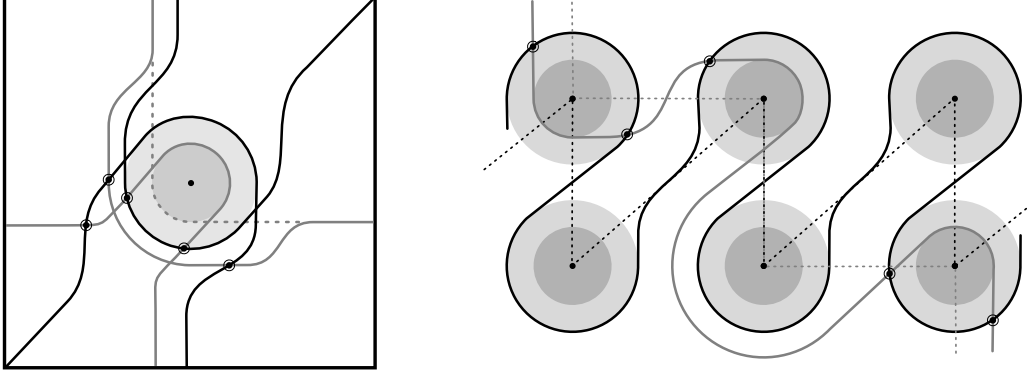


Figure 53. The pairing of γ_0 (gray) consisting of two segments of slopes 0 and ∞ with γ_1 (black) consisting of two segments of slopes 1 and ∞ , shown both in the torus and in the covering space $\mathbb{R}^2 \setminus \mathbb{Z}^2$. This corresponds to a gluing of two trefoil complements. The result of the gluing is an integer homology sphere, since there is ± 1 intersection point counted with sign.

thought of as an element of $H_1(\partial M_0)$, must be primitive (in particular, the two segments cannot have the same slope).

The intersection points counted so far all occur near the peg. More precisely, if the radii shrink to zero in the transverse peg-board diagram, the intersection points get arbitrarily close to the basepoint. We now observe that any two segments of slope r_1 and r_2 in the singular peg-board diagram intersect d times, where $d = \Delta(r_1, r_2)$ is the distance between the slopes. One of these intersection points is at the endpoints, but the remaining $d - 1$ intersection points occur in the interior of the segments; these intersections remain in a (non-singular) peg-board diagram and are a finite distance from the peg. It follows that if γ_0 and γ_1 have segments with slope of distance greater than 1, $\#(\gamma_0 \cap \gamma_1)$ is at least 5.

So far we have shown that if $\dim(\widehat{HF}(Y)) < 5$ then γ_0 is a single curve whose singular diagram has two segments of slope r_1 and $r_2 \neq r_1$, γ_1 is a single curve with two segments of slope q_1 and q_2 , and $\Delta(p_1, q_1)$, $\Delta(p_1, q_2)$, $\Delta(p_2, q_1)$, and $\Delta(p_2, q_2)$ are all at most 1. Note that for each curve, the pair of slopes realized in the singular peg-board representative determines the homotopy class of the curve. This statement implicitly assumes that there is no peg-wrapping (i.e. the curve never wraps fully around a peg); this subtlety will follow from results in the next subsection. In particular, with the present set-up both M_0 and M_1 are Floer simple, and thus by Lemma 55 there is no peg-wrapping in γ_0 or γ_1 .

If the pairs of slopes $\{p_1, p_2\}$ and $\{q_1, q_2\}$ agree, then $\gamma_0 \sim \gamma_1$. The curves have 4 intersection points but also bound an immersed annulus; the finger move required to achieve admissibility introduces two more intersection points, forcing $\dim(\widehat{HF}(Y))$ to be at least 6. Now suppose the slopes p_1, p_2, r_1 , and r_2 are all distinct. Without loss of generality, suppose that $p_1 = \infty$; it follows that q_1 and q_2 are integers, and since they are each distance one from p_2 it follows that $p_2 = n$, and q_1 and q_2 are $n \pm 1$. But this cannot happen, since the sum of a segment of slope $n + 1$ and a segment of slope $n - 1$ is not primitive as an element of $H_1(\partial M_0)$. The only remaining case is that $p_1 = q_1$ and $p_2 \neq q_2$. Without loss of generality, set $p_1 = \infty$ and note that p_2 and q_2 are consecutive integers; up to reparametrizing the torus, we can take them to be 0 and 1. This case is depicted in Figure 53 and has 5 intersection points. \square

The case in Figure 53 is realized by gluing two trefoil complements. For instance, it arises from gluing the complement of two right handed trefoil complements by identifying 0-framed longitude with meridian and meridian with 1-framed longitude. This provides an example of a toroidal integer homology sphere Y realizing $\dim \widehat{HF}(Y) = 5$.

With this example in hand, consider the function f taking values in the natural numbers defined by

$$f(n) = \min_Y \{ \dim \widehat{HF}(Y) \mid Y \text{ is a rational homology sphere with } n \text{ separating JSJ tori} \}$$

and note that $f(0) = 1$ (realized by the three-sphere or the Poincaré homology sphere) and $f(1) = 5$ (realized by gluing two trefoil exteriors as in Theorem 57, see Figure 53). For Heegaard Floer aficionados, we propose:

Question 53. Is it possible to determine f or describe properties of f as n grows?

If we further assume that Y is an L-space, we can in fact strengthen the result of Theorem 8 by enumerating all examples with $\dim \widehat{HF}(Y) < 8$; see Theorem 57. This will make use of a result specific to L-spaces. Toward establishing this result, we now turn our attention to properties of the immersed curve invariants relevant to L-spaces.

7.5. Characterizing L-space slopes. Given a manifold with torus boundary M , let \mathcal{L}_M denote the set of L-space slopes, that is, the subset of slopes giving rise to L-spaces on Dehn filling, and let \mathcal{L}_M° denote the interior of \mathcal{L}_M . This section gives a characterization of the set \mathcal{L}_M° in terms of the collection of curves $\widehat{HF}(M)$.

Given an immersed curve γ in T and a slope r in $\mathbb{R}P^1$, we say that r is a tangent slope of γ if every smooth immersed curve homotopic to γ has a tangent line with slope r . For a spin^c structure \mathfrak{s} on M , consider the curve(s) $\widehat{HF}(M; \mathfrak{s})$ (recall that we think of these curves as lifted to the covering space \widehat{T}_M). Let $S(M; \mathfrak{s}) \subset \mathbb{R}P^1$ denote the set of tangent slopes to $\widehat{HF}(M; \mathfrak{s})$ if $\widehat{HF}(M; \mathfrak{s})$ consists of a single immersed curve with the trivial one-dimensional local system, with the convention that $S(M; \mathfrak{s}) = \mathbb{R}P^1$ if $\widehat{HF}(M; \mathfrak{s})$ has more than one component or a non-trivial local system. We define $S(M)$ to be the union of $S(M; \mathfrak{s})$ over all spin^c structures.

An equivalent, and more convenient, definition for $S(M)$ can be given using peg-board representatives. For a given ϵ and spin^c structure s , let $S_\epsilon(M; s)$ be the set of tangent slopes of the ϵ radius peg-board representative of $\widehat{HF}(M; s)$, or $\mathbb{R}P^1$ if $\widehat{HF}(M; s)$ is disconnected or has a non-trivial local system. $S(M; s)$ can be realized by taking $\epsilon \rightarrow 0$, in the sense that $S(M; s) = \bigcap_{n=N}^\infty S_{\frac{1}{n}}(M; s)$; once again, $S(M)$ is the union of $S(M; s)$ over all spin^c structures. In practice, $S(M)$ can be computed from the singular peg-board diagram for (the lift of) $\widehat{HF}(M)$; we define $S^{\text{sing}}(M)$ to be the set of slopes of tangent lines to the singular peg-board representative, where we say a line L through a corner is a tangent line if L coincides with one of the two segments at that corner or if both segments lie on the same side of L . Equivalently, $S^{\text{sing}}(M)$ is the set of tangent slopes after smoothing the corners in a singular peg-board diagram. Each corner determines a closed interval of tangent slopes, bounded by the slopes of the incoming and outgoing segments, and $S^{\text{sing}}(M)$ is the union of these intervals. The singular peg-board representative may contain a degenerate corner, where the incoming and outgoing segments coincide; any slope is a tangent slope at such a corner. If there are no corners, then the singular peg-board representative for $\widehat{HF}(M)$ is a collection of straight lines of some rational slope α (the slope of the rational longitude), and $S^{\text{sing}}(M) = \{\alpha\}$. As with $S(M)$, we set $S^{\text{sing}}(M) = \mathbb{R}P^1$ if $\widehat{HF}(M)$ has more than one curve in any spin^c structure or a non-trivial local system.

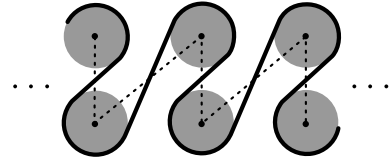


Figure 54. The peg board diagram and singular peg board diagram (dashed) associated with the curve of the right hand trefoil, lifted to $\mathbb{R}^2 \setminus \mathbb{Z}^2$.

Note that passing from a peg-board diagram to a singular peg-board diagram loses some information. In particular, in a peg-board diagram a curve may wrap entirely around a peg (that is, it changes direction by an angle of at least π); we call this *peg wrapping*. A singular peg-board diagram only records the slopes of the incoming and outgoing segments each time the curve passes a peg; it can not determine if peg-wrapping occurs. It is clear that the two sets of slopes $S(M)$ and $S^{\text{sing}}(M)$ are

the same unless there is peg-wrapping in $\tilde{\gamma}(M)$, in which case $S(M) = \mathbb{R}P^1$. For arbitrary curves in $\mathbb{R}^2 \setminus \mathbb{Z}^2$, these two intervals of tangent slopes need not be the same, but in fact we will see that they agree for any collection of curves $\widehat{HF}(M)$ arising from a 3-manifold M . That is, $S(M) = S^{sing}(M)$.

Using tangent slopes in peg-board diagrams, we can give a new interpretation of L-space slopes for a loop type manifold.

Theorem 54. *If M is a manifold with torus boundary then \mathcal{L}_M° is the complement of the set $S_{\mathbb{Q}}^{sing}(M) = S^{sing}(M) \cap \mathbb{Q}P^1$.*

Proof. By the pairing theorem, $\widehat{HF}(M(\alpha))$ is equivalent to the intersection Floer homology of $\widehat{HF}(M)$ and a straight line with slope α , which we denote L_α . Suppose first that α is a non-L-space slope, so that the Dehn filling $M(\alpha)$ is not an L-space and there is some \mathfrak{s} so that $\dim \widehat{HF}(M(\alpha); \mathfrak{s}) > 1$. It follows that (for any homotopy representative of $\widehat{HF}(M)$) there are two intersection points x and y between $\widehat{HF}(M)$ and the line L_α with the same spin^c -grading. This means that x and y correspond to intersection points \tilde{x} and \tilde{y} between (a lift of) L_α and $\widehat{HF}(M; \mathfrak{s})$ in the covering space $\mathbb{R}^2 \setminus \mathbb{Z}^2$. If $\widehat{HF}(M; \mathfrak{s})$ contains more than one curve then $S^{sing}(M) = \mathbb{R}P^1$ by definition and $\alpha \in S_{\mathbb{Q}}^{sing}(M)$, so suppose that $\widehat{HF}(M; \mathfrak{s})$ contains a single curve. The intersection points \tilde{x} and \tilde{y} exist for any homotopy representative of $\widehat{HF}(M; \mathfrak{s})$ (in particular the peg-board representatives for arbitrarily small ϵ) and since L_α can be taken to be some finite distance away from every peg, we can in fact take \tilde{x} and \tilde{y} to be intersections of the singular peg-board representative of $\widehat{HF}(M; \mathfrak{s})$ with a lift of L_α . Note that the corners of the singular representative for $\widehat{HF}(M; \mathfrak{s})$ can be smoothed without affecting intersections with L_α and that $S^{sing}(M)$ is precisely the set of tangent slopes after this smoothing. By the (extended) mean value theorem, there is a point on the smoothing of the singular representative of $\widehat{HF}(M; \mathfrak{s})$ for which the tangent line has slope α . We conclude that $\alpha \in S_{\mathbb{Q}}^{sing}(M)$ as claimed. We have proved that $\mathcal{L}_M^c \subset S_{\mathbb{Q}}^{sing}(M)$; in fact, since $S_{\mathbb{Q}}^{sing}(M)$ is closed (as a subset of $\mathbb{Q}P^1$), we have $\overline{\mathcal{L}_M^c} = (\mathcal{L}_M^\circ)^c \subset S_{\mathbb{Q}}^{sing}(M)$.

Conversely consider a slope α in $S_{\mathbb{Q}}^{sing}(M)$. We will work with the singular peg-board representative of $\widehat{HF}(M)$. If $S^{sing}(M) = \{\alpha\}$, then α is the rational longitude of M and thus not an L-space slope. Otherwise, α is in the interval of tangent slopes determined by some corner c ; let s_1 and s_2 denote the two line segments meeting at c . First suppose α is in the interior of the interval for the corner c . Let L_α be the line of slope α through c ; since L_α is a tangent line, s_1 and s_2 both lie on one side of line L_α . Let L'_α be a small pushoff of L_α that intersects the segments s_1 and s_2 and is disjoint from all lattice points. For sufficiently small ϵ (smaller than the minimum distance between L'_α and any lattice point), replacing the singular representative for $\widehat{HF}(M)$ with the radius ϵ peg-board representative preserves these two intersection points. These points give two generators with the same spin^c grading in the intersection Floer chain complex of $\widehat{HF}(M)$ with L' . Since both L'_α and $\widehat{HF}(M)$ are peg-board representatives relative to the radius ϵ and they have transverse intersection, they are in minimal position and both generators survive in homology. It follows that $M(\alpha)$ is not an L-space, that is, $\alpha \notin \mathcal{L}_M$. Now suppose α is a boundary of the interval of slopes determined by the corner c ; there are slopes arbitrarily close to α in the interior of this interval, and these slopes are not in \mathcal{L}_M , so $\alpha \notin \mathcal{L}_M^\circ$. \square

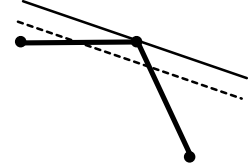


Figure 55. Intersection points for a slope in $S^{sing}(M)$.

Theorem 54 is in fact true for arbitrary immersed curves in T (using an appropriate definition of the set of L-space slopes for a curve), not just for the collections of curves associated to loop type manifolds. For curves arising from loop type manifolds, however, we can replace $S^{sing}(M)$ with $S(M)$. To prove this, we first make the following observation about Floer simple manifolds:

Lemma 55. *If M is Floer simple, then $S(M) \neq \mathbb{R}P^1$.*

Proof. If M is Floer simple, then by [15, Proposition 6] M has simple loop type, that is, for some parametrization (α, β) of ∂M , $\widehat{CFD}(M, \alpha, \beta)$ is a collection of loops (one for each Spin^c structure on M) consisting only of ρ_1 , ρ_3 and ρ_{23} arrows. It follows that the corresponding curves in the plane travel only up and right. Clearly $S(M)$ contains only positive slopes (relative to the chosen parametrization), and so $S(M) \neq \mathbb{R}P^1$. Note that reparametrizing the boundary changes this interval but does not change whether or not it is all of $\mathbb{R}P^1$. \square

Corollary 56. *For any loop type manifold M , $S(M) = S^{sing}(M)$.*

Proof. In the absence of peg-wrapping $S(M) = S^{sing}(M)$. If there is peg-wrapping, then $S(M) = \mathbb{R}P^1$, and by Lemma 55, M is not Floer simple. It follows that $\mathcal{L}_M^\circ = \emptyset$, and by Theorem 54 $S^{sing}(M) = \mathbb{R}P^1$. \square

We remark that, as an immediate corollary of Theorem 54, the set \mathcal{L}_M° is either empty, an open interval with rational endpoints, or all of $\mathbb{Q}P^1$ but the rational longitude λ ; this is because $S(M)$ contains at least λ and is a closed interval. More generally, it is possible to characterize the set \mathcal{L}_M in terms of the tangent slopes in a singular peg-board diagram: roughly speaking, \mathcal{L}_M is the complement of the set $S'(M)$ obtained by taking the union over all corners of the *interior* of the set of tangent slopes determined by the corner, with the convention that a degenerate corner with two segments of slope α contributes $\mathbb{R}P^1 \setminus \{\alpha\}$, along with the slope of any segment such that $\widehat{HF}(M)$ turns left at both of the corners connected by the segment or turns right at both corners. It follows that \mathcal{L}_M is either empty, a single point, a closed interval with rational endpoints, or $\mathbb{Q}P^1 \setminus \{\lambda\}$; this recovers Theorem 1.6 of [30] (see also Theorem 1.2 of [17]).

7.6. The L-space gluing theorem. We now turn to the proof of Theorem 13. In previous works [17, 30, 15] the authors and S. Rasmussen prove this L-space gluing criterion when the manifolds have simple loop type (equivalently, when the manifolds are Floer simple). Interpreting bordered Floer homology as immersed curves with local systems allows us to give an elegant proof of this gluing theorem without requiring the simple loop type hypothesis on the manifolds.

Proof of Theorem 13. By the pairing theorem, $M_0 \cup_h M_1$ is equivalent to the intersection Floer homology of $\gamma_0 = \widehat{HF}(M_0)$ and $\gamma_1 = \bar{h}(\widehat{HF}(M_1))$. Suppose first that $M_0 \cup_h M_1$ is not an L-space, implying that there is some \mathfrak{s} so that $\dim \widehat{HF}(M_0 \cup_h M_1, \mathfrak{s}) > 1$. In other words, there are two intersection points x and y between γ_0 and γ_1 with the same spin^c grading. This means, in particular, that x and y are intersection points of $\gamma_{0, \mathfrak{s}_0} = \widehat{HF}(M_0; \mathfrak{s}_0)$ and $\gamma_{1, \mathfrak{s}_1} = \bar{h}(\widehat{HF}(M_1; \mathfrak{s}_1))$ for some $\mathfrak{s}_0 \in \text{Spin}^c(M_0)$ and $\mathfrak{s}_1 \in \text{Spin}^c(M_1)$. We will assume for $i \in \{0, 1\}$ that $\gamma_{i, \mathfrak{s}_i}$ contains only one curve with a trivial local system, since otherwise $\mathcal{L}_{M_i}^\circ$ is empty and $\mathcal{L}_{M_0}^\circ \cup h(\mathcal{L}_{M_1}^\circ) \neq \mathbb{Q}P^1$. Let c_0 be the path from x to y in $\gamma_{0, \mathfrak{s}_0}$ and let c_1 be the path from x to y in $\gamma_{1, \mathfrak{s}_1}$. The fact that x and y have the same spin^c grading implies that $[c_0 - c_1] = 0 \in H_1(T)$, or equivalently that the paths lift to form a bigon in \mathbb{R}^2 , the corners of which are lifts \tilde{x} and \tilde{y} of x and y . Let α be the slope of the line segment connecting \tilde{x} and \tilde{y} . By the (extended) mean value theorem, \tilde{c}_0 and \tilde{c}_1 each contain a point with slope α .

This argument applies for any homotopy representative of γ_0 and γ_1 . In particular, if we take peg-board representatives relative to some peg radius $\frac{1}{n}$ we find a slope α_n that is a tangent slope to both curves. It follows that $\alpha_n \in S_{\frac{1}{n}}(M_0) \cap h(S_{\frac{1}{n}}(M_1))$. Here, by abuse of notation, h refers to the map on slopes induced by h ; note that, as maps on slopes, \bar{h} and h agree since the elliptic involution preserves slopes. Since $S_{\frac{1}{n}}(M_0) \cap h(S_{\frac{1}{n}}(M_1))$ for positive integers n gives a nested sequence of nonempty closed sets there is some slope α in the total intersection, which is simply $S(M_0) \cap h(S(M_1))$. Moreover, we can take this α to be rational, since $S(M_0)$ and $h(S(M_1))$ have rational endpoints. By Theorem 54 and Corollary 56, $S_{\mathbb{Q}}(M_0) = (\mathcal{L}_{M_0}^\circ)^c$ and $S_{\mathbb{Q}}(M_1) = (\mathcal{L}_{M_1}^\circ)^c$. Thus α is not in $\mathcal{L}_{M_0}^\circ \cup h(\mathcal{L}_{M_1}^\circ)$.

Conversely, suppose that there is a slope α not in $\mathcal{L}_{M_0}^\circ \cup h(\mathcal{L}_{M_1}^\circ)$. Equivalently, α is in both $S_{\mathbb{Q}}^{\text{sing}}(M_0)$ and $h(S_{\mathbb{Q}}^{\text{sing}}(M_1))$, so α is a tangent slope of both γ_0 and γ_1 in a singular peg-board diagram. Let c_0 and c_1 be components of γ_0 and γ_1 , respectively, for which α is a tangent slope to the singular peg-board representative. We may assume that c_0 and c_1 are not solid torus like components. If, for example, c_0 were solid torus like then α would be the rational longitude of M_0 and every component of γ_0 would have a tangent line of slope α ; we could then replace c_0 by another component, at least one of which is not solid torus like because M_0 is not solid torus like. By reparametrizing ∂M_0 and ∂M_1 , we may assume that $\alpha = 0$.

Fixing a small peg radius ϵ , consider transverse peg-board representatives of c_0 and c_1 with a chosen orientation on each curve. Since c_0 and c_1 are in minimal position, to show that $M_0 \cup_h M_1$ is not an L-space it is enough to find two intersection points between c_0 and c_1 with the same $\mathbb{Z}/2\mathbb{Z}$ -grading. It is easy to find two such generators if both curves have peg-wrapping. In this case the curves c_0 and c_1 contain complete circles of radius ϵ_0 and ϵ_1 around the puncture, with $\epsilon_0 \neq \epsilon_1$. Suppose, without loss of generality, that $\epsilon_0 < \epsilon_1$. Then c_0 also contains two line segments tangent at their ends to the circle of radius ϵ_0 , one oriented toward the circle and one oriented away from it. These two segments clearly intersect the oriented circle of radius ϵ_1 with opposite sign, and the two corresponding generators of $HF(\gamma_0, \gamma_1)$ have opposite $\mathbb{Z}/2\mathbb{Z}$ grading. Thus we may assume that there is no peg-wrapping in c_0 .

In the singular peg-board diagram for c_0 , the line segments connecting corners can be classified as moving upwards, downwards, or horizontally (once we have fixed an orientation on c_0). The segments can not be all upward or all downward, since then $\alpha = 0$ would not be a tangent slope. If the slopes are not all horizontal, we can choose a corner so that the segments preceding and following the corner are up and down, up and horizontal, or horizontal and down. Note that the corresponding corner in a radius ϵ peg-board diagram for c_0 has a point of horizontal tangency on the top side of the peg, at the point $(0, \epsilon)$. If every line segment in c_0 is horizontal, then every corner has horizontal tangency to the peg, and we can choose the corner so that this point of tangency is on the top side of the peg. Moving away from this point of tangency in either direction, c_0 moves either horizontally or downwards. If it moves horizontally it wraps once around the torus and returns to the peg at another horizontal tangency on the top of the peg; after some number of horizontal segments like this, c_0 must move downwards. Thus, c_0 contains an upward moving piece c_0^I oriented toward the point $(0, \epsilon)$ and a downward moving piece c_0^O oriented away from $(0, \epsilon)$, as in Figure 56(a). Note that c_0 may traverse any number of horizontal segments between c_0^I and c_0^O ; we will ignore these horizontal segments. Similarly, we can choose a corner of c_1 such that the preceding segment in the singular peg-board diagram moves downward or horizontally and the following segment moves horizontally or upward, and such that in a radius ϵ peg-board diagram there is a horizontal tangency to the peg at $(0, -\epsilon)$. Let c_1^I be the horizontal or downward piece of c_1 oriented toward $(0, -\epsilon)$ and let c_1^O be the horizontal or upward piece oriented away from $(0, -\epsilon)$, as in Figure 56(b). Note that we ignore any full wraps around the peg between c_1^I and c_1^O . We consider these curves in one fundamental domain of T , the square $[-\frac{1}{2}, \frac{1}{2}] \times [-\frac{1}{2}, \frac{1}{2}]$. The intersection of c_0^I and c_0^O with the boundary of this square can be any point with non-positive y -coordinate; the intersection of c_1^I and c_1^O with the boundary of this square can have any non-negative y -coordinate or y -coordinate $-\epsilon$.

We can overlay the portions of c_0 and c_1 described above in a transverse peg-board diagram. We may assume that the corner of c_0 has larger peg radius; since the corner of c_1 passes through $(0, -\epsilon)$ and the corner of c_0 does not, this is consistent with the partial order on corners. It is clear that if both c_0^I and c_0^O intersect the boundary of the square $[-\frac{1}{2}, \frac{1}{2}] \times [-\frac{1}{2}, \frac{1}{2}]$ with strictly negative y -value or if both c_1^I and c_1^O intersect the boundary of the square with strictly positive y -value (equivalently, if the corresponding segments in the singular diagram are not horizontal), then there are two intersection points with opposite $\mathbb{Z}/2\mathbb{Z}$ grading (see Figure 56(c)).

The remaining case is when one of the specified segments in both c_0 and c_1 correspond to horizontal segments in a singular diagram. We consider the case that c_0^O and c_1^O are both horizontal moving

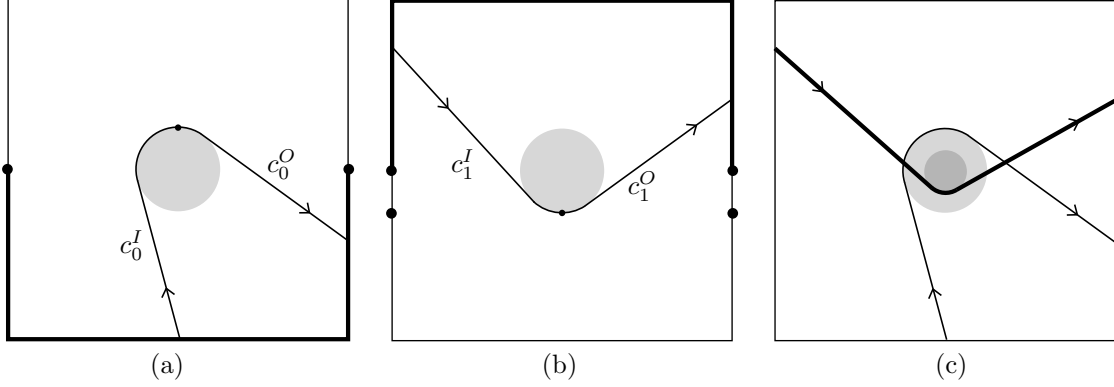


Figure 56. (a) The segments c_0^I and c_0^O in c_0 ; these segments can enter/leave the square anywhere in the bottom half of its boundary. (b) The segments c_1^I and c_1^O in c_1 ; these segments can enter/leave the square anywhere in the top half of its boundary or through the points $(\pm\frac{1}{2}, -\epsilon)$. (c) A transverse peg-board diagram for $c_0^I \cup c_0^O$ and $c_1^I \cup c_1^O$.

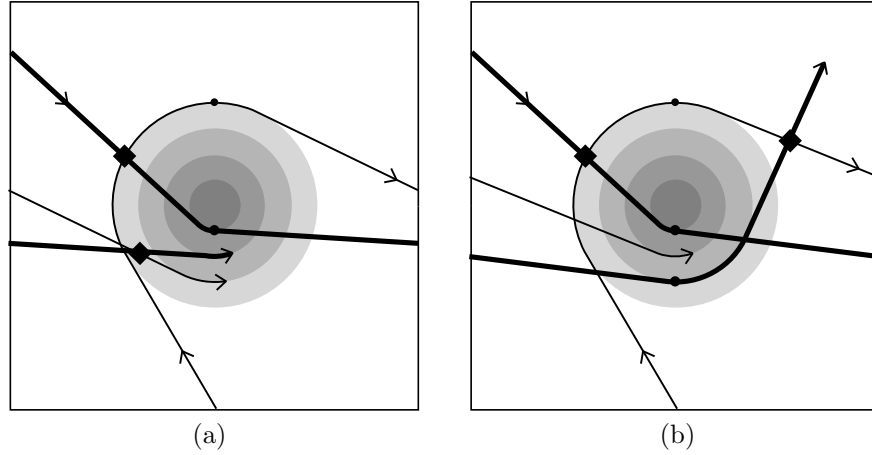


Figure 57. A transverse peg-board diagram for $c_0^I \cup c_0^O$ and $c_1^I \cup c_1^O$ when c_0^O and c_1^O both correspond to horizontal segments in singular diagrams for c_0 and c_1 . There are two cases, depending on the partial order on corners; in either case there are two intersection points between c_0 and c_1 with opposite sign.

to the right (see Figure 57); cases when the incoming segments or both segments are horizontal are similar. In this case, we do not get two intersection points of $c_0^I \cup c_0^O$ and $c_1^I \cup c_1^O$ if we restrict to one fundamental domain of T . However, c_0^O and c_1^O both wrap once around T horizontally, leading to new corners of c_0 and c_1 , respectively. In the transverse peg-board diagram, let ϵ_1 and ϵ_2 be the peg radii associated with these two corners. If $\epsilon_2 < \epsilon_1$, then c_0^O intersects c_1^O before reaching the next corner (Figure 57(a)). If $\epsilon_1 > \epsilon_2$, then c_1 must not have peg-wrapping at this corner. It follows that c_1 must continue by leaving the peg horizontally or upwards. If it leaves the peg moving upwards, it will intersect with $c_0^I \cup c_0^O$ (Figure 57(b)). If it leaves the peg horizontally, it wraps around T once more to a new corner with some radius ϵ_3 , and we repeat the argument using this corner in place of the corner with radius ϵ_2 . In either case, we find two intersection points between c_0 and c_1 with the opposite sign, as desired. \square

7.7. Enumerating toroidal L-spaces. As our first application of the L-space gluing theorem, we classify small toroidal L-spaces.

Theorem 57. *If Y is a prime toroidal L-space then $|H_1(Y)| = 5$ or $|H_1(Y)| \geq 7$. Moreover, if $|H_1(Y)| = 5$ then Y is one of precisely 4 manifolds obtained by gluing trefoil exteriors.*

Proof of Theorem 57. We begin by setting conventions. Consider manifolds M_0 and M_1 with torus boundary, and let $h: \partial M_1 \rightarrow \partial M_0$ be an orientation reversing homeomorphism. Since we are interested in rational homology spheres $Y = M_0 \cup_h M_1$, we may assume that both M_0 and M_1 are rational homology solid tori, with slopes $\lambda_i \in \partial M_i$ representing the rational longitude for $i = 0, 1$. Recall that

$$|H_1(M_0 \cup_h M_1; \mathbb{Z})| = t_0 t_1 |\lambda_0| |\lambda_1| |\Delta(\lambda_0, h(\lambda_1))|$$

where t_i is the order of the torsion subgroup of $H_1(M_i; \mathbb{Z})$ and $|\lambda_i|$ is the order of λ_i in $H_1(M_i; \mathbb{Z})$. The integer $\Delta(\lambda_0, h(\lambda_1))$ is the distance between the relevant slopes, that is, the minimal geometric intersection in ∂M_0 . If we fix Spin^c structures \mathfrak{s}_i on M_i , the quantity $|\lambda_0| |\lambda_1| |\Delta(\lambda_0, h(\lambda_1))|$ is the number of Spin^c structures on Y that restrict to \mathfrak{s}_0 on M_0 and \mathfrak{s}_1 on M_1 .

Since M_i is boundary incompressible, there is at least one $\mathfrak{s}_i \in \text{Spin}^c(M_i)$ for which $\gamma_i = \widehat{HF}(M_i, \mathfrak{s}_i)$ is not loose. The argument used in the proof of Theorem 8 shows that the curves representing γ_0 and γ_1 intersect in at least four points. Since Y is an L-space, this implies that $|\lambda_0| |\lambda_1| |\Delta(\lambda_0, h(\lambda_1))| \geq 4$. To have $H_1(Y) \leq 6$, we must have $t_0 = t_1 = 1$, *i.e.* both M_i are integer homology solid tori.

By abuse of notation we identify h with a matrix $\begin{pmatrix} s & r \\ q & p \end{pmatrix}$, acting on the right, where $(1, 0)$ is identified with λ_1 and $(0, 1)$ represents a meridian μ_1 . With this notation, one checks that $|r| = \Delta(\lambda_0, h(\lambda_1))$. Towards minimizing $|H_1(M_0 \cup_h M_1; \mathbb{Z})|$, we may assume that the M_i are integer homology solid tori, so that $c_0 = c_1 = 1$ and $|H_1(M_0 \cup_h M_1; \mathbb{Z})| = |r|$.

Now suppose that Y is an L-space; the intervals $\mathcal{L}_i = \mathcal{L}_{M_i}$ are necessarily non-empty. Since $H_1(M_i) = \mathbb{Z}$, the M_i cannot be Floer homology solid tori. Let $a_i \mu_i + b_i \lambda_i$ be an endpoint of \mathcal{L}_i , where without loss of generality we assume $a_i > 0$. The characterization of \mathcal{L}_i proved in [30] implies that \mathcal{L}_i is contained either in the interval $[a_i/b_i, a_i/(b_i+1)]$ or in the interval $[a_i/(b_i-1), a_i/b_i]$. (Here our notation denotes the cyclic interval with those endpoints which does not contain 0). By choosing μ_i appropriately, we may assume that $0 > b_i > -a_i$ in the first case, and that $0 < b_i < a_i$ in the second, so that $\mathcal{L}_i \subset [-\infty, -1]$ or $\mathcal{L}_i \subset [1, \infty]$. Finally, by reversing the global orientation on Y , we may assume that $\mathcal{L}_1 \subset [1, \infty]$.

We consider the images $h(0, 1) = (q, p)$, $h(1, 0) = (s, r)$, and $h(1, 1) = (q + s, p + r)$ relative to the interval of slopes \mathcal{L}_0 . If Y is an L-space then we must have $1 < h(\alpha) < \infty$ for each of these slopes or $-\infty < h(\alpha) < -1$ for each of these slopes.

First consider the case where $\mathcal{L}_0 \subset [1, \infty]$. Then

$$\begin{aligned} 1 < \frac{p}{q} < \infty &\Rightarrow 1 < |q| < |p| \\ 1 < \frac{r}{s} < \infty &\Rightarrow 1 < |s| < |r| \end{aligned}$$

and, considering the inverse homeomorphism $h^{-1} = \begin{pmatrix} -p & r \\ q & -s \end{pmatrix}$,

$$\begin{aligned} 1 < -\frac{s}{q} < \infty &\Rightarrow 1 < |q| < |s| \\ 1 < -\frac{r}{p} < \infty &\Rightarrow 1 < |p| < |r| \end{aligned}$$

where p and q and r and s have the same sign, while p and r and q and s have opposite signs. Additionally, note that $\det(h) = ps - qr = -1$ since h reverses orientation. Without loss of generality, we may assume that $r > 0$; one checks that there are no matrices with $r = 1, 2$ satisfying this list of constraints.

When $r = 3, 4$ the only possible matrices are $\begin{pmatrix} 2 & 3 \\ -1 & -2 \end{pmatrix}$, $\begin{pmatrix} 3 & 4 \\ -2 & -3 \end{pmatrix}$. However a homeomorphism of the form $\begin{pmatrix} r-1 & r \\ -r & -r \end{pmatrix}$ is always ruled out since $h(1, 1) = (1, 1)$ in this case (so a boundary L-space slope is not mapped to an interior L-space slope, as required). The same argument applies in the case $r = 6$

From this discussion we observe that in fact we seek to list matrices with determinant -1 satisfying $1 < \frac{p+r}{q+s} < \frac{r}{s} < \frac{p}{q} < \infty$. For $r = 5$, this leaves $\begin{pmatrix} 3 & 5 \\ -1 & -2 \end{pmatrix}$ and $\begin{pmatrix} 2 & 5 \\ -1 & -3 \end{pmatrix}$ as a complete list of possible L-space gluings in this case.

The case where $\mathcal{L}_0 \subset [-\infty, -1]$ is similar. Potential examples of L-spaces for which $r < 5$ or $r = 6$ are ruled out, by the requirement that $-\infty < \frac{p+r}{q+s} < \frac{r}{s} < \frac{p}{q} < -1$, leaving $\begin{pmatrix} -3 & 5 \\ 2 & -3 \end{pmatrix}$ and $\begin{pmatrix} -2 & 5 \\ 1 & -2 \end{pmatrix}$ as a complete list of L-space gluings for $r = 5$.

Next, we claim that in each of these four cases, we must have $\mathcal{L}_1 = [1, \infty]$. We give the argument for $H = \begin{pmatrix} 2 & 5 \\ -1 & -3 \end{pmatrix}$; the other cases are very similar. As we observed above, if a/b is the right endpoint of \mathcal{L}_1 , then $\mathcal{L}_1 \subset [a/(b+1), a/b]$. On the other hand, $\frac{p+r}{q+s} = 2$ and $\frac{p}{q} = 3$ must be in \mathcal{L}_1° . We deduce that $\frac{a}{b+1} < 2$ and $\frac{a}{b} > 3$, or equivalently $\frac{b+1}{a} > \frac{1}{2}$ and $\frac{b}{a} < \frac{1}{3}$. From this it follows that $a < 6$, and we quickly check by hand that there are no solutions with $0 < b < a < 6$. Thus the right-hand endpoint of \mathcal{L}_1 is ∞ , which implies that M_1 has an integer-homology sphere L-space filling. In turn, this implies that $\mathcal{L}_1 = [2g - 1, \infty]$, where g is the genus of M_1 . Since $2 \in \mathcal{L}_1^\circ$, we must have $g = 1$.

Reversing the roles of M_0 and M_1 , we see that $\mathcal{L}_0 = [1, \infty]$ or $\mathcal{L}_1 = [-\infty, -1]$. In either case, both M_0 and M_1 are prime, boundary incompressible and have two different L-space homology sphere fillings. It follows that they are both homeomorphic to trefoil complements. \square

We expect that there will only be finitely many toroidal L-spaces with $|H_1(Y)| = 7$, but cannot prove it, since we can't classify Floer simple manifolds with the same Alexander polynomial as $T(2, 5)$. In contrast, it is possible to obtain infinitely many toroidal L-spaces with $|H_1(Y)| = 8$ by gluing the trefoil complement to the twisted I -bundle over the Klein bottle.

7.8. Satellite L-space knots. Given a pattern knot P and a companion knot C , both in the three-sphere, denote by $P(C)$ the result of forming a satellite knot (note that this depends on some additional choices). The following is a conjecture of Hom, Lidman, and Vafaee [20, Conjecture 1.7]:

Conjecture 58. *If $P(C)$ is an L-space knot, then P and C are L-space knots as well.*

We conclude this section by proving that this conjecture holds.

Proof of Theorem 14. Consider the toroidal L-space Y resulting from surgery on a satellite knot K and write $Y = M_0 \cup_h M_1$. By Theorem 13, $\mathcal{L}_{M_0}^\circ \cup h(\mathcal{L}_{M_1}^\circ) = \mathbb{Q}P^1$ so that the manifolds M_0 and M_1 are, in fact, Floer simple manifolds (that is, the sets $\mathcal{L}_{M_i}^\circ$ are non-empty). In particular, M_0 the complement of an L-space knot C in S^3 (the companion knot). Since the Seifert longitude λ_C of C is not an L-space slope, it must be that $\lambda_C \in h(\mathcal{L}_{M_1}^\circ)$ so that $\alpha_P = h^{-1}(\lambda_C)$ gives an L-space $M_1(\alpha_P)$.

Now consider the pattern knot P in $D^2 \times S^1$, obtained from $M_K \setminus M_0$, where the boundary of $D^2 \times S^1$ is framed so that $\alpha_P \simeq \{\text{pt}\} \times S^1$. Note that filling this manifold along α_P gives a knot in S^3 (the pattern knot), which we will also denote by P . Further, P must be an L-space knot since there is more than one choice α , which existed by Floer simplicity of M_K (and was required for the construction of Y). This establishes the conjecture. \square

There is a converse to this statement which only requires a weaker version of the L-space gluing theorem from [15]; see Hom [19].

APPENDIX A. THREE MANIFOLD INVARIANTS ARE EXTENDABLE

We outline the proof of Theorem 4, which is mainly a matter of assembling the correct elements from [25] and checking that they still apply in our situation. We will assume the reader is familiar with the notation and terminology of [25].

Suppose that (M, α_1, α_2) is a compact oriented three-manifold with parametrized T^2 boundary, and that $\mathcal{H} = (\Sigma, \alpha, \beta)$ is a bordered Heegaard diagram representing it. (There is a notation clash here with our previous use of α, β for the parametrization.)

Our first step is to describe the moduli spaces of pseudo-holomorphic maps used to define the generalized coefficient maps D_I . The extended torus algebra \tilde{A} has a natural basis $\langle \rho_I \rangle$, where each ρ_I corresponds to a Reeb chord on the ideal contact boundary $\mathcal{Z} = \partial\bar{\Sigma}$. Suppose that x, y are generators for \mathcal{H} , that $B \in \tilde{\pi}_2(x, y)$, and that $\vec{\rho}$ is a sequence of Reeb chords whose product is equal to ρ_I . (Here, the notation $\tilde{\pi}_2$ indicates that we consider domains which may have nonzero multiplicity at z , as in [25, Section 10.2]).

We consider decorated sources as in [25, Definition 5.2], but with boundary punctures labeled by arbitrary Reeb chords ρ_I on \mathcal{Z} , including those which pass through the basepoint z . (Sources of this type are not sufficient for a bordered theory of HFK^- , since they lack interior punctures, but they are good enough for our needs.) Given a decorated source S^\flat we can consider the moduli space $\tilde{\mathcal{M}}^B(x, y; S^\flat)$ of pseudoholomorphic maps $U: S \rightarrow \Sigma \times [0, 1] \times \mathbb{R}$ which represent the homology class B as in [25, Definition 5.3], but omitting axiom (M-9) (the requirement that S has 0 multiplicity near the basepoint). Similarly, if \vec{P} is an ordering of the punctures of S , we can consider the open subset $\tilde{\mathcal{M}}^B(x, y; S^\flat; \vec{P})$ for which projection to the \mathbb{R} direction induces the given ordering \vec{P} . Finally, we let $\mathcal{M}^B(x, y; S^\flat; \vec{P})$ be the corresponding reduced moduli space.

Most of the analysis of pseudo-holomorphic curves in [25, Sections 5.2-5.6] carries over unchanged to this context, with the notable exception of the fact that boundary degenerations (see [25, Lemma 5.48]) can (and do) occur. More specifically, the proof of [25, Lemma 5.48] relies on the fact that $\pi_2(\Sigma, \alpha) = 0$. Since we are allowing sources whose boundary maps to ρ_0 , we must instead consider $\tilde{\pi}_2(\Sigma, \alpha) = \mathbb{Z}$. The generator of this group is the domain $[\Sigma]$, whose boundary is $\sum_{i=0}^3 \rho_i$. (Notice that since we do not allow sources with interior punctures, $\tilde{\pi}_2(\Sigma, \beta) = 0$.)

Now suppose we are given a sequence of Reeb chords $\vec{\rho}$ and that B is compatible with $\vec{\rho}$ in the sense of [25, Definition 5.68]. Following [25, Definition 5.68], we let $\mathcal{M}^B(x, y; \vec{\rho})$ be the union of those moduli spaces $\mathcal{M}^B(x, y; S^\flat)$ whose constituent pseudo-holomorphic curves are *embedded* and for which $[\vec{P}] = \vec{\rho}$.

Finally, following [25, Definition 6.3], we let

$$D_I(x) = \sum_y \sum_{\{\vec{\rho} | \alpha(-\vec{\rho}) = \rho_I\}} \sum_{\{B | \text{ind}(B, \rho) = 1\}} \#(\mathcal{M}^B(x, y; \vec{\rho}))y$$

and define $\tilde{\partial}^2(x) = \sum_I \rho_I \otimes D_I(x)$, where the sum runs over all indices I which contain at most one 0.

Proof of Theorem 4. We must show that $\tilde{\partial}^2(x) = W \otimes x$ modulo terms of the form $\rho_I \otimes y$, where I contains at least two 0's. To do so, we argue as in the proofs of [25, Proposition 6.7] and [25, Proposition 11.30]. Write

$$\tilde{\partial}^2(x) = \sum_I \sum_y n_{xy, I} \rho_I y.$$

Fix y and I which contains at most one 0, and consider the moduli space

$$\mathcal{M}(x, y; \rho_I) = \bigcup_{\{\bar{\rho} | \alpha(-\bar{\rho}) = \rho_I\}} \bigcup_{\{B | \text{ind}(B, \bar{\rho}) = 2\}} \mathcal{M}^B(x, y; \bar{\rho})$$

As in the proof of [25, Theorem 6.7], $n_{xy, I}$ is the mod 2 number of ends $\mathcal{M}(x, y; \rho_I)$ which do not correspond to boundary degenerations.

Suppose that boundary degenerations appear as ends of $\mathcal{M}(x, y; \rho_I)$. Index considerations dictate that such a degeneration must be of the form $\varphi_1 \vee \varphi_2$, where $\varphi_1 \in \mathcal{M}^{B_1}$ for some $B_1 \in \pi_2(\Sigma, \alpha)$ with index k , and $\varphi_2 \in \mathcal{M}^{B_2}$, where $B_2 \in \pi_2(x, y)$ has index $-k$. Assuming we have chosen a generic almost complex structure, all moduli spaces have their expected dimensions, and $k = 0$. Thus φ_2 is a union of trivial strips. The domain of B_1 is some multiple of the generator of $\pi_2(\Sigma, \alpha)$. Since 0 occurs in I at most once, the domain of B_1 must be Σ , which implies that $|I| = 4$. We conclude that if $|I| \neq 4$ or $x \neq y$, there are no boundary degenerations and $n_{xy, I} = 0$. The case $|I| = 4$ and $x = y$ was studied by Lipshitz, Ozsváth, and Thurston in [25, Proposition 11.30]. They showed that the number of boundary degenerations in this case is equal to $1 \pmod{2}$, so $n_{xy, I} = 1$. \square

REFERENCES

- [1] Akram Alishahi and Robert Lipshitz. Bordered Floer homology and incompressible surfaces. Preprint, arXiv:1708.05121.
- [2] Denis Auroux. Fukaya categories and bordered Heegaard-Floer homology. In *Proceedings of the International Congress of Mathematicians. Volume II*, pages 917–941. Hindustan Book Agency, New Delhi, 2010.
- [3] Denis Auroux. Fukaya categories of symmetric products and bordered Heegaard-Floer homology. *J. Gökova Geom. Topol. GGT*, 4:1–54, 2010.
- [4] Kenneth L. Baker and Kimihiko Motegi. Twist families of L-space knots, their genera, and Seifert surgeries. Preprint, arXiv:1506.04455.
- [5] Michel Boileau, Steven Boyer, and Cameron McA. Gordon. Branched covers of quasipositive links and L-spaces. In preparation.
- [6] Steven Boyer and Adam Clay. Foliations, orders, representations, L-spaces and graph manifolds. Preprint, arXiv:1401.7726.
- [7] Steven Boyer, Cameron McA. Gordon, and Liam Watson. On L-spaces and left-orderable fundamental groups. *Math. Ann.*, 356(4):1213–1245, 2013.
- [8] Eaman Eftekhary. Bordered Floer homology and existence of incompressible tori in homology spheres. Preprint, arXiv:1504.05329.
- [9] Thomas Gillespie. L-space fillings and generalized solid tori. Preprint, arXiv:1603.05016.
- [10] Cameron Gordon and Tye Lidman. Corrigendum to “taut foliations, left-orderability, and cyclic branched covers”. *Acta Mathematica Vietnamica*, Jun 2017.
- [11] Cameron McA. Gordon and Tye Lidman. Taut foliations, left-orderability, and cyclic branched covers. *Acta Math. Vietnam.*, 39(4):599–635, 2014.
- [12] Fabian Haiden, Ludmil Katzarkov, and Maxim Kontsevich. Flat surfaces and stability structures. Preprint, arXiv:1409.8611.
- [13] Jonathan Hanselman. Splicing integer framed knot complements and bordered Heegaard Floer homology. Preprint, arXiv:1409.1912.
- [14] Jonathan Hanselman. Bordered Heegaard Floer homology and graph manifolds. *Algebr. Geom. Topol.*, 16(6):3103–3166, 2016.
- [15] Jonathan Hanselman, Jacob Rasmussen, Sarah Dean Rasmussen, and Liam Watson. Taut foliations on graph manifolds. Preprint, arXiv:1508.05911.
- [16] Jonathan Hanselman, Jacob Rasmussen, and Liam Watson. Heegaard Floer homology for manifolds with torus boundary: properties and examples. In preparation.
- [17] Jonathan Hanselman and Liam Watson. A calculus for bordered Floer homology. Preprint, arXiv:1508.05445.
- [18] Matthew Hedden and Adam Simon Levine. Splicing knot complements and bordered Floer homology. *J. Reine Angew. Math.*, 2016:129–154, 2014.
- [19] Jennifer Hom. Satellite knots and L-space surgeries. *Bull. Lond. Math. Soc.*, 48(5):771–778, 2016.
- [20] Jennifer Hom, Tye Lidman, and Faramarz Vafaee. Berge-Gabai knots and L-space satellite operations. *Algebr. Geom. Topol.*, 14(6):3745–3763, 2014.
- [21] Jennifer Hom, Tye Lidman, and Liam Watson. The Alexander module, Seifert forms, and categorification. *Journal of Topology*, 10(1):22–100, 2017.
- [22] Yankı Lekili and Timothy Perutz. Fukaya categories of the torus and Dehn surgery. *Proc. Natl. Acad. Sci. USA*, 108(20):8106–8113, 2011.

- [23] Adam Simon Levine. Knot doubling operators and bordered Heegaard Floer homology. *J. Topol.*, 5(3):651–712, 2012.
- [24] Robert Lipshitz. *A Heegaard Floer invariant of bordered three-manifolds*. PhD thesis, Stanford University, 2006.
- [25] Robert Lipshitz, Peter Ozsváth, and Dylan Thurston. Bordered Heegaard Floer homology: Invariance and pairing. To appear in *Mem. Amer. Math. Soc.*, arXiv:0810.0687.
- [26] Robert Lipshitz, Peter S. Ozsváth, and Dylan P. Thurston. Bimodules in bordered Heegaard Floer homology. *Geom. Topol.*, 19(2):525–724, 2015.
- [27] András Némethi. Links of rational singularities, L-spaces and LO fundamental groups. *Inventiones mathematicae*, Apr 2017.
- [28] Peter Ozsváth and Zoltán Szabó. Heegaard diagrams and holomorphic disks. In *Different faces of geometry*, volume 3 of *Int. Math. Ser. (N. Y.)*, pages 301–348. Kluwer/Plenum, New York, 2004.
- [29] Ina Petkova. The decategorification of bordered Heegaard Floer homology. Preprint, arXiv:1212.4529.
- [30] Jacob Rasmussen and Sarah Dean Rasmussen. Floer simple manifolds and L-space intervals. To appear in *Adv. Math.*, arXiv:1508.05900.
- [31] Sarah Dean Rasmussen. L-space intervals for graph manifolds and cables. *Compos. Math.*, 153(5):1008–1049, 2017.
- [32] Peter Scott. The geometries of 3-manifolds. *Bull. London Math. Soc.*, 15(5):401–487, 1983.
- [33] Liam Watson. Heegaard Floer homology solid tori. AMS special session: Knots, links, and three-manifolds, San Diego, January 2013.

DEPARTMENT OF MATHEMATICS, PRINCETON UNIVERSITY.

E-mail address: `jh66@princeton.edu`

DEPARTMENT OF PURE MATHEMATICS AND MATHEMATICAL STATISTICS, UNIVERSITY OF CAMBRIDGE.

E-mail address: `J.Rasmussen@dpms.cam.ac.uk`

DÉPARTEMENT DE MATHÉMATIQUES, UNIVERSITÉ DE SHERBROOKE.

E-mail address: `Liam.Watson@USherbrooke.ca`